FedAvg with Fine Tuning: Local Updates Lead to Representation Learning

Liam Collins
ECE Department
The University of Texas at Austin
liamc@utexas.edu

Hamed Hassani
ESE Department
University of Pennsylvania
hassani@seas.upenn.edu

Aryan Mokhtari
ECE Department
The University of Texas at Austin
mokhtari@austin.utexas.edu

Sanjay Shakkottai
ECE Department
The University of Texas at Austin
sanjay.shakkottai@utexas.edu

Abstract

The Federated Averaging (FedAvg) algorithm, which consists of alternating between a few local stochastic gradient updates at client nodes, followed by a model averaging update at the server, is perhaps the most commonly used method in Federated Learning. Notwithstanding its simplicity, several empirical studies have illustrated that the model output by FedAvg leads to a model that generalizes well to new unseen tasks after a few fine-tuning steps. This surprising performance of such a simple method, however, is not fully understood from a theoretical point of view. In this paper, we formally investigate this phenomenon in the multi-task linear regression setting. We show that the reason behind the generalizability of the FedAvg output is FedAvg's power in learning the common data representation among the clients' tasks, by leveraging the diversity among client data distributions via multiple local updates between communication rounds. We formally establish the iteration complexity required by the clients for proving such result in the setting where the underlying shared representation is a linear map. To the best of our knowledge, this is the first result showing that FedAvg learns an expressive representation in any setting. Moreover, we show that multiple local updates between communication rounds are necessary for representation learning, as distributed gradient methods that make only one local update between rounds provably cannot recover the ground-truth representation in the linear setting, and empirically yield neural network representations that generalize drastically worse to new clients than those learned by FedAvg trained on heterogeneous image classification datasets.

1 Introduction

Federated Learning (FL) [1] provides a communication-efficient and privacy preserving means to learn from data distributed across clients such as cell phones, autonomous vehicles, and hospitals. FL aims for each client to benefit from collaborating in the learning process without sacrificing data privacy or paying a substantial communication cost. Federated Averaging (FedAvg) [1] is the predominant FL algorithm. In FedAvg, also known as Local SGD [2–4], the clients achieve communication efficiency by making multiple local updates of a shared global model before sending the result to the server, which averages the locally updated models to compute the next global model.

FedAvg is motivated by settings with *homogeneous* data across clients, since multiple local updates should improve model performance on all other clients' data when their data is similar. In contrast,

36th Conference on Neural Information Processing Systems (NeurIPS 2022).

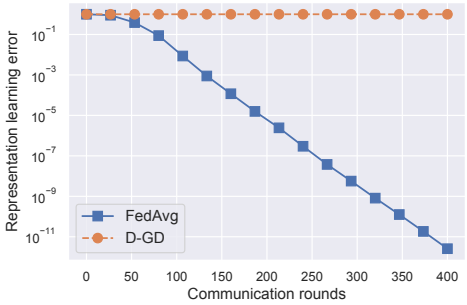

Figure 1: In multi-task linear regression with population losses, FedAvg linearly converges to the ground-truth representation, while D-GD (FedAvg with one local update) fails to learn it.

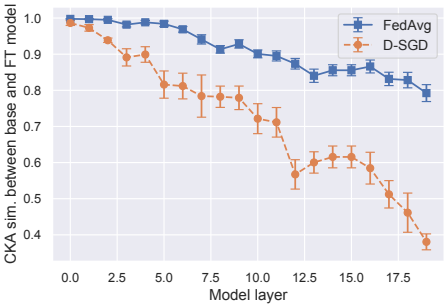

Figure 2: The NN representation learned by FedAvg on CIFAR-100 with 5 classes/client does not change significantly when fine-tuned on a new dataset (CIFAR-10), unlike D-SGD.

FedAvg faces two major challenges in more realistic *heterogeneous* data settings: learning a single global model may not necessarily yield good performance for each individual client, and, multiple local updates may cause the FedAvg updates to drift away from solutions of the global objective [5–9]. Despite these challenges, several empirical studies [10–12] have observed that this shared global model trained by FedAvg *with several local updates per round* when further fine-tuned for individual clients is surprisingly effective in heterogeneous FL settings. These studies motivate us to explore the impact of local updates on post-fine-tuning performance.

Meanwhile, a large number of recent works have shown that representation learning is a powerful paradigm for attaining high performance in multi-task settings, including FL. This is because the tasks' data often share a small set of features which are useful for downstream tasks, even if the datasets as a whole are heterogeneous. Consider, for example, heterogeneous federated image classification in which each client (task) may have images of different types of animals. It is safe to assume the images share a small number of features, such as body shape and color, which admit a simple and accurate mapping from feature space to label space. Since the number of important features is much smaller than the dimension of the data, knowing these features greatly simplifies each client's task.

To explore the connection between local updates and representation learning, we first study multi-task linear regression sharing a common ground-truth representation (Figure 1). We observe that FedAvg converges (exponentially fast) to the ground-truth representation in principal angle distance, while Distributed-GD (D-GD), which is effectively FedAvg with one local gradient update, fails to learn the shared representation. A similar concept can be shown in the nonlinear setting. We study a multi-layer CNN on a heterogeneous partition of CIFAR-100 (Figure 2). Since there is not necessarily a ground-truth model here, we evaluate representation learning as follows. We first train the models with FedAvg and Distributed-SGD (D-SGD) then fine-tune the pre-trained models on clients from a new dataset, CIFAR-10. Finally we evaluate the quality of the learned representation by measuring the amount that each model layer changes during fine-tuning using CKA similarity [13]. Observe that the early layers of FedAvg's pre-trained model (corresponding to the representation) change much less than those of D-SGD. More details for both experiments are in Section 5 and Appendix C. These observations suggest that FedAvg learns a shared representation that generalizes to new clients, even when trained in a heterogeneous setting. Hence, a natural question that arises is:

Does FedAvg provably learn effective representations of heterogeneous data?

We answer "yes" to this question by proving that FedAvg recovers the ground-truth representation in the case of multi-task linear regression. Critically, we show that FedAvg's local updates leverage the diversity among client data distributions to learn their common representation. This is surprising because FedAvg is a general-purpose algorithm not designed for representation learning. Our analysis thus yields new insights on how FedAvg finds generalizable models. Our contributions are:

- **Representation learning guarantees.** We study the behavior of FedAvg in multi-task linear regression with common representation. Here, each client aims to solve a d-dimensional regression with ground-truth solution that belongs to a shared k-dimensional subspace of $\mathbb{R}^d$, where $k \ll d$. Our results show that FedAvg with $\tau \geq 2$ local updates learns the representation

at a linear rate when each client accesses population gradients. *To the best of our knowledge, this is the first result showing that FedAvg learns an effective representation in any setting.*

- **Insights on the importance of local updates.** Our analysis reveals that executing more than one local update between communication rounds *exploits the diversity* of the clients' ground truth regressors to improve the learned representation in all k directions in the linear setting. In contrast, we prove that D-GD fails to learn the representation.

- **Empirical evidence of representation learning.** We provide experimental results showing Fedavg learns a generalizable representation when we use deep neural networks on image classification datasets. In contrast, the representations learned by D-SGD generalize drastically worse to data from new clients. This suggests that the main massage of our theoretical results that local updates facilitate representation learning can generalize to more complex scenarios beyond the bilinear setting.

Related work. Recently there has been a surge of interest motivated by FL in analyzing FedAvg/Local SGD in heterogeneous settings. Multiple works have shown that FedAvg converges to a global optimum (resp. stationary point) of the global objective in convex (resp. nonconvex) settings but with decaying learning rate [5, 14–17], leading to sublinear rates and communication complexity sometimes dominated by Distributed-SGD [18]. These results are tight in the sense that FedAvg with fixed learning rate may *not* converge to a stationary point of the global objective in the presence of data heterogeneity, as its multiple local updates cause it to optimize a distinct, unknown objective [6–9, 16, 19, 20]. Several methods have tried to correct this objective inconsistency via gradient tracking [5, 19, 21–25], local regularization [20, 26–28], operator splitting [7], and strategic client sampling [29–31]. In contrast, we show that local updates with *constant* learning rate benefit *learning* in heterogeneous settings by resulting in linear convergence to generalizable models.

Several papers have also studied FedAvg from a generalization perspective. It was shown in [32] that in a setting with strongly convex losses, either local training or FedAvg with fine-tuning (but not both) achieves minimax risk, depending on the level of data heterogeneity. Similarly, [33] argued that FedAvg with fine-tuning generalizes as well as more sophisticated methods, including Model-Agnostic Meta-Learning (MAML) [34, 35], in a strongly convex regularized linear regression setting. Additional work has studied the generalization of FedAvg in kernel regression, but for convex objectives that do not allow for representation learning [36], and the generalization of a variant of FedAvg, known as Reptile [37], on wide two-layer ReLU networks with homogeneous data [38]. We focus on the multi-task linear representation learning setting [39], which has become popular in recent years as it is an expressive but tractable nonconvex setting for studying the sample-complexity benefits of learning representations and the representation learning abilities of popular algorithms in data heterogeneous settings [11, 40–46]. Remarkably, our study of FedAvg reveals that it can learn an effective representation even though it was not designed for this goal, unlike a variety of personalized FL methods specifically tailored for representation learning [11, 47–51].

Notations. We use $\mathcal{N}(\mathbf{u}, \mathbf{\Sigma})$ to signify the multivariate Gaussian distribution with mean $\mathbf{u}$ and covariance $\mathbf{\Sigma}$. $\mathcal{O}^{d\times k}$ denotes the set of matrices in $\mathbb{R}^{d\times k}$ with orthonormal columns. The notation $\mathrm{col}(\mathbf{B})$ represents the column space of the matrix $\mathbf{B}$, and $\mathrm{col}(\mathbf{B})^{\perp}$ is the orthogonal complement to this space. The norm $\|\cdot\|$ is the spectral norm and $\mathbf{I}_d$ is the identity matrix in $\mathbb{R}^{d\times d}$. We use $[m]$ to indicate the set of natural numbers up to and including m.

2 Problem Formulation

Consider a federated setting with a central server and M clients. Each client $i \in [M]$ has a training dataset $\hat{\mathcal{D}}_i$ of n_i labeled samples drawn from a distribution $\mathcal{D}_i$ over $\mathcal{X} \times \mathcal{Y}$, where $\mathcal{X}$ is the input space and $\mathcal{Y}$ is the label space. The learning model is given by $h_{\boldsymbol{\theta}} : \mathcal{X} \to \mathcal{Y}$ for model parameters $\boldsymbol{\theta} \in \mathbb{R}^D$. The loss of the model on a sample $(\mathbf{x}, \mathbf{y}) \in \mathcal{X} \times \mathcal{Y}$ is given by $\ell(h_{\boldsymbol{\theta}}(\mathbf{x}), \mathbf{y})$, which may be, for example, the squared or cross entropy loss. The loss of model parameters $\boldsymbol{\theta}$ on the i-th client is the average loss of the model $h_{\boldsymbol{\theta}}$ on the samples in $\hat{\mathcal{D}}_i$, namely $f_i(\boldsymbol{\theta}) := \frac{1}{n_i}\sum_{j=1}^{n_i} \ell(h_{\boldsymbol{\theta}}(\mathbf{x}_{i,j}), \mathbf{y}_{i,j})$, where $(\mathbf{x}_{i,j}, \mathbf{y}_{i,j})$ is the j-th sample in $\hat{\mathcal{D}}_i$. The server aims to leverage all of the data across clients to find models that achieve small loss $f_i(\boldsymbol{\theta})$ for each client. To do so, the standard approach is to find

a single model $\boldsymbol{\theta}$ that minimizes the average of the client losses weighted by number of samples:

$$\min_{\boldsymbol{\theta}} \frac{1}{N} \sum_{i=1}^{M} n_i f_i(\boldsymbol{\theta}) \;=\; \frac{1}{N} \sum_{i=1}^{M} \sum_{j \in \hat{\mathcal{D}}_i} \ell(h_{\boldsymbol{\theta}}(\mathbf{x}_{i,j}), \mathbf{y}_{i,j})), \tag{1}$$

where $N = \sum_{i=1}^{M} n_i$. Due to communication and privacy constraints, the clients cannot share their local data $\hat{\mathcal{D}}_i$, so (1) must be solved in a federated manner.

FedAvg. The most common FL method is FedAvg. On each round t of FedAvg, the server uniformly samples a set $\mathcal{I}_t$ of $m \leq M$ clients. Each selected client receives the current global parameters $\boldsymbol{\theta}_t$, executes multiple SGD steps on its local data starting from $\boldsymbol{\theta}_t$, then sends the result back to the server. The server then computes $\boldsymbol{\theta}_{t+1}$ as the weighted average of the updates. Specifically, upon receiving the global model $\boldsymbol{\theta}_t$, client i computes

$$\boldsymbol{\theta}_{t,i,s+1} = \boldsymbol{\theta}_{t,i,s} - \alpha \mathbf{g}_{t,i,s}(\boldsymbol{\theta}_{t,i,s}), \tag{2}$$

for $s = 0, \ldots, \tau - 1$, where τ is the number of local steps, $\boldsymbol{\theta}_{t,i,0} = \boldsymbol{\theta}_t$ and $\mathbf{g}_{t,i,s}(\boldsymbol{\theta}_{t,i,s})$ is a stochastic gradient of f_i evaluated at $\boldsymbol{\theta}_{t,i,s}$ using b samples from $\hat{\mathcal{D}}_i$. The client then sends $\boldsymbol{\theta}_{t,i,\tau}$ back to the server, which computes the next global iterate as:

$$\boldsymbol{\theta}_{t+1} = \frac{1}{N_t} \sum_{i \in \mathcal{I}_t} n_i \boldsymbol{\theta}_{t,i,\tau}, \tag{3}$$

where $N_t \coloneqq \sum_{i \in \mathcal{I}_t} n_i$. Note that $\tau = 1$ corresponds to D-SGD, also known as mini-batch SGD whose convergence properties are well-understood [18, 52–54]. FedAvg improves the communication efficiency of D-SGD by making $\tau \geq 2$ local updates between communication rounds.

Fine-tuning. After training for T communication rounds, the global parameters $\boldsymbol{\theta}_T$ learned by FedAvg are typically fine-tuned on each client before testing. In particular, starting from $\boldsymbol{\theta}_T$, client i executes τ' steps of SGD on its local data as follows:

$$\boldsymbol{\theta}_{T,i,s+1} = \boldsymbol{\theta}_{T,i,s} - \alpha \mathbf{g}_{T,i,s}(\boldsymbol{\theta}_{t,i,s}) \tag{4}$$

for $s = 0, \ldots, \tau - 1$. The fine-tuned model ultimately used for testing is $\boldsymbol{\theta}_{T,i,\tau'}$. Note that a new client, indexed by $M + 1$, entering the system after FedAvg training has completed can also fine-tune $\boldsymbol{\theta}_T$ using the same procedure to obtain a personalized solution $\boldsymbol{\theta}_{T,M+1,\tau'}$.

Representation learning. We aim to answer why the fine-tuned models $\{\boldsymbol{\theta}_{T,i,\tau'}\}_{i=1}^{M+1}$ perform well in practice by taking a representation learning perspective. We show that the output of FedAvg, i.e., θ_T, has learned the common data representation among clients assuming that such a representation exists. To formalize this result, we consider a class of models that can be written as the composition of a representation h^{rep} and a prediction module, i.e. head, denoted as h^{head}. Let the model parameters be split as $\boldsymbol{\theta} \coloneqq [\boldsymbol{\phi}, \boldsymbol{\psi}]$, where $\boldsymbol{\phi}$ contains the representation parameters and $\boldsymbol{\psi}$ contains the head parameters. Then, for any $\mathbf{x} \in \mathcal{X}$, the prediction of the learning model is $h_{\boldsymbol{\theta}}(\mathbf{x}) = (h^{\text{head}}_{\boldsymbol{\psi}} \circ h^{\text{rep}}_{\boldsymbol{\phi}})(\mathbf{x}) = h^{\text{head}}_{\boldsymbol{\psi}}(h^{\text{rep}}_{\boldsymbol{\phi}}(\mathbf{x}))$. For instance, if $h_{\boldsymbol{\theta}}$ is a neural network with weights $\boldsymbol{\theta}$, then $h^{\text{rep}}_{\boldsymbol{\phi}}$ is the first many layers of the network with weights $\boldsymbol{\phi}$, and $h^{\text{head}}_{\boldsymbol{\psi}}$ is the network last few layers with weights $\boldsymbol{\psi}$. A standard assumption in multi-task settings, including the settings we consider, is the existence of a common representation $h^{\text{rep}}_{\boldsymbol{\phi}_*}$ that admits an easily learnable head $h^{\text{rep}}_{\boldsymbol{\psi}_{*,i}}$ such that $h^{\text{head}}_{\boldsymbol{\psi}_{*,i}} \circ h^{\text{rep}}_{\boldsymbol{\phi}_*}$ performs well for task i. As a result, in these settings it is of interest to all the clients to learn $h^{\text{rep}}_{\boldsymbol{\phi}_*}$.

3 Main Results

To rigorously study the representation learning abilities of FedAvg, we employ the standard setting used for algorithmic representation learning analysis: multi-task linear regression [11, 40, 41, 46, 55, 56]. In this setting, samples $(\mathbf{x}_{i,j}, y_{i,j})$ for each client i are drawn independently from a distribution $\mathcal{D}_i$ on $\mathbb{R}^d \times \mathbb{R}$ such that

$$\mathbf{x}_{i,j} \overset{\text{i.i.d.}}{\sim} p_{\mathbf{x}}, \;\; y_{i,j} = \langle \boldsymbol{\beta}_{*,i}, \mathbf{x}_{i,j} \rangle + \zeta_{i,j} \;\; \text{where} \;\; \zeta_{i,j} \overset{\text{i.i.d.}}{\sim} p_{\zeta}$$

for an unobserved ground-truth regressor $\boldsymbol{\beta}_{*,i} \in \mathbb{R}^d$ and label noise $\zeta_{i,j}$. We assume the distributions $p_{\mathbf{x}}$ and p_{ζ} are such that $\mathbb{E}[\mathbf{x}_{i,j}] = \mathbf{0}$, $\mathbb{E}[\mathbf{x}_{i,j}\mathbf{x}_{i,j}^{\top}] = \mathbf{I}_d$, $\mathbb{E}[\zeta_{i,j}] = 0$.

To incentivize representation learning, each $\boldsymbol{\beta}_{*,i}$ belongs to the same k-dimensional subspace of $\mathbb{R}^d$, where $k \ll d$. Let $\mathbf{B}_* \in \mathcal{O}^{d\times k}$ have columns that form an orthogonal basis for the shared subspace, so that $\boldsymbol{\beta}_{*,i} = \mathbf{B}_*\mathbf{w}_{*,i}$ for some $\mathbf{w}_{*,i} \in \mathbb{R}^k$ for each i. In other words, there exists a low-dimensional set of parameters known as the "head" that can specify the ground-truth model for client i once the shared representation, i.e., $\mathrm{col}(\mathbf{B}_*)$, is known. It is advantageous to learn $\mathrm{col}(\mathbf{B}_*)$ because once it is known, all clients (including potentially new clients entering the system) have sample complexity $O(k) \ll d$ as they only need to learn the parameters of their head [40, 41].

Each client i ultimately aims to learn a model $\hat{\boldsymbol{\beta}}_i$ that approximates $\boldsymbol{\beta}_{*,i}$ in order to achieve good generalization on its local distribution. To eventually achieve this for each client, FedAvg with fine-tuning first aims to learn a global model consisting of a representation $\mathbf{B} \in \mathbb{R}^{d\times k}$ and a head $\mathbf{w} \in \mathbb{R}^k$ that minimizes the average loss across clients. The loss for client i is $f_i(\mathbf{B}, \mathbf{w}) := \frac{1}{2n_i}\sum_{j=1}^{n_i}(y_{i,j} - \langle \mathbf{B}\mathbf{w}, \mathbf{x}_{i,j}\rangle)^2$, i.e. the average squared loss on the local data, so FedAvg tries to learn a global model that solves the nonconvex problem:

$$\min_{\mathbf{B}\in\mathbb{R}^{d\times k}, \mathbf{w}\in\mathbb{R}^k} \frac{1}{N}\sum_{i=1}^{M} n_i \Big\{ f_i(\mathbf{B}, \mathbf{w}) := \frac{1}{2n_i}\sum_{j=1}^{n_i}(y_{i,j} - \langle \mathbf{B}\mathbf{w}, \mathbf{x}_{i,j}\rangle)^2 \Big\}. \tag{5}$$

where $N = \sum_{i=1}^{M} n_i$. To solve (5) in a distributed manner, FedAvg dictates that each client makes a series of local updates of the current global model before returning the models to the server for averaging (see Section 2). Our aim is to show that FedAvg training learns the column space of $\mathbf{B}_*$. First, we make standard diversity and normalization assumptions on the ground-truth heads.

Assumption 1 (Client normalization)**.** *There exists $L < \infty$ s.t. $\forall i \in [M]$, $\|\mathbf{w}_{*,i}\|_2 \le L\sqrt{k}$.*

Assumption 2 (Client diversity)**.** *There exists $\mu > 0$ s.t. $\sigma_{\min}(\frac{1}{M}\sum_{i=1}^{M}(\mathbf{w}_{*,i} - \bar{\mathbf{w}}_*)(\mathbf{w}_{*,i} - \bar{\mathbf{w}}_*)^\top) \ge \mu^2$, where $\bar{\mathbf{w}}_* := \frac{1}{M}\sum_{i=1}^{M}\mathbf{w}_{*,i}$. Define $\kappa := L/\mu$.*

Assumption 2 is very similar to typical task diversity assumptions except that it quantifies the diversity of the centered rather than un-centered tasks [40, 41]. Intuitively, task diversity is required so that all of the directions in $\mathrm{col}(\mathbf{B}_*)$ are observed. The smaller κ, the more evenly spread the ground-truth heads are, and the larger the task (i.e. client) diversity. Next, to obtain convergence results we must define the variance of the ground-truth heads and the principal angle distance between representations.

Definition 1 (Client variance)**.** *For $\gamma > 0$, define: $\gamma^2 := \frac{1}{kM}\sum_{i=1}^{M}\|\mathbf{w}_{*,i} - \bar{\mathbf{w}}_*\|^2$, where $\bar{\mathbf{w}}_*$ is defined in Assumption 2. For $H > 0$, define $H^4 := \frac{1}{k^2 M}\sum_{i=1}^{M}\|\mathbf{w}_{*,i}\mathbf{w}_{*,i}^\top - \frac{1}{M}\sum_{i'=1}^{M}\mathbf{w}_{*,i'}\mathbf{w}_{*,i'}^\top\|^2$.*

Definition 2 (Principal angle distance)**.** *For two matrices $\mathbf{B}_1, \mathbf{B}_2 \in \mathbb{R}^{d\times k}$, the* principal angle distance *between $\mathbf{B}_1$ and $\mathbf{B}_2$ is defined as $\mathrm{dist}(\mathbf{B}_1, \mathbf{B}_2) := \|\bar{\mathbf{B}}_{1,\perp}^\top \bar{\mathbf{B}}_2\|_2$, where the columns of $\bar{\mathbf{B}}_{1,\perp} \in \mathcal{O}^{d\times(d-k)}$ and $\bar{\mathbf{B}}_2 \in \mathcal{O}^{d\times k}$ form orthonormal bases for $\mathrm{col}(\mathbf{B}_1)^\perp$ and $\mathrm{col}(\mathbf{B}_2)$, respectively.*

Intuitively, the principal angle distance between $\mathbf{B}_1$ and $\mathbf{B}_2$ is the sine of the largest angle between the subspaces spanned by their columns. Now we are ready to state our main result. We suppose each client has $n_i = \infty$ samples, i.e. it accesses the gradients of the population loss on its local distribution.

Theorem 1. *Consider the case that each client takes gradient steps with respect to their population loss $f_i(\mathbf{B}, \mathbf{w}) := \frac{1}{2}\|\mathbf{B}\mathbf{w} - \mathbf{B}_*\mathbf{w}_{*,i}\|^2$ and all losses are weighed equally in the global objective. Suppose Assumptions 1-2 hold, the number of clients participating each round satisfies $m \ge \min(M, 20((\gamma/L)^2 + (H/L)^4)(\alpha L\sqrt{k})^{-4}\log(kT))$, and the initial parameters satisfy (i) $\delta_0 := \mathrm{dist}(\mathbf{B}_0, \mathbf{B}_*) \le \sqrt{1 - E_0}$ for any $E_0 \in (0, 1]$, (ii) $\|\mathbf{I} - \alpha\mathbf{B}_0^\top\mathbf{B}_0\|_2 = O(\alpha^2\tau L^2\kappa^2 k^2)$ and (iii) $\|\mathbf{w}_0\|_2 = O(\alpha^{2.5}\tau L^3 k^{1.5})$. Choose step size $\alpha = O(\frac{1-\delta_0}{\sqrt{\tau}L\kappa^2 k^{1.5}})$. Then for any $\epsilon \in (0, 1)$, the distance of the representation learned by FedAvg with $\tau \ge 2$ local updates satisfies $\mathrm{dist}(\mathbf{B}_T, \mathbf{B}_*) < \epsilon$ after at most $T = O\big(\frac{\log(1/\epsilon)}{\alpha^2\tau\mu^2 E_0}\big)$ communication rounds with probability at least $1 - 4(kT)^{-99}$.*

Theorem 1 shows that FedAvg converges exponentially fast to the ground-truth representation when executed on the clients' population losses. We provide intuition for the proof in Section 4 and the full proof in Appendix B. First, some comments are in order.

Mild initial conditions. Theorem 1 holds under benign initial conditions. In particular, condition (i) requires that the initial distance is only a constant smaller than 1. Condition (ii) ensures that the

initial representation is well-conditioned with appropriate scaling, and (iii) guarantees the initial head is not too large. The last two conditions can be easily achieved by normalizing the inputs.

Generalization without convergence in terms of the global loss. When each client accesses its population loss as in Theorem 1, the global objective (5) becomes:

$$\min_{\mathbf{B}\in\mathbb{R}^{d\times k},\mathbf{w}\in\mathbb{R}^k} \frac{1}{M}\sum_{i=1}^{M} \|\mathbf{B}\mathbf{w}-\mathbf{B}_*\mathbf{w}_{*,i}\|^2 \tag{6}$$

However, Theorem 1 does not imply that FedAvg solves (6). In fact, our simulations in Section 5 show that it does not even reach a stationary point of (6). This is consistent with prior works that have noticed the "objective inconsistency" phenomenon of FedAvg: it solves an unknown objective distinct from the global objective due to the fact that after multiple local updates, local gradients are no longer unbiased estimates of gradients of (6) [9]. Nevertheless, our results show that FedAvg is able to learn a generalizable model *even when it does not optimize the global loss in data heterogeneous settings*.

Multiple local updates critically harness client diversity, whereas Distributed GD (D-GD) does not learn the representation. Key to the proof of Theorem 1 is that the locally-updated heads become *diverse*, meaning that they cover all directions in $\mathbb{R}^k$, with greater diversity corresponding to more even covering in all directions. We will show in Section 4 that the locally-updated heads become roughly as diverse as the ground-truth heads, and this causes the representation to move towards the ground-truth at rate depending on the diversity level. Theorem 1 reflects this: the convergence rate improves with the diversity metric μ/L. In this way FedAvg *exploits* data heterogeneity to learn the representation, as more diverse $\{\mathbf{w}_{*,i}\}_{i\in[M]}$ implies more heterogeneous data. Moreover, since τ also appears in the denominator of the communication round complexity, additional local updates improve the convergence rate up to $\tau = O(\alpha^{-2})$, which is the limit imposed due to the upper bound on α.

Importantly, head diversity only benefits the global representation update if $\tau \geq 2$. We formally prove that D-GD (equivalent to FedAvg with $\tau=1$ and $m=M$) cannot recover $\mathrm{col}(\mathbf{B}_*)$ in the following result.

Proposition 1 (Distributed GD lower bound)**.** *Suppose we are in the setting described in Section 3 and $d > k > 1$. Then for any set of ground-truth heads $\{\mathbf{w}_{*,i}\}_{i=1}^M$, full-rank initialization $\mathbf{B}_0 \in \mathbb{R}^{d\times k}$, initial distance $\delta_0 \in (0, 1/2]$, step size $\alpha > 0$, and number of rounds T, there exists $\mathbf{B}_* \in \mathcal{O}^{d\times k}$ satisfying $\mathrm{dist}(\mathbf{B}_0, \mathbf{B}_*) = \delta_0$ and $\mathrm{dist}(\mathbf{B}_T^{\text{D-GD}}, \mathbf{B}_*) \geq 0.7\delta_0$, where $\mathbf{B}_T^{\text{D-GD}} \equiv \mathbf{B}_T^{\text{D-GD}}(\mathbf{B}_0, \mathbf{B}_*, \{\mathbf{w}_{*,i}\}_{i=1}^M, \alpha)$ is the result of D-GD with step size α and initialization $\mathbf{B}_0$ in the setting with ground-truth representation $\mathbf{B}_*$ and ground-truth heads $\{\mathbf{w}_{*,i}\}_{i=1}^M$.*

Proposition 1 shows that for any choice of $\delta_0 \in (0, 1/2]$, non-degenerate initialization $\mathbf{B}_0$, and ground-truth heads, there exists a $\mathbf{B}_*$ whose column space is δ_0-close to $\mathrm{col}(\mathbf{B}_0)$, yet is at least $0.7\delta_0$-far from the representation learned by D-GD in the setting with $\mathbf{B}_*$ as ground-truth. Therefore, even allowing for a strong initialization, D-GD cannot guarantee to recover the ground-truth representation. This negative result combined with our previous results suggest that even if we had an infinite communication budget, it would still be advantageous to execute multiple local updates between communication rounds in order to achieve better generalization through representation learning.

4 Intuitions and Proof Sketch

Next we highlight the key ideas behind the importance of local updates and why FedAvg learns $\mathrm{col}(\mathbf{B}_*)$, while D-GD fails to achieve this goal.

Global update $\mathbf{B}_{t+1}$. To build intuition for why FedAvg can learn $\mathrm{col}\,(\mathbf{B}_*)$, we examine the global update of the representation in the full participation case ($m = M$):

$$\mathbf{B}_{t+1} = \mathbf{B}_t \underbrace{\left[\frac{1}{M}\sum_{i=1}^{M}\prod_{s=0}^{\tau-1}(\mathbf{I}_k - \alpha\mathbf{w}_{t,i,s}\mathbf{w}_{t,i,s}^\top)\right]}_{\text{prior weight}} + \mathbf{B}_* \underbrace{\left[\frac{\alpha}{M}\sum_{i=1}^{M}\mathbf{w}_{*,i}\sum_{s=0}^{\tau-1}\mathbf{w}_{t,i,s}^\top\prod_{r=s+1}^{\tau-1}(\mathbf{I}_k - \alpha\mathbf{w}_{t,i,r}\mathbf{w}_{t,i,r}^\top)\right]}_{\text{signal weight}}$$

Notice that $\mathbf{B}_{t+1}$ is a mixture of $\mathbf{B}_t$ and $\mathbf{B}_*$ with weight matrices in $\mathbb{R}^{k\times k}$. We aim to show that

(I) the 'prior weight' on $\mathbf{B}_t$ has spectral norm strictly less than 1, and

(II) the 'signal weight' on $\mathbf{B}_*$ adds energy from $\mathrm{col}(\mathbf{B}_*)$ to $\mathbf{B}_{t+1}$ so that $\sigma_{\min}(\mathbf{B}_{t+1}) \approx \sigma_{\min}(\mathbf{B}_t)$.

These two conditions imply that the contribution from $\mathrm{col}(\mathbf{B}_t)$ in $\mathrm{col}(\mathbf{B}_{t+1})$ contracts, while energy from $\mathrm{col}(\mathbf{B}_*)$ replaces the lost energy from $\mathrm{col}(\mathbf{B}_t)$. Hence, $\mathrm{col}(\mathbf{B}_{t+1})$ moves to $\mathrm{col}(\mathbf{B}_*)$ in all k directions.

The role of head diversity and multiple local updates. To show (I) and (II), it is imperative to use the diversity of the locally-updated heads when $\tau \geq 2$. First consider (I). Notice that for each i, $\prod_{s=0}^{\tau-1}(\mathbf{I}_k - \alpha \mathbf{w}_{t,i,s}\mathbf{w}_{t,i,s}^\top)$ has singular values at most 1, and strictly less than 1 corresponding to directions spanned by $\{\mathbf{w}_{t,i,s}\}_{s\in[\tau-1]}$. Thus, the maximum singular value of the average of these matrices should be strictly less than 1 as long as $\{\mathbf{w}_{t,i,s}\}_{s\in[\tau-1],i\in[M]}$ spans $\mathbb{R}^k$, i.e. the locally-updated heads are diverse. Similarly, the signal weight is rank-k if the locally-updated heads span $\mathbb{R}^k$, which leads to (II) as discussed below. In contrast, if $\tau = 1$, then the global update of the representation does *not* leverage head diversity, as it is only a function of the global head and the average ground-truth head: $\mathbf{B}_{t+1} = \mathbf{B}_t(\mathbf{I}_k - \alpha \mathbf{w}_t\mathbf{w}_t^\top) + \alpha \mathbf{B}_*\bar{\mathbf{w}}_*\mathbf{w}_t^\top$ in this case. As a result, $\mathrm{col}(\mathbf{B}_{t+1})$ can only improve in one direction, so D-GD ultimately fails to learn $\mathrm{col}(\mathbf{B}_*)$ (see Proposition 1).

Achieving head diversity: the necessity of controlling $\mathbf{I}_k - \alpha\mathbf{B}_t^\top\mathbf{B}_t$. We have discussed the intuition for why head diversity implies (I) and (II) for FedAvg. Next, we investigate why the heads become diverse. Let us examine client i's first local update for the head at round t:

$$\mathbf{w}_{t,i,1} = (\mathbf{I}_k - \alpha\mathbf{B}_t^\top\mathbf{B}_t)\mathbf{w}_t + \alpha\mathbf{B}_t^\top\mathbf{B}_*\mathbf{w}_{*,i}$$

From this equation we see that if $\mathbf{\Delta}_t \coloneqq \mathbf{I}_k - \alpha\mathbf{B}_t^\top\mathbf{B}_t \approx \mathbf{0}$ and $\|\mathbf{w}_t\|$ is bounded, then $\mathbf{w}_{t,i,1} \approx \alpha\mathbf{B}_t^\top\mathbf{B}_*\mathbf{w}_{*,i}$. If this approximation holds, then $\{\mathbf{w}_{t,i,1}\}_{i\in[M]}$ inherits the diversity of $\{\mathbf{w}_{*,i}\}_{i\in[M]}$, which is indeed diverse due to Assumption 2, meaning that the local heads are diverse after just one local update. Moreover, it can be shown that if $\mathbf{\Delta}_t \approx \mathbf{0}$ and the heads become diverse after one local update, then they remain diverse for all local updates due to the observation that each $\mathbf{B}_{t,i,s}$ changes slowly over s. Note that in addition to implying local head diversity, $\mathbf{\Delta}_t \approx \mathbf{0}$ for all t implies $\sigma_{\min}(\mathbf{B}_t) \approx \sigma_{\min}(\mathbf{B}_{t+1}) \approx \frac{1}{\sqrt{\alpha}}$, which directly ensures (II). Thus we aim to show $\mathbf{\Delta}_t \approx \mathbf{0}$ for all communication rounds, i.e. $\mathbf{B}_t$ remains close to a scaled orthonormal matrix.

However, it is surprising why $\|\mathbf{\Delta}_t\|$ remains small: $\mathbf{B}_{t+1}$ is the average of nonlinearly locally-updated representations, and the local updates could 'overfit' by adding more energy to some columns than others, and/or lead to cancellation when summed, so it is not intuitive why $\sqrt{\alpha}\mathbf{B}_t$ remains almost orthonormal. Nor does the expression above for $\mathbf{B}_{t+1}$ provide any clarity on this. Nevertheless, through a careful induction we show that $\mathbf{\Delta}_t$ indeed stays close to zero since the local heads converge quickly and the projection of the local representation gradient onto $\mathrm{col}(\mathbf{B}_t)$ is exponentially decaying.

Inductive argument. While the above intuitions seem to simplify the behavior of FedAvg, showing that they all hold simultaneously is not at all obvious. To study this, we are inspired by recent work [44] that developed an inductive argument for representation learning in the context of gradient based-meta-learning. To formalize our intuition discussed previously, in our proof we need to show that (i) the learned representation does not overfit to each client's loss despite *many local updates* and simultaneously the heads quickly become diverse, and (ii) the update at the global server preserves the learned representation despite *averaging* many nonlinearly perturbed representations gathered from clients after local updates. To address these challenges, we construct a pair of intertwined inductive hypotheses over time, one for tracking the effect of local updates, and another for tracking the global averaging. Each inductive hypothesis (local and global) itself consists of several hypotheses (in effect, a nested induction) that evolve within communication rounds.

Local induction. The proof leverages the following local inductive hypotheses for every t, i:

1. $A_{1,t,i}(s) \coloneqq \{\|\mathbf{w}_{t,i,s'} - \alpha\mathbf{B}_{t,i,s'-1}^\top\mathbf{B}_*\mathbf{w}_{*,i}\|_2 = c_1\alpha^{2.5}\tau L_{\max}^3\kappa_{\max}^2 E_0^{-1}\ \forall s' \in \{1,\dots,s\}\}$
2. $A_{2,t,i}(s) \coloneqq \{\|\mathbf{w}_{t,i,s'}\|_2 \leq c_2\sqrt{\alpha}L_{\max} \quad \forall s' \in \{1,\dots,s\}\}$
3. $A_{3,t,i}(s) \coloneqq \{\|\mathbf{I}_k - \alpha\mathbf{B}_{t,i,s'}^\top\mathbf{B}_{t,i,s'}\|_2 = c_3\alpha^2 L_{\max}^2\kappa_{\max}^2 E_0^{-1} \quad \forall s' \in \{1,\dots,s\}\}$
4. $A_{4,t,i}(s) \coloneqq \{\mathrm{dist}(\mathbf{B}_{t,i,s'}, \mathbf{B}_*) \leq c_4\,\mathrm{dist}(\mathbf{B}_t, \mathbf{B}_*) \quad \forall s' \in \{1,\dots,s\}\}$

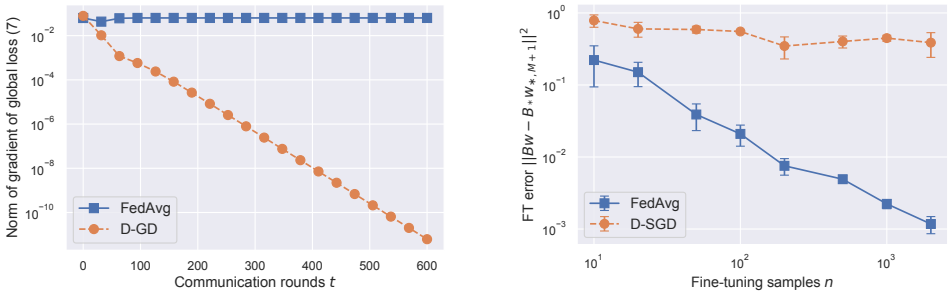

Figure 3: (Left) D-GD converges to a stationary point of the global objective (6), unlike FedAvg, yet (Right) FedAvg achieves smaller error after fine-tuning with various numbers of samples.

The local induction tracks the effect of updates at each client node: At the end of τ local updates, $A_{1,t,i}(\tau)$ captures the diversity of the local heads, $A_{2,t,i}(\tau)$ ensures that the heads remain uniformly bounded, $A_{3,t,i}(\tau)$ shows that the locally adapted representations stay close to a scaled orthonormal matrix, and $A_{4,t,i}(\tau)$ shows that the locally adapted representations do not diverge too quickly from the ground-truth. The second set of inductions below controls the global behavior.

Global induction. The global induction utilizes a similar set of inductive hypotheses.

1. $A_1(t) := \{\|\mathbf{w}_{t'} - \alpha(\mathbf{I}_k + \mathbf{\Delta}_{t'})\mathbf{B}_{t'}^\top \mathbf{B}_* \bar{\mathbf{w}}_{*,t'}\|_2 = c_1' \alpha^{2.5} \tau L_{\max}^3 \quad \forall t' \in \{1, \dots, t\}\}$
2. $A_2(t) := \{\|\mathbf{w}_{t'}\|_2 \le c_2' \sqrt{\alpha} L_{\max} \quad \forall t' \in \{1, \dots, t\}\}$
3. $A_3(t) := \{\|\mathbf{\Delta}_{t'}\|_2 = c_3' \alpha^2 \tau L_{\max}^2 \kappa_{\max}^2 E_0^{-1} \quad \forall t' \in \{1, \dots, t\}\}$
4. $A_4(t) := \{\|\mathbf{B}_{*,\perp}^\top \mathbf{B}_{t'}\|_2 \le (1 - c_4' \alpha^2 \tau \mu^2 E_0) \|\mathbf{B}_{*,\perp}^\top \mathbf{B}_{t'-1}\|_2 \quad \forall t' \in \{1, \dots, t\}\}$
5. $A_5(t) := \{\mathrm{dist}(\mathbf{B}_t, \mathbf{B}_*) \le (1 - c_5' \alpha^2 \tau \mu^2 E_0)^{t-1} \quad \forall t' \in \{1, \dots, t\}\}$

Hypotheses $A_1(t)$, $A_2(t)$ and $A_3(t)$ are analogous to $A_{1,t,i}(s)$, $A_{2,t,i}(s)$ and $A_{3,t,i}(s)$, respectively. $A_4(t)$ shows that the energy of $\mathrm{col}(\mathbf{B}_t)$ that is orthogonal to the ground-truth subspace is contracting, and $A_5(t)$ finally shows that the principal angle distance between the learned and ground-truth representations is exponentially decreasing. Our main claim follows from $A_5(T)$. However, proving this result requires showing that all the above local and global hypotheses hold for all times $t \ge 1$, as these hypotheses are heavily coupled. As mentioned previously, the most difficult challenge is controlling $\|\mathbf{\Delta}_t\|$ ($A_3(t)$) despite many local updates, and doing so requires leveraging both local and global properties. The details of this local-global induction argument are in Appendix B.

5 Experiments

In this section, we conduct experiments to (I) verify our theoretical results in the linear setting and (II) determine whether our established insights generalize to deep neural networks. Notably, demonstrating the competitive performance of FedAvg plus fine-tuning for personalized FL is *not* a goal of this section, as this is evident from prior experiments [10–12, 33]. Rather, to achieve (II) we test whether FedAvg learns effective representations when trained with neural networks in heterogeneous data settings via three popular benchmarks for evaluating the quality of learned representations. Since our main claim is that local updates are key to representation learning, we use D-(S)GD as our baseline in all experiments.

5.1 Multi-task linear regression

We first experiment with the regression setting from our theory. We randomly generate $\mathbf{B}_* \in \mathbb{R}^{d \times k}$ and $\{\mathbf{w}_{*,i}\}_{i \in [M]}$ by sampling each element i.i.d. from the normal distribution, where $d = 100$, $k = 5$ and $M = 40$, and then orthogonalizing $\mathbf{B}_*$. Then we run FedAvg with $\tau = 2$ local updates and D-GD, both sampling $m = M$ clients per round. We have seen in Figure 1 that the principal angle distance between the representation learned by FedAvg and the ground-truth representation linearly converges to zero, whereas D-GD does not learn the ground-truth representation. Conversely, Figure 3 (left) tracks the gradient of the global loss (6) and shows that D-GD linearly converges to stationary point of (6), while FedAvg does not converge to one at all. Although D-GD optimizes

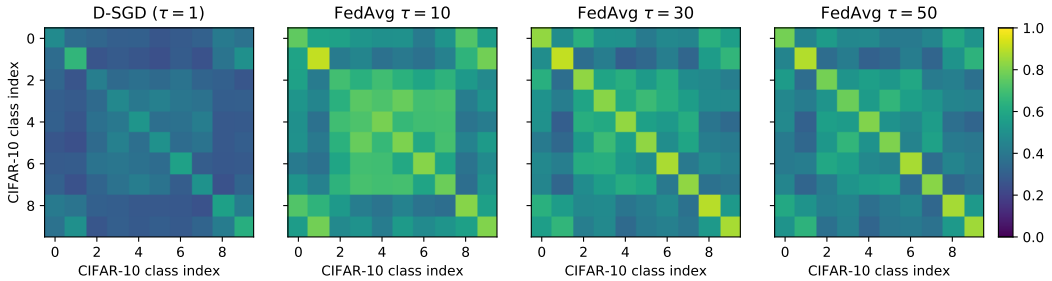

Figure 4: Average cosine similarity for features learned by D-SGD and FedAvg with varying numbers of local updates on a heterogeneous partition of CIFAR-10.

the global loss, it does not generalize as well as FedAvg to new clients as demonstrated by Figure 3 (right). Here, we fine-tune the models learned by FedAvg and D-GD on a new client with n samples generated by $\mathbf{x}_{M+1} \sim \mathcal{N}(\mathbf{0}, \mathbf{I}_d)$, $\zeta_{M+1} \sim \mathcal{N}(0, 0.01)$, and $y_{M+1} = \langle \mathbf{B}_* \mathbf{w}_{*,M+1}, \mathbf{x}_{M+1} \rangle + \zeta_{M+1}$. We fine-tune using GD for $\tau' = 200$ iterations with batch size $b = n$, and plot the final error $\|\mathbf{B}_{T,M+1,\tau'} \mathbf{w}_{T,M+1,\tau'} - \mathbf{B}_* \mathbf{w}_{*,M+1}\|^2$. Both plots are generated by averaging 10 runs.

5.2 Image classification with neural networks

Next we evaluate FedAvg's representation learning ability on nonlinear neural networks. For fair comparison, in every experiment all methods make the same total amount of local updates during the course of training (e.g. D-SGD is trained for $50\times$ more rounds than FedAvg with $\tau = 50$).

Datasets and models. We use the image classification datasets CIFAR-10 and CIFAR-100 [57], which consist of 10 and 100 classes of RGB images, respectively. We use a convolutional neural network (CNN) with three convolutional blocks followed by a three-layer multi-layer perceptron, with each convolutional block consisting of two convolutional layers and a max pooling layer.

Cosine similarity of features. A desirable property of representations for downstream classification tasks is that features of examples from the same class are similar to each other, while features of examples from different classes are dissimilar [58]. In Figure 4 we examine whether the representations learned by FedAvg satisfy this property. Here we have trained FedAvg with varying τ and D-SGD (FedAvg with $\tau = 1$) on CIFAR-10. Image classes are heterogeneously allocated to $M = 100$ clients according to the Dirichlet distribution with parameter 0.6 as in [59]. Each subplot is a 10x10 matrix whose (i, j)-th element gives the average cosine similarity between features of images from the i-th and j-th classes learned by the corresponding model. Ideally, diagonal elements are close to 1 (high similarity) and off-diagonal elements are close to 0 (low similarity). Figure 4 shows that FedAvg indeed learns features with high intra-class similarity and low inter-class similarity, with representation quality improving with more local updates between communications. Meanwhile, D-SGD does not learn such features. The leftmost subplot shows that all of the features learned by D-SGD are dissimilar, regardless of whether two images belong to the same class.

Fine-tuning performance. We evaluate the generalization ability of the representations learned by FedAvg to new classes and also new datasets. An effective representation identifies universally important features, so it should generalize to new data, with perhaps a small amount of fine-tuning needed to learn a new mapping from feature space to label space. The transfer learning performance of fine-tuned models is a popular metric for evaluating the quality of learned representations [60, 61]. We first study how models trained by FedAvg and D-SGD generalize to unseen classes from the same dataset. To do so, we train models on heterogeneous partitions of CIFAR-100 using both FedAvg with $\tau = 50$ as well as D-SGD. In the left plot of Figure 5, we illustrate the case that models are trained on 80 clients each with 500 total images from C classes sub-selected from 80 classes of CIFAR-100, and tested on new clients with images from the remaining 20 classes of CIFAR-100. We fine-tune the trained models on the new clients with 10 epochs of SGD, with varying numbers of samples per epoch as listed on the x-axis, before testing. Next, we investigate how well models trained by FedAvg and D-SGD generalize to an unseen dataset. In the right plot of Figure 5, we train models with C classes/client from CIFAR-100, then test on new clients with samples drawn from CIFAR-10 (a different dataset, but with presumably similar "basic" features). Specifically, for these new clients, we fine-tune for 10 epochs as previously, then test the post-fine-tuned models on the test

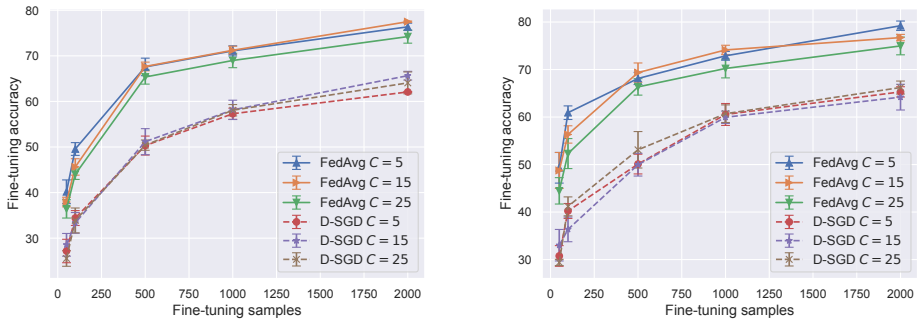

Figure 5: Average fine-tuning accuracies on new clients for models trained by FedAvg and D-SGD. (Left) Models trained on 80 classes from CIFAR-100 (with C classes/client) and fine-tuned on new clients from 20 new classes from CIFAR-100. (Right) Models trained on CIFAR-100 with C classes/client and fine-tuned on new clients from CIFAR-10 (10 classes/client). For FedAvg, $\tau = 50$ in all cases, and error bars give standard deviations over five trials with five new clients tested per trial.

data for each client. In both left and right plots, we observe that FedAvg significantly outperforms D-SGD, indicating that FedAvg has learned a representation that generalizes better to new classes.

6 Conclusion

We showed that FedAvg learns the ground-truth representation in the multi-task linear regression setting. To our knowledge, this is the first theoretical study showing FedAvg learns an effective representation in any setting. Our analysis reveals that multiple local updates are critical to FedAvg's representation learning ability, which is supported empirically on both linear and nonlinear models. These experimental results suggest future work can extend our findings to more complex settings.

Acknowledgements

This research is supported in part by NSF Grants 2127697, 2019844, 2107037, and 2112471, ARO Grant W911NF2110226, ONR Grant N00014-19-1-2566, the Machine Learning Lab (MLL) at UT Austin, and the Wireless Networking and Communications Group (WNCG) Industrial Affiliates Program.

References

[1] B. McMahan, E. Moore, D. Ramage, S. Hampson, and B. A. y Arcas, "Communication-efficient learning of deep networks from decentralized data," in *Artificial Intelligence and Statistics*, pp. 1273–1282, PMLR, 2017.

[2] S. U. Stich, "Local sgd converges fast and communicates little," in *International Conference on Learning Representations*, 2018.

[3] S. U. Stich and S. P. Karimireddy, "The error-feedback framework: Better rates for sgd with delayed gradients and compressed communication," *arXiv preprint arXiv:1909.05350*, 2019.

[4] J. Wang and G. Joshi, "Cooperative sgd: A unified framework for the design and analysis of communication-efficient sgd algorithms," in *ICML Workshop on Coding Theory for Machine Learning*, 2019.

[5] S. P. Karimireddy, S. Kale, M. Mohri, S. Reddi, S. Stich, and A. T. Suresh, "Scaffold: Stochastic controlled averaging for federated learning," in *International Conference on Machine Learning*, pp. 5132–5143, PMLR, 2020.

[6] G. Malinovskiy, D. Kovalev, E. Gasanov, L. Condat, and P. Richtarik, "From local sgd to local fixed-point methods for federated learning," in *International Conference on Machine Learning*, pp. 6692–6701, PMLR, 2020.

[7] R. Pathak and M. J. Wainwright, "Fedsplit: An algorithmic framework for fast federated optimization," *Advances in Neural Information Processing Systems*, vol. 33, pp. 7057–7066, 2020.

[8] Z. Charles and J. Konečnỳ, "Convergence and accuracy trade-offs in federated learning and meta-learning," in *International Conference on Artificial Intelligence and Statistics*, pp. 2575–2583, PMLR, 2021.

[9] J. Wang, Q. Liu, H. Liang, G. Joshi, and H. V. Poor, "Tackling the objective inconsistency problem in heterogeneous federated optimization," *arXiv preprint arXiv:2007.07481*, 2020.

[10] T. Yu, E. Bagdasaryan, and V. Shmatikov, "Salvaging federated learning by local adaptation," *arXiv preprint arXiv:2002.04758*, 2020.

[11] L. Collins, H. Hassani, A. Mokhtari, and S. Shakkottai, "Exploiting shared representations for personalized federated learning," in *International Conference on Machine Learning*, pp. 2089–2099, PMLR, 2021.

[12] T. Li, S. Hu, A. Beirami, and V. Smith, "Ditto: Fair and robust federated learning through personalization," *arXiv: 2012.04221*, 2020.

[13] S. Kornblith, M. Norouzi, H. Lee, and G. Hinton, "Similarity of neural network representations revisited," in *International Conference on Machine Learning*, pp. 3519–3529, PMLR, 2019.

[14] A. Khaled, K. Mishchenko, and P. Richtárik, "Tighter theory for local sgd on identical and heterogeneous data," in *International Conference on Artificial Intelligence and Statistics*, pp. 4519–4529, PMLR, 2020.

[15] A. Koloskova, N. Loizou, S. Boreiri, M. Jaggi, and S. Stich, "A unified theory of decentralized sgd with changing topology and local updates," in *International Conference on Machine Learning*, pp. 5381–5393, PMLR, 2020.

[16] X. Li, K. Huang, W. Yang, S. Wang, and Z. Zhang, "On the convergence of fedavg on non-iid data," in *International Conference on Learning Representations*, 2019.

[17] Z. Qu, K. Lin, J. Kalagnanam, Z. Li, J. Zhou, and Z. Zhou, "Federated learning's blessing: Fedavg has linear speedup," *arXiv preprint arXiv:2007.05690*, 2020.

[18] B. E. Woodworth, K. K. Patel, and N. Srebro, "Minibatch vs local sgd for heterogeneous distributed learning," *Advances in Neural Information Processing Systems*, vol. 33, pp. 6281–6292, 2020.

[19] A. Mitra, R. Jaafar, G. J. Pappas, and H. Hassani, "Linear convergence in federated learning: Tackling client heterogeneity and sparse gradients," *Advances in Neural Information Processing Systems*, vol. 34, pp. 14606–14619, 2021.

[20] K. Wang, R. Mathews, C. Kiddon, H. Eichner, F. Beaufays, and D. Ramage, "Federated evaluation of on-device personalization," *arXiv preprint arXiv:1910.10252*, 2019.

[21] F. Haddadpour, M. M. Kamani, A. Mokhtari, and M. Mahdavi, "Federated learning with compression: Unified analysis and sharp guarantees," in *International Conference on Artificial Intelligence and Statistics*, pp. 2350–2358, PMLR, 2021.

[22] X. Liang, S. Shen, J. Liu, Z. Pan, E. Chen, and Y. Cheng, "Variance reduced local sgd with lower communication complexity," *arXiv preprint arXiv:1912.12844*, 2019.

[23] T. Murata and T. Suzuki, "Bias-variance reduced local sgd for less heterogeneous federated learning," in *International Conference on Machine Learning*, pp. 7872–7881, PMLR, 2021.

[24] E. Gorbunov, F. Hanzely, and P. Richtárik, "Local sgd: Unified theory and new efficient methods," in *International Conference on Artificial Intelligence and Statistics*, pp. 3556–3564, PMLR, 2021.

[25] C. Xi and U. A. Khan, "Dextra: A fast algorithm for optimization over directed graphs," *IEEE Transactions on Automatic Control*, vol. 62, no. 10, pp. 4980–4993, 2017.

[26] T. Li, A. K. Sahu, M. Zaheer, M. Sanjabi, A. Talwalkar, and V. Smith, "Federated optimization in heterogeneous networks," *arXiv preprint arXiv:1812.06127*, 2018.

[27] F. Zhang, K. Kuang, Z. You, T. Shen, J. Xiao, Y. Zhang, C. Wu, Y. Zhuang, and X. Li, "Federated unsupervised representation learning," *arXiv preprint arXiv:2010.08982*, 2020.

[28] C. T Dinh, N. Tran, and J. Nguyen, "Personalized federated learning with moreau envelopes," *Advances in Neural Information Processing Systems*, vol. 33, pp. 21394–21405, 2020.

[29] M. Ribero and H. Vikalo, "Communication-efficient federated learning via optimal client sampling," *arXiv preprint arXiv:2007.15197*, 2020.

[30] W. Chen, S. Horvath, and P. Richtarik, "Optimal client sampling for federated learning," *arXiv preprint arXiv:2010.13723*, 2020.

[31] Y. J. Cho, J. Wang, and G. Joshi, "Client selection in federated learning: Convergence analysis and power-of-choice selection strategies," *arXiv preprint arXiv:2010.01243*, 2020.

[32] S. Chen, Q. Zheng, Q. Long, and W. J. Su, "A theorem of the alternative for personalized federated learning," *arXiv preprint arXiv:2103.01901*, 2021.

[33] G. Cheng, K. Chadha, and J. Duchi, "Fine-tuning is fine in federated learning," *arXiv preprint arXiv:2108.07313*, 2021.

[34] C. Finn, P. Abbeel, and S. Levine, "Model-agnostic meta-learning for fast adaptation of deep networks," in *Proceedings of the 34th International Conference on Machine Learning-Volume 70*, pp. 1126–1135, JMLR. org, 2017.

[35] A. Fallah, A. Mokhtari, and A. Ozdaglar, "Personalized federated learning: A meta-learning approach," 2020.

[36] L. Su, J. Xu, and P. Yang, "Achieving statistical optimality of federated learning: Beyond stationary points," *arXiv preprint arXiv:2106.15216*, 2021.

[37] A. Nichol and J. Schulman, "Reptile: a scalable metalearning algorithm," *arXiv preprint arXiv:1803.02999*, vol. 2, p. 2, 2018.

[38] B. Huang, X. Li, Z. Song, and X. Yang, "Fl-ntk: A neural tangent kernel-based framework for federated learning convergence analysis," *arXiv preprint arXiv:2105.05001*, 2021.

[39] A. Maurer, M. Pontil, and B. Romera-Paredes, "The benefit of multitask representation learning," *Journal of Machine Learning Research*, vol. 17, no. 81, pp. 1–32, 2016.

[40] S. S. Du, W. Hu, S. M. Kakade, J. D. Lee, and Q. Lei, "Few-shot learning via learning the representation, provably," in *International Conference on Learning Representations*, 2020.

[41] N. Tripuraneni, C. Jin, and M. Jordan, "Provable meta-learning of linear representations," in *International Conference on Machine Learning*, pp. 10434–10443, PMLR, 2021.

[42] W. Kong, R. Somani, S. Kakade, and S. Oh, "Robust meta-learning for mixed linear regression with small batches," *Advances in neural information processing systems*, vol. 33, pp. 4683–4696, 2020.

[43] K. K. Thekumparampil, P. Jain, P. Netrapalli, and S. Oh, "Statistically and computationally efficient linear meta-representation learning," *Advances in Neural Information Processing Systems*, vol. 34, 2021.

[44] L. Collins, A. Mokhtari, S. Oh, and S. Shakkottai, "Maml and anil provably learn representations," *arXiv preprint arXiv:2202.03483*, 2022.

[45] Y. Sun, A. Narang, I. Gulluk, S. Oymak, and M. Fazel, "Towards sample-efficient overparameterized meta-learning," *Advances in Neural Information Processing Systems*, vol. 34, 2021.

[46] P. Jain, J. Rush, A. Smith, S. Song, and A. G. Thakurta, "Differentially private model personalization," 2021.

[47] P. P. Liang, T. Liu, L. Ziyin, R. Salakhutdinov, and L.-P. Morency, "Think locally, act globally: Federated learning with local and global representations," *arXiv preprint arXiv:2001.01523*, 2020.

[48] M. G. Arivazhagan, V. Aggarwal, A. K. Singh, and S. Choudhary, "Federated learning with personalization layers," *arXiv preprint arXiv:1912.00818*, 2019.

[49] J. Oh, S. Kim, and S.-Y. Yun, "Fedbabu: Towards enhanced representation for federated image classification," *arXiv preprint arXiv:2106.06042*, 2021.

[50] S.-J. Hahn, M. Jeong, and J. Lee, "Subspace learning for personalized federated optimization," *arXiv preprint arXiv:2109.07628*, 2021.

[51] W. Zhuang, X. Gan, Y. Wen, S. Zhang, and S. Yi, "Collaborative unsupervised visual representation learning from decentralized data," in *Proceedings of the IEEE/CVF International Conference on Computer Vision*, pp. 4912–4921, 2021.

[52] L. Nguyen, P. H. Nguyen, M. Dijk, P. Richtárik, K. Scheinberg, and M. Takác, "Sgd and hogwild! convergence without the bounded gradients assumption," in *International Conference on Machine Learning*, pp. 3750–3758, PMLR, 2018.

[53] O. Shamir and N. Srebro, "Distributed stochastic optimization and learning," in *2014 52nd Annual Allerton Conference on Communication, Control, and Computing (Allerton)*, pp. 850–857, IEEE, 2014.

[54] R. M. Gower, N. Loizou, X. Qian, A. Sailanbayev, E. Shulgin, and P. Richtárik, "Sgd: General analysis and improved rates," in *International Conference on Machine Learning*, pp. 5200–5209, PMLR, 2019.

[55] K. K. Thekumparampil, P. Jain, P. Netrapalli, and S. Oh, "Sample efficient linear meta-learning by alternating minimization," *arXiv preprint arXiv:2105.08306*, 2021.

[56] K. Chua, Q. Lei, and J. D. Lee, "How fine-tuning allows for effective meta-learning," *Advances in Neural Information Processing Systems*, vol. 34, 2021.

[57] A. Krizhevsky, G. Hinton, *et al.*, "Learning multiple layers of features from tiny images," *Citeseer*, 2009.

[58] R. Hadsell, S. Chopra, and Y. LeCun, "Dimensionality reduction by learning an invariant mapping," in *2006 IEEE Computer Society Conference on Computer Vision and Pattern Recognition (CVPR'06)*, vol. 2, pp. 1735–1742, IEEE, 2006.

[59] D. A. E. Acar, Y. Zhao, R. Matas, M. Mattina, P. Whatmough, and V. Saligrama, "Federated learning based on dynamic regularization," in *International Conference on Learning Representations*, 2021.

[60] W. F. Whitney, M. J. Song, D. Brandfonbrener, J. Altosaar, and K. Cho, "Evaluating representations by the complexity of learning low-loss predictors," *arXiv preprint arXiv:2009.07368*, 2020.

[61] T. Chen, S. Kornblith, M. Norouzi, and G. Hinton, "A simple framework for contrastive learning of visual representations," in *International conference on machine learning*, pp. 1597–1607, PMLR, 2020.

[62] F. Haddadpour, M. M. Kamani, M. Mahdavi, and V. Cadambe, "Local sgd with periodic averaging: Tighter analysis and adaptive synchronization," *Advances in Neural Information Processing Systems*, vol. 32, 2019.

[63] H. Yu, S. Yang, and S. Zhu, "Parallel restarted sgd with faster convergence and less communication: Demystifying why model averaging works for deep learning," in *Proceedings of the AAAI Conference on Artificial Intelligence*, vol. 33, pp. 5693–5700, 2019.

[64] A. Spiridonoff, A. Olshevsky, and I. Paschalidis, "Communication-efficient sgd: From local sgd to one-shot averaging," *Advances in Neural Information Processing Systems*, vol. 34, 2021.

[65] B. Woodworth, K. K. Patel, S. Stich, Z. Dai, B. Bullins, B. Mcmahan, O. Shamir, and N. Srebro, "Is local sgd better than minibatch sgd?," in *International Conference on Machine Learning*, pp. 10334–10343, PMLR, 2020.

[66] F. Zhou and G. Cong, "On the convergence properties of a k-step averaging stochastic gradient descent algorithm for nonconvex optimization," *arXiv preprint arXiv:1708.01012*, 2017.

[67] Z. Charles and J. Konečnỳ, "On the outsized importance of learning rates in local update methods," *arXiv preprint arXiv:2007.00878*, 2020.

[68] J. Wang, Z. Xu, Z. Garrett, Z. Charles, L. Liu, and G. Joshi, "Local adaptivity in federated learning: Convergence and consistency," *arXiv preprint arXiv:2106.02305*, 2021.

[69] A. Nedić and A. Olshevsky, "Distributed optimization over time-varying directed graphs," *IEEE Transactions on Automatic Control*, vol. 60, no. 3, pp. 601–615, 2014.

[70] M. Assran, N. Loizou, N. Ballas, and M. Rabbat, "Stochastic gradient push for distributed deep learning," in *International Conference on Machine Learning*, pp. 344–353, PMLR, 2019.

[71] M. S. Assran and M. G. Rabbat, "Asynchronous gradient push," *IEEE Transactions on Automatic Control*, vol. 66, no. 1, pp. 168–183, 2020.

[72] Q. Li, B. He, and D. Song, "Model-contrastive federated learning," in *Proceedings of the IEEE/CVF Conference on Computer Vision and Pattern Recognition*, pp. 10713–10722, 2021.

[73] N. Tripuraneni, M. Jordan, and C. Jin, "On the theory of transfer learning: The importance of task diversity," *Advances in Neural Information Processing Systems*, vol. 33, pp. 7852–7862, 2020.

[74] Z. Xu and A. Tewari, "Representation learning beyond linear prediction functions," *Advances in Neural Information Processing Systems*, vol. 34, 2021.

[75] D. Gross and V. Nesme, "Note on sampling without replacing from a finite collection of matrices," *arXiv preprint arXiv:1001.2738*, 2010.

[76] A. Subramanian, "torch-cka." `https://github.com/AntixK/PyTorch-Model-Compare`, 2021.

Checklist

1. For all authors...
   (a) Do the main claims made in the abstract and introduction accurately reflect the paper's contributions and scope? [Yes]
   (b) Did you describe the limitations of your work? [Yes] Our theoretical results only hold for the multi-task linear setting. This point is explicitly mentioned in the abstract, Introduction (Section 1), and Main Results (Section 3).
   (c) Did you discuss any potential negative societal impacts of your work? [N/A]
   (d) Have you read the ethics review guidelines and ensured that your paper conforms to them? [Yes]
2. If you are including theoretical results...
   (a) Did you state the full set of assumptions of all theoretical results? [Yes] Please see the Main Results (Section 3).
   (b) Did you include complete proofs of all theoretical results? [Yes] Please see Appendix B.
3. If you ran experiments...

(a) Did you include the code, data, and instructions needed to reproduce the main experimental results (either in the supplemental material or as a URL)? [Yes] Please see Appendix C and the supplementary material.

(b) Did you specify all the training details (e.g., data splits, hyperparameters, how they were chosen)? [Yes] Please see Appendix C.

(c) Did you report error bars (e.g., with respect to the random seed after running experiments multiple times)? [Yes] Please see Figures 2, 3 and 5.

(d) Did you include the total amount of compute and the type of resources used (e.g., type of GPUs, internal cluster, or cloud provider)? [Yes] Please see Appendix C.

4. If you are using existing assets (e.g., code, data, models) or curating/releasing new assets...

   (a) If your work uses existing assets, did you cite the creators? [Yes]

   (b) Did you mention the license of the assets? [N/A]

   (c) Did you include any new assets either in the supplemental material or as a URL? [No]

   (d) Did you discuss whether and how consent was obtained from people whose data you're using/curating? [N/A]

   (e) Did you discuss whether the data you are using/curating contains personally identifiable information or offensive content? [N/A]

5. If you used crowdsourcing or conducted research with human subjects...

   (a) Did you include the full text of instructions given to participants and screenshots, if applicable? [N/A]

   (b) Did you describe any potential participant risks, with links to Institutional Review Board (IRB) approvals, if applicable? [N/A]

   (c) Did you include the estimated hourly wage paid to participants and the total amount spent on participant compensation? [N/A]

A Additional Related Work

In this section we provide further discussion of the related works.

Convergence of FedAvg. The convergence of FedAvg, also known as Local SGD, has been the subject of intense study in recent years due to the algorithm's effectiveness combined with the difficulties of analyzing it. In homogeneous data settings, local updates are easier to reconcile with solving the global objective, allowing much progress to be made in understanding convergence rates in this case [2–4, 62–66]. In the heterogeneous case multiple works have shown that FedAvg with fixed learning rate may *not* solve the global objective because the local updates induce a non-vanishing bias by drifting towards local solutions, even with full gradient steps and and strongly convex objectives [5–9, 16, 20, 67, 68]. As a remedy, several papers have analyzed FedAvg with learning rate that decays over communication rounds, and have shown that this approach indeed reaches a stationary point of the global objective, but at sublinear rates [5, 14–17] that can be strictly slower than the convergence rates of D-SGD [5, 18]. Sublinear convergence rates to stationary points of the global objective have also been shown for gossip algorithms that generalize FedAvg when operating on time-varying communication graphs [69–71], but these rates have exponential dependence on M and τ.

Another line of work has shown that in overparameterized settings with strongly convex losses, FedAvg achieves linear convergence to the global optimum [15, 17]. We consider more challenging nonconvex losses, and our setting is not overparameterized in the same sense (in these works overparameterized implies that the model class contains a single model that achieves zero loss for all clients). Lastly, like our work, [72] empirically observed that FedAvg learns strong representations, but relative to local-only training (i.e., without any communication), thus they did not study the role of local updates between communication rounds in learning representations, nor did they provide theoretical analysis.

Multi-task representation learning. Multiple works have studied the multi-task linear representation learning setting [39] in recent years. [41] and [42] give statistical rates for a method-of-moments estimator for learning the representation and [45] analyze a projection and eigen-weighting based algorithm designed for the case in which ground-truth representation is unknown. Other works have studied alternating minimization procedures for learning $\mathrm{col}(\mathbf{B}_*)$ in the context of meta-learning [43], federated learning [11], and differentially private optimization [46]. However, these methods require a unique head for each client, which greatly simplifies the analysis since head diversity is guaranteed prior to local updates and is not applicable to some cross-device FL settings which cannot tolerate stateful clients. Outside of the multi-task linear regression setting, [73] and [74] have demonstrated the necessity of task diversity to learning generalizable representations from a learning theoretic perspective, and [40] considered the statistical rates of representation learning by solving an ERM with unique heads per task.

B Proof of Theorem Main Results

B.1 Proof of Theorem 1

In this section we provide the proof of Theorem 1. We make use of the notations in Table 1.

Table 1: Notations.

Notation	Definition
μ	$\lambda_{\min}^{0.5}\left(\frac{1}{M}\sum_{i=1}^{M}(\mathbf{w}_{*,i}-\bar{\mathbf{w}}_*)(\mathbf{w}_{*,i}-\bar{\mathbf{w}}_*)^\top\right)$
$L_{\max}$	$\max_{i\in[M]}\|\mathbf{w}_{*,i}\|_2$, note that $L_{\max}\coloneqq L\sqrt{k}$ where L is defined in Assumption 1
$\kappa_{\max}$	${}^{L_{\max}}/_{\mu}$, note that $\kappa_{\max}\coloneqq\kappa\sqrt{k}$ where κ is defined in Assumption 2
$\bar{\mathbf{w}}_*$	$\frac{1}{M}\sum_{i=1}^{M}\mathbf{w}_{*,i}$
$\bar{\mathbf{w}}_{*,t}$	$\frac{1}{m}\sum_{i\in\mathcal{I}_t}\mathbf{w}_{*,i}$
$\mathbf{B}_{t,i,s},\mathbf{w}_{t,i,s}$	the results of s local updates of the global model at round t by the i-th client
$\mathbf{B}_{t,i,0},\mathbf{w}_{t,i,0}$	$\mathbf{B}_t,\mathbf{w}_t$, respectively
$\mathbf{e}_{t,i,s}$	$\mathbf{B}_{t,i,s}\mathbf{w}_{t,i,s}-\mathbf{B}_*\mathbf{w}_{*,i}$, i.e. product error for s-th local update for task i, round t
$\mathbf{G}_{t,i,s}$	$(\mathbf{B}_{t,i,s+1}-\mathbf{B}_{t,i,s})/\alpha$, such that $\mathbf{B}_{t,i,s+1}=\mathbf{B}_{t,i,s}-\alpha\mathbf{G}_{t,i,s}$
$\mathbf{G}_t$	$(\mathbf{B}_{t+1}-\mathbf{B}_t)/\alpha$, such that $\mathbf{B}_{t+1}=\mathbf{B}_t-\alpha\mathbf{G}_t$
$\mathbf{\Delta}_t$	$\mathbf{I}_k-\alpha\mathbf{B}_t^\top\mathbf{B}_t$
$\bar{\mathbf{\Delta}}_t$	$\mathbf{I}_d-\alpha\mathbf{B}_t\mathbf{B}_t^\top$
dist_t	$\mathrm{dist}(\mathbf{B}_t,\mathbf{B}_*)$
δ_0	dist_0
E_0	$1-\mathrm{dist}_0^2$
$\mathrm{col}(\mathbf{B}),\mathrm{col}(\mathbf{B})^\perp$	column space of $\mathbf{B}$, orthogonal complement to column space of $\mathbf{B}$, respectively

Here the local updates are given by

$$\begin{aligned}\mathbf{B}_{t,i,s+1}&=\mathbf{B}_{t,i,s}-\alpha(\mathbf{B}_{t,i,s}\mathbf{w}_{t,i,s}-\mathbf{B}_*\mathbf{w}_{*,i})\mathbf{w}_{t,i,s}^\top\\ \mathbf{w}_{t,i,s+1}&=\mathbf{w}_{t,i,s}-\alpha\mathbf{B}_{t,i,s}^\top(\mathbf{B}_{t,i,s}\mathbf{w}_{t,i,s}-\mathbf{B}_*\mathbf{w}_{*,i})\\ &=\mathbf{\Delta}_{t,i,s}\mathbf{w}_{t,i,s}+\alpha\mathbf{B}_{t,i,s}^\top\mathbf{B}_*\mathbf{w}_{*,i}\end{aligned}$$

and the global updates are given by

$$\begin{aligned}\mathbf{B}_{t+1}&=\tfrac{1}{m}\sum_{i\in\mathcal{I}_t}\mathbf{B}_{t,i,\tau}\\ \mathbf{w}_{t+1}&=\tfrac{1}{m}\sum_{i\in\mathcal{I}_t}\mathbf{w}_{t,i,\tau}.\end{aligned}$$

First we control the ground-truth heads sampled on each round.

Lemma 1. *Suppose* $m\geq\min(M,20(({}^{\gamma}/_{L})^2+({}^{H}/_{L})^4)(\alpha L\sqrt{k})^{-4}\log(kT))$. *Then the event*

$$\begin{aligned}A_0\coloneqq\Bigg\{&\left\|\frac{1}{m}\sum_{i\in\mathcal{I}_t}\mathbf{w}_{*,i}-\bar{\mathbf{w}}_*\right\|\leq 4\alpha^2L_{\max}^3,\\ &\left\|\frac{1}{m}\sum_{i\in\mathcal{I}_t}\mathbf{w}_{*,i}\mathbf{w}_{*,i}^\top-\frac{1}{M}\sum_{i'=1}^{M}\mathbf{w}_{*,i'}\mathbf{w}_{*,i'}^\top\right\|\leq 4\alpha^2L_{\max}^4\quad\forall t\in[T]\Bigg\}\end{aligned}$$

occurs with probability at least $1-4(kT)^{-99}$, *where* $L_{\max}\coloneqq L\sqrt{k}$.

Proof. If $m=M$ then A_0 holds almost surely. Otherwise, first let $\mathbf{W}_{*,i}\coloneqq\mathrm{diag}(\mathbf{w}_{*,i})\in\mathbf{R}^{k\times k}$, and let $\bar{\mathbf{W}}_*\coloneqq\frac{1}{M}\sum_{i=1}^{M}\mathrm{diag}(\mathbf{w}_{*,i})$. For any $t\in[T]$, $\{\mathbf{W}_{*,i}\}_{i\in\mathcal{I}_t}$ is a set of Hermitian matrices sampled uniformly without replacement from $\{\mathbf{W}_{*,i}\}_{i\in[M]}$, $\|\mathbf{W}_{*,i}\|\leq L\sqrt{k}$ almost surely, and

$\left\|\frac{1}{M}\sum_{i=1}^{M}(\mathbf{W}_{*,i}-\bar{\mathbf{W}}_*)^2\right\| \leq \frac{1}{M}\sum_{i=1}^{M}\|\mathbf{w}_{*,i}-\bar{\mathbf{w}}_*\|^2 = \gamma^2 k$ by the triangle and Cauchy-Schwarz inequalities and Definition 1. Thus, we can apply Theorem 1 in [75] to obtain

$$\mathbb{P}\left(\left\|\sum_{i\in\mathcal{I}_t}\mathbf{W}_{*,i}-\bar{\mathbf{W}}_*\right\| > t\right) \leq 2k\exp(\tfrac{-t^2}{4m\gamma^2 k}) \tag{7}$$

as long as $t \leq 2m\gamma^2\sqrt{k}/L$. Choose $t = 4m\alpha^2 L^3 k^{1.5}$. Note that indeed $t \leq 2m\gamma^2\sqrt{k}$ since $\gamma^2 = \frac{1}{k}\sum_{l=1}^{k}\frac{1}{M}\sum_{i=1}^{M}\mathbf{u}_l^\top(\mathbf{w}_{*,i}-\bar{\mathbf{w}}_*)(\mathbf{w}_{*,i}-\bar{\mathbf{w}}_*)^\top\mathbf{u}_l \geq \mu^2$, where $\mathbf{u}_l$ is the l-th standard basis vector, and $\alpha \leq \mu^2/(2L^4k^2)$. Thus we obtain

$$\mathbb{P}\left(\left\|\sum_{i\in\mathcal{I}_t}\mathbf{W}_{*,i}-\bar{\mathbf{W}}_*\right\| > 4m\alpha^2L^3k^{1.5}\right) \leq 2k\exp\left(\tfrac{-4m\alpha^4L^6k^2}{\gamma^2}\right)$$

$$\implies \mathbb{P}\left(\left\|\frac{1}{m}\sum_{i\in\mathcal{I}_t}\mathbf{W}_{*,i}-\bar{\mathbf{W}}_*\right\| > 4\alpha^2L^3k^{1.5}\right) \leq 2k\exp\left(-100\log(kT)\right)$$

since $m \geq 20(\frac{\gamma^2}{L^2})(\alpha^4L^4k^2)^{-1}\log(kT)$. An analogous argument, without needing to lift the matrices to higher dimensions, yields

$$\mathbb{P}\left(\left\|\frac{1}{m}\sum_{i\in\mathcal{I}_t}\left(\mathbf{w}_{*,i}\mathbf{w}_{*,i}^\top - \frac{1}{M}\sum_{i'=1}^{M}\mathbf{w}_{*,i'}\mathbf{w}_{*,i'}^\top\right)\right\| > 4\alpha^2L^4k^2\right) \leq 2k\exp\left(-100\log(kT)\right)$$

Union bounding, we obtain that $\left\|\frac{1}{m}\sum_{i\in\mathcal{I}_t}\mathbf{W}_{*,i}-\bar{\mathbf{W}}_*\right\| \leq 4\alpha^2L^3k^{1.5}$ and $\left\|\frac{1}{m}\sum_{i\in\mathcal{I}_t}\left(\mathbf{w}_{*,i}\mathbf{w}_{*,i}^\top - \frac{1}{M}\sum_{i'=1}^{M}\mathbf{w}_{*,i'}\mathbf{w}_{*,i'}^\top\right)\right\| \leq 4\alpha^2L^4k^2$ with probability at least $1-4k\exp(-100\log(kT)) = 1-4k^{-99}T^{-100}$. Union bounding over all $t\in[T]$ completes the proof. □

Next we state and prove the version of Theorem 1 with explicit constants. Note that the constants are not optimized.

Theorem 2 (FedAvg Representation Learning)**.** *Consider the case that each client takes gradient steps with respect to their population loss $f_i(\mathbf{B},\mathbf{w}) := \frac{1}{2}\|\mathbf{B}\mathbf{w}-\mathbf{B}_*\mathbf{w}_{*,i}\|^2$ and all losses are weighted equally in the global objective. Suppose Assumptions 1 and 2 hold, the number of clients participating each round satisfies $m \geq \min(M, 20((\gamma/L)^2+(H/L)^4)(\alpha L\sqrt{k})^{-4}\log(kT))$, and the initial parameters satisfy (i) $\delta_0 := \mathrm{dist}(\mathbf{B}_0,\mathbf{B}_*) \leq \sqrt{1-E_0}$ for any $E_0\in(0,1]$, (ii) $\|\mathbf{I}-\alpha\mathbf{B}_0^\top\mathbf{B}_0\|_2 \leq \alpha^2\tau L^2\kappa^2k^2$ and (iii) $\|\mathbf{w}_0\|_2 \leq \alpha^{2.5}\tau L^3k^{1.5}$. Choose step size $\alpha \leq \frac{1-\delta_0}{4800\sqrt{\tau}L\kappa^2k^{1.5}}$. Then for any $\epsilon\in(0,1)$, the distance of the representation learned by FedAvg with $\tau\geq 2$ local updates satisfies $\mathrm{dist}(\mathbf{B}_T,\mathbf{B}_*) < \epsilon$ after at most*

$$T \leq \frac{25}{\alpha^2\tau\mu^2E_0}\log(1/\epsilon)$$

communication rounds with probability at least $1-4(kT)^{-99}$.

Proof. In this proof we use the notation $L_{\max} := L\sqrt{k}$ and $\kappa_{\max} := \kappa\sqrt{k}$. First we condition on the event A_0, which occurs with probability at least $1-4(kT)^{-99}$ by Lemma 1. Conditioned on this event, we will show that that the following two sets of inductive hypotheses hold for all $s\in[\tau]$, $i\in\mathcal{I}_t$, and $t\in[T]$. The first set of inductive hypotheses controls local behavior. We apply the below local induction in parallel for each client $i\in[M]$ at every communication round $t\geq 0$, starting from the base case $s=1$.

1. $A_{1,t,i}(s) := \{\|\mathbf{w}_{t,i,s'} - \alpha\mathbf{B}_{t,i,s'-1}^\top\mathbf{B}_*\mathbf{w}_{*,i}\|_2 \leq 4c_3\alpha^{2.5}\tau L_{\max}^3\kappa_{\max}^2E_0^{-1} \quad \forall s' \in \{1,\dots,s\}\}$
2. $A_{2,t,i}(s) := \{\|\mathbf{w}_{t,i,s'}\|_2 \leq 2\alpha^{0.5}L_{\max} \quad \forall s'\in\{1,\dots,s\}\}$
3. $A_{3,t,i}(s) := \{\|\mathbf{\Delta}_{t,i,s'}\|_2 \leq 2c_3\alpha^2\tau L_{\max}^2\kappa_{\max}^2E_0^{-1} \quad \forall s'\in\{1,\dots,s\}\}$

4. $A_{4,t,i}(s) \coloneqq \{\text{dist}(\mathbf{B}_{t,i,s'}, \mathbf{B}_*) \leq 1.1\,\text{dist}(\mathbf{B}_t, \mathbf{B}_*) \quad \forall s' \in \{1, \ldots, s\}\}$

The second set of inductions controls the global behavior, starting from $t = 1$ as the base case:

1. $A_1(t) \coloneqq \{\|\mathbf{w}_{t'} - \alpha(\mathbf{I}_k + \mathbf{\Delta}_{t'})\mathbf{B}_{t'}^\top \mathbf{B}_* \bar{\mathbf{w}}_{*,t'}\|_2 \leq 91\alpha^{2.5}\tau L_{\max}^3 \quad \forall t' \in \{1, \ldots, t\}\}$
2. $A_2(t) \coloneqq \{\|\mathbf{w}_{t'}\|_2 \leq 2\alpha^{0.5} L_{\max} \quad \forall t' \in \{1, \ldots, t\}\}$
3. $A_3(t) \coloneqq \{\|\mathbf{\Delta}_{t'}\|_2 \leq c_3 \alpha^2 \tau L_{\max}^2 \kappa_{\max}^2 E_0^{-1} \quad \forall t' \in \{1, \ldots, t\}\}$
4. $A_4(t) \coloneqq \{\|\mathbf{B}_{*,\perp}^\top \mathbf{B}_{t'}\|_2 \leq (1 - 0.04\alpha^2\tau\mu^2 E_0)\|\mathbf{B}_{*,\perp}^\top \mathbf{B}_{t'-1}\|_2 \quad \forall t' \in \{1, \ldots, t\}\}$
5. $A_5(t) \coloneqq \{\text{dist}_t \leq (1 - 0.04\alpha^2\tau\mu^2 E_0)^{t-1} \quad \forall t' \in \{1, \ldots, t\}\}$

where $c_3 = 4800$. Without loss of generality let $\alpha \leq \frac{1-\delta_0}{c_3\sqrt{\tau}L_{\max}\kappa_{\max}^2}$. For ease of presentation we refer to c_3 symbolically rather than by its value throughout the proof.

The above inductions are applied in the following manner. First, the global initialization at $t = 0$ implies that the local inductive hypotheses hold after one local update (the base case). Then, by the local inductive argument, these conditions continue to hold for all subsequent local updates. This in turn implies that the global inductive hypotheses hold after the first global averaging step, i.e. $A_1(1), A_2(1)$ and $A_3(1)$ hold. Next, the global hypotheses holding at $t = 1$ implies that the local inductions hold in their base case at $t = 1$ (after one local update, i.e. $s = 1$), which implies they continue to hold for all subsequent local updates. Again, this implies the global hypotheses hold at $t = 2$, which implies the base case for the local inductions at $t = 2$, and so on. In summary, the ordering of the inductions is:

$$\begin{aligned}\text{Initialization at } t{=}0 \implies &\text{Local inductions at } t{=}0 \implies \text{Global inductions at } t{=}1 \\ &\implies \text{Local inductions at } t{=}1 \implies \ldots\end{aligned}$$

We start by showing that the base case $s = 1$ holds for the local inductions. The proof is identical for all $i \in [M]$ and $t \geq 0$.

- **If $t = 0$: initial conditions $\implies A_{1,t,i}(1)$, else $A_2(t) \cap A_3(t) \implies A_{1,t,i}(1)$.**

  Note that at initialization, $\|\mathbf{\Delta}_0\mathbf{w}_0\| \leq \|\mathbf{\Delta}_0\|\|\mathbf{w}_0\| \leq \alpha^{2.5}\tau L_{\max}^3\kappa_{\max}^2 \leq 4c_3\alpha^{2.5}\tau L_{\max}^3\kappa_{\max}^2 E_0^{-1}$. Likewise, at arbitrary t, $\|\mathbf{\Delta}_t\mathbf{w}_t\| \leq 4c_3\alpha^{2.5}\tau L_{\max}^3\kappa_{\max}^2 E_0^{-1}$ due to $A_2(t)$ and $A_3(t)$. Thus, since $\mathbf{w}_{t,i,1} = \mathbf{\Delta}_t\mathbf{w}_t + \alpha\mathbf{B}_t^\top\mathbf{B}_*\mathbf{w}_{*,i}$, we have

  $$\|\mathbf{w}_{t,i,1} - \alpha\mathbf{B}_t^\top\mathbf{B}_*\mathbf{w}_{*,i}\| = \|\mathbf{\Delta}_t\mathbf{w}_t\| \leq \|\mathbf{\Delta}_t\|\|\mathbf{w}_t\| \leq 4c_3\alpha^{2.5}\tau L_{\max}^3\kappa_{\max}^2 E_0^{-1}$$

  as desired (recall that $\mathbf{B}_{t,i,0} \equiv \mathbf{B}_t$).

- **If $t = 0$: initial conditions $\cap\ A_{1,t,i}(1) \implies A_{2,t,i}(1)$, else $A_3(t) \cap A_{1,t,i}(1) \implies A_{2,t,i}(1)$.**

  For any $t \geq 0$, we have $\|\mathbf{\Delta}_t\| \leq c_3\alpha^2\tau L_{\max}^2\kappa_{\max}^2 E_0^{-1}$ due to either the initialization ($t = 0$) or $A_3(t)$ ($t > 0$). This implies that $\|\mathbf{B}_t\| \leq \sqrt{\frac{1+c_3\alpha^2\tau L_{\max}^2\kappa_{\max}^2 E_0^{-1}}{\alpha}} \leq \frac{1.1}{\sqrt{\alpha}}$ since α is sufficiently small (noting that $\frac{(1-\delta)^2}{E_0} = \frac{(1-\delta)^2}{1-\delta^2} \leq 1$. Now we use $A_{1,t,i}(1)$ and the triangle inequality to obtain:

  $$\begin{aligned}\|\mathbf{w}_{t,i,1}\| &\leq \|\mathbf{w}_{t,i,1} - \alpha\mathbf{B}_t^\top\mathbf{B}_*\mathbf{w}_{*,i}\| + \|\alpha\mathbf{B}_t^\top\mathbf{B}_*\mathbf{w}_{*,i}\| \\ &\leq 4c_3\alpha^{2.5}\tau L_{\max}^3\kappa_{\max}^2 E_0^{-1} + \alpha\|\mathbf{B}_t\|\|\mathbf{w}_{*,i}\| \\ &\leq 2\sqrt{\alpha}L_{\max}.\end{aligned}$$

  as desired.

- **If $t = 0$: initial conditions $\implies A_{3,t,i}(1)$, else $A_2(t) \cap A_3(t) \implies A_{3,t,i}(1)$.**

We have

$$\begin{aligned}\mathbf{\Delta}_{t,i,1} &= \mathbf{I}_k - \alpha \mathbf{B}_{t,i,1}^\top \mathbf{B}_{t,i,1} \\ &= \mathbf{\Delta}_t + \alpha^2 \mathbf{B}_t^\top (\mathbf{B}_t \mathbf{w}_t - \mathbf{B}_* \mathbf{w}_{*,i}) \mathbf{w}_t^\top \\ &\quad + \alpha^2 \mathbf{B}_t^\top (\mathbf{B}_t \mathbf{w}_t - \mathbf{B}_* \mathbf{w}_{*,i}) \mathbf{w}_t^\top - \alpha^3 \mathbf{w}_t \mathbf{w}_t^\top \|\mathbf{B}_t \mathbf{w}_t - \mathbf{B}_* \mathbf{w}_{*,i}\|_2^2 \end{aligned} \tag{8}$$

By the initial conditions and by inductive hypotheses $A_1(t)$ and $A_2(t)$, for any $t \geq 0$ we have $\|\mathbf{w}_t\|_2 \leq 2\sqrt{\alpha} L_{\max}$, $\|\mathbf{\Delta}_t\| \leq c_3 \alpha^2 \tau L_{\max}^2 \kappa_{\max}^2 E_0^{-1}$, and $\|\mathbf{B}_t\|_2 \leq \frac{1.1}{\sqrt{\alpha}}$. This implies $\|\mathbf{B}_t \mathbf{w}_t - \mathbf{B}_* \mathbf{w}_{*,i}\|_2 \leq \|\mathbf{B}_t\| \|\mathbf{w}_t\| + \|\mathbf{B}_* \mathbf{w}_{*,i}\| \leq 3.2 L_{\max}$. Therefore using (8), we obtain

$$\begin{aligned}\|\mathbf{\Delta}_{t,i,1}\|_2 &\leq \|\mathbf{\Delta}_t\|_2 + 2\alpha^2 \|\mathbf{B}_t^\top (\mathbf{B}_t \mathbf{w}_t - \mathbf{B}_* \mathbf{w}_{*,i}) \mathbf{w}_t^\top\|_2 + \alpha^3 \|\mathbf{w}_t\|_2^2 \|\mathbf{B}_t \mathbf{w}_t - \mathbf{B}_* \mathbf{w}_{*,i}\|_2^2 \\ &\leq \|\mathbf{\Delta}_t\|_2 + 15\alpha^2 L_{\max}^2 + 41\alpha^4 L_{\max}^4 \\ &\leq 2c_3 \alpha^2 \tau L_{\max}^2 \kappa_{\max}^2 E_0^{-1} \end{aligned} \tag{9}$$

as desired.

- **If $t = 0$: initial conditions $\implies A_{4,t,i}(1)$, else $A_{3,t,i}(1) \cap A_2(t) \cap A_3(t) \implies A_{4,t,i}(1)$.**

  Note that

  $$\|\mathbf{B}_{*,\perp}^\top \mathbf{B}_{t,i,1}\|_2 = \|\mathbf{B}_{*,\perp}^\top \mathbf{B}_t (\mathbf{I}_k - \alpha \mathbf{w}_t \mathbf{w}_t^\top)\|_2 \leq \|\mathbf{B}_{*,\perp}^\top \mathbf{B}_t\| \|\mathbf{I}_k - \alpha \mathbf{w}_t \mathbf{w}_t^\top\|_2 \leq \|\mathbf{B}_{*,\perp}^\top \mathbf{B}_t\|_2$$

  as $\alpha \|\mathbf{w}_t\|^2 \leq 1$ by either the initialization (if $t = 0$) or $A_2(t)$ (if $t \geq 1$) and the choice of α sufficiently small. Thus, letting $\hat{\mathbf{B}}_{t,i,1} \mathbf{R}_{t,i,1} = \mathbf{B}_{t,i,1}$ denote the QR-decomposition of $\mathbf{B}_{t,i,1}$, we have

  $$\begin{aligned}\operatorname{dist}(\mathbf{B}_{t,i,1}, \mathbf{B}_*) &= \|\mathbf{B}_{*,\perp}^\top \hat{\mathbf{B}}_{t,i,1}\|_2 \\ &\leq \tfrac{1}{\sigma_{\min}(\mathbf{B}_{t,i,1})} \|\mathbf{B}_{*,\perp}^\top \mathbf{B}_{t,i,1}\|_2 \\ &\leq \tfrac{1}{\sigma_{\min}(\mathbf{B}_{t,i,1})} \|\mathbf{B}_{*,\perp}^\top \mathbf{B}_t\|_2 \\ &\leq \tfrac{\|\mathbf{B}_t\|}{\sigma_{\min}(\mathbf{B}_{t,i,1})} \operatorname{dist}(\mathbf{B}_t, \mathbf{B}_*) \\ &\leq \sqrt{\tfrac{1 + c_3 \alpha^2 \tau L_{\max}^2 \kappa_{\max}^2 E_0^{-1}}{1 - 2c_3 \alpha^2 \tau L_{\max}^2 \kappa_{\max}^2 E_0^{-1}}} \operatorname{dist}_t \qquad (10) \\ &\leq 1.1 \operatorname{dist}(\mathbf{B}_t, \mathbf{B}_*) \qquad (11)\end{aligned}$$

  where the (10) follows by $A_{3,t,i}(1)$ and either the initial condition on $\|\mathbf{\Delta}_t\|$ (if $t = 0$) or $A_3(t)$ (if $t > 0$), and (11) follows as α is sufficiently small.

Now we show that the global inductions hold at global round $t = 1$ following the local updates at round $t = 0$.

- **Initialization $\cap \big(\cap_{i \in \mathcal{I}_0} A_{1,0,i}(\tau) \cap A_{2,0,i}(\tau) \cap A_{3,0,i}(\tau) \big) \implies A_1(1) \cap A_2(1) \cap A_4(1) \cap A_5(1)$.**

  To show each of these hypotheses hold we can apply the proofs of Lemmas 6, 7 9 and 11 respectively, since they only rely on inductive hypotheses $A_{1,0,i}(\tau)$, $A_{2,0,i}(\tau)$ and $A_{3,0,i}(\tau)$ and appropriate scaling of $\|\mathbf{B}_0\|$ and $\|\mathbf{w}_0\|$, which is guaranteed by the initialization. In particular, the proof of these inductive hypotheses is identical for all $t \geq 1$.

- **Initialization $\cap \big(\cap_{i \in \mathcal{I}_0} A_{2,0,i}(\tau) \cap A_{3,0,i}(\tau) \big) \implies A_2(1)$.**

  In the proof of $A_2(t)$ for $t \geq 2$ (Lemma 9) we leverage the fact that $\mathbf{w}_{t-1}$ is close to a matrix times the average of the $\bar{\mathbf{w}}_{*,t-1}$. Our initialization cannot guarantee that this holds for $\mathbf{w}_0$. Instead, we show that $\|\mathbf{\Delta}_1\|$ may increase from $\|\mathbf{\Delta}_0\|$ at a large rate that would cause $\|\mathbf{\Delta}_t\|$ to blow up if continued indefinitely, but since it only grows at this rate for the first round, this is ok. In particular, let $\mathbf{G}_0 = \frac{1}{\alpha}(\mathbf{B}_0 - \mathbf{B}_1)$ such that $\mathbf{B}_1 = \mathbf{B}_0 - \alpha \mathbf{G}_0$. Then

  $$\mathbf{\Delta}_1 = \mathbf{\Delta}_0 + \alpha^2 \mathbf{B}_0^\top \mathbf{G}_0 + \alpha^2 \mathbf{G}_0^\top \mathbf{B}_0 - \alpha^3 \mathbf{G}_0^\top \mathbf{G}_0$$

Moreover,

$$\|\mathbf{G}_0\| = \left\| \frac{1}{m} \sum_{i \in \mathcal{I}_0} \sum_{s=0}^{\tau-1} (\mathbf{B}_{0,i,s}\mathbf{w}_{0,i,s} - \mathbf{B}_*\mathbf{w}_{*,i})\mathbf{w}_{0,i,s}^\top \right\| \leq 7\sqrt{\alpha}\tau L_{\max}^2$$

by the initialization and $A_{2,0,i}(\tau)$ and $A_{3,0,i}(\tau)$, thus

$$\|\mathbf{B}_0^\top \mathbf{G}_0\| \leq 8\tau L_{\max}^2, \qquad \|\mathbf{G}_0^\top \mathbf{G}_0\| \leq 49\alpha\tau^2 L_{\max}^4$$

which implies that $\|\mathbf{\Delta}_1\| \leq \|\mathbf{\Delta}_0\| + 10\alpha^2\tau L_{\max}^2 \leq c_3\alpha^2\tau L_{\max}^2\kappa_{\max}^2 E_0^{-1}$, as desired.

Assume that the inductive hypotheses hold up to time t and local round $s \geq 1$. We first show that the local inductive hypotheses hold for local round $s+1$. Then, we show that the global inductions hold at time $t+1$. This is achieved by the following lemmas.

Local inductions.

- $A_{2,t,i}(s) \cap A_{3,t,i}(s) \implies A_{1,t,i}(s+1)$. This is Lemma 2.
- $A_{1,t,i}(s+1) \cap A_{2,t,i}(s) \cap A_{3,t,i}(s) \implies A_{2,t,i}(s+1)$. This is Lemma 3.
- $A_{2,t,i}(s) \cap A_{3,t,i}(s) \implies A_{3,t,i}(s+1)$. This is Lemma 4.
- $A_{2,t,i}(s) \cap A_{3,t,i}(s+1) \cap A_3(t) \implies A_{4,t,i}(s+1)$. This is Lemma 5.

Global inductions.

- $\cap_{i \in \mathcal{I}_t} \big(A_{1,t,i}(\tau-1) \cap A_{3,t,i}(\tau-1)\big) \cap A_1(t) \cap A_2(t) \cap A_3(t) \implies A_1(t+1)$. This is Lemma 6.
- $\cap_{i \in \mathcal{I}_t} A_{2,t,i}(\tau) \implies A_2(t+1)$. This is Lemma 7.
- $\cap_{i \in \mathcal{I}_t} \big(\cap_{h=1}^4 A_{h,t,i}(\tau)\big) \cap A_1(t) \cap A_2(t) \cap A_3(t) \cap A_5(t) \implies A_3(t+1)$. This is Lemma 9.
- $\cap_{i \in \mathcal{I}_t} \big(A_{1,t,i}(\tau) \cap A_{2,t,i}(\tau) \cap A_{3,t,i}(\tau)\big) \cap A_2(t) \cap A_3(t) \implies A_4(t+1)$. This is Lemma 10.
- $A_3(t+1) \cap A_4(t+1) \cap A_5(t) \implies A_5(t+1)$. This is Lemma 11.

These inductions complete the proof. □

Lemma 2. $A_{2,t,i}(s) \cap A_{3,t,i}(s) \implies A_{1,t,i}(s+1)$.

Proof. Since $\mathbf{w}_{t,i,s+1} = \mathbf{\Delta}_{t,i,s}\mathbf{w}_{t,i,s} + \alpha\mathbf{B}_{t,i,s}^\top\mathbf{B}_*\mathbf{w}_{*,i}$, we have

$$\begin{aligned} \|\mathbf{w}_{t,i,s+1} - \alpha\mathbf{B}_{t,i,s}^\top\mathbf{B}_*\mathbf{w}_{*,i}\| &= \|\mathbf{\Delta}_{t,i,s}\mathbf{w}_{t,i,s}\|_2 \\ &\leq \|\mathbf{\Delta}_{t,i,s}\|\|\mathbf{w}_{t,i,s}\|_2 \\ &\leq 4c_3\alpha^{2.5}\tau L_{\max}^3\kappa_{\max}^2 \end{aligned} \tag{12}$$

where the last inequality follows by $A_{2,t,i}(s)$ and $A_{3,t,i}(s)$. □

Lemma 3. $A_{1,t,i}(s+1) \cap A_{3,t,i}(s) \implies A_{2,t,i}(s+1)$.

Proof. Note that by the triangle inequality,

$$\begin{aligned} \|\mathbf{w}_{t,i,s+1}\| &\leq \|\mathbf{w}_{t,i,s+1} - \alpha\mathbf{B}_{t,i,s}^\top\mathbf{B}_*\mathbf{w}_{*,i}\| + \|\alpha\mathbf{B}_{t,i,s}^\top\mathbf{B}_*\mathbf{w}_{*,i}\| \\ &\leq 4c_3\alpha^{2.5}\tau L_{\max}^3\kappa_{\max}^2 E_0^{-1} + \|\alpha\mathbf{B}_{t,i,s}^\top\mathbf{B}_*\mathbf{w}_{*,i}\| \qquad (13) \\ &\leq 4c_3\alpha^{2.5}\tau L_{\max}^3\kappa_{\max}^2 E_0^{-1} + 1.1\sqrt{\alpha}L_{\max} \qquad (14) \\ &\leq 2\sqrt{\alpha}L_{\max} \end{aligned}$$

where (13) follows by $A_{1,t,i}(s)$ and (14) follows by the fact that $\|\mathbf{B}_{t,i,s}\| \leq \frac{1.1}{\sqrt{\alpha}}$ by $A_{3,t,i}(s)$, and choice of $\alpha \leq (1-\delta_0)(c_3\sqrt{\tau}L_{\max}\kappa_{\max}^2)^{-1}$. □

Lemma 4. $A_{2,t,i}(s) \cap A_{3,t,i}(s) \implies A_{3,t,i}(s+1)$.

Proof. Let $\mathbf{e}_{t,i,s} \coloneqq \mathbf{B}_{t,i,s}\mathbf{w}_{t,i,s} - \mathbf{B}_*\mathbf{w}_{*,i}$ and $\mathbf{G}_{t,i,s} \coloneqq \mathbf{e}_{t,i,s}\mathbf{w}_{t,i,s}$. We have

$$\mathbf{\Delta}_{t,i,s+1} = \mathbf{\Delta}_{t,i,s} + \alpha^2\mathbf{B}_{t,i,s}^\top\mathbf{G}_{t,i,s} + \alpha^2\mathbf{G}_{t,i,s}^\top\mathbf{B}_{t,i,s} - \alpha^3\mathbf{G}_{t,i,s}^\top\mathbf{G}_{t,i,s}$$

We use $A_{2,t,i}(s)$ and $A_{3,t,i}(s)$ throughout the proof. Recall that $A_{3,t,i}(s)$ directly implies $\|\mathbf{B}_{t,i,s}\| \leq \frac{1.1}{\sqrt{\alpha}}$. This bound as well as the bound on $\|\mathbf{w}_{t,i,s}\|$ from $A_{2,t,i}(s)$ and the Cauchy Schwarz inequality implies $\|\mathbf{e}_{t,i,s}\| \leq 3.2L_{\max}$ and $\|\mathbf{G}_{t,i,s}\|_2 \leq 7\sqrt{\alpha}L_{\max}^2$, thus $\|\alpha^3\mathbf{G}_{t,i,s}^\top\mathbf{G}_{t,i,s}\| \leq 49\alpha^4L_{\max}^4$. Next,

$$\begin{aligned}
\mathbf{B}_{t,i,s}^\top\mathbf{G}_{t,i,s} &= \mathbf{B}_{t,i,s}^\top\mathbf{e}_{t,i,s}\mathbf{w}_{t,i,s}^\top \\
&= \alpha\mathbf{B}_{t,i,s}^\top\mathbf{e}_{t,i,s}\mathbf{w}_{*,i}^\top\mathbf{B}_*^\top\mathbf{B}_{t,i,s-1} + \mathbf{B}_{t,i,s}^\top\mathbf{e}_{t,i,s}\mathbf{w}_{t,i,s-1}^\top\mathbf{\Delta}_{t,i,s-1} \\
&= \alpha\mathbf{B}_{t,i,s}^\top\mathbf{e}_{t,i,s}\mathbf{w}_{*,i}^\top\mathbf{B}_*^\top\mathbf{B}_{t,i,s} + \alpha\mathbf{B}_{t,i,s}^\top\mathbf{e}_{t,i,s}\mathbf{w}_{*,i}^\top\mathbf{B}_*^\top(\mathbf{B}_{t,i,s-1} - \mathbf{B}_{t,i,s}) \\
&\quad + \mathbf{B}_{t,i,s}^\top\mathbf{e}_{t,i,s}\mathbf{w}_{t,i,s-1}^\top\mathbf{\Delta}_{t,i,s-1}
\end{aligned}$$

where, by the Cauchy-Schwarz inequality and $A_{2,t,i}(s)$ and $A_{3,t,i}(s)$

$$\begin{aligned}
\|\alpha\mathbf{B}_{t,i,s}^\top\mathbf{e}_{t,i,s}\mathbf{w}_{*,i}^\top\mathbf{B}_*^\top(\mathbf{B}_{t,i,s-1} - \mathbf{B}_{t,i,s})\| &= \alpha^2\|\mathbf{B}_{t,i,s}^\top\mathbf{e}_{t,i,s}\mathbf{w}_{*,i}^\top\mathbf{B}_*^\top\mathbf{e}_{t,i,s-1}\mathbf{w}_{t,i,s-1}^\top\| \leq 23\alpha^2L_{\max}^4, \\
\|\mathbf{B}_{t,i,s}^\top\mathbf{e}_{t,i,s}\mathbf{w}_{t,i,s-1}^\top\mathbf{\Delta}_{t,i,s-1}\| &\leq 15c_3\alpha^2\tau L_{\max}^4\kappa_{\max}^2E_0^{-1},
\end{aligned} \tag{15}$$

and

$$\begin{aligned}
&\|\alpha\mathbf{B}_{t,i,s}^\top\mathbf{e}_{t,i,s}\mathbf{w}_{*,i}^\top\mathbf{B}_*^\top\mathbf{B}_{t,i,s}\| \\
&\quad= \|\alpha^2\mathbf{B}_{t,i,s}^\top\mathbf{B}_{t,i,s}\mathbf{B}_{t,i,s-1}^\top\mathbf{B}_*\mathbf{w}_{*,i}\mathbf{w}_{*,i}^\top\mathbf{B}_*^\top\mathbf{B}_{t,i,s} - \alpha\mathbf{B}_{t,i,s}^\top\mathbf{B}_*\mathbf{w}_{*,i}\mathbf{w}_{*,i}^\top\mathbf{B}_*^\top\mathbf{B}_{t,i,s} \\
&\qquad + \alpha^2\mathbf{B}_{t,i,s}^\top\mathbf{B}_{t,i,s}\mathbf{\Delta}_{t,i,s-1}\mathbf{w}_{t,i,s-1}\mathbf{w}_{*,i}^\top\mathbf{B}_*^\top\mathbf{B}_{t,i,s}\| \\
&\quad= \|-\alpha\mathbf{\Delta}_{t,i,s}\mathbf{B}_{t,i,s}^\top\mathbf{B}_*\mathbf{w}_{*,i}\mathbf{w}_{*,i}^\top\mathbf{B}_*^\top\mathbf{B}_{t,i,s} \\
&\qquad + \alpha^2\mathbf{B}_{t,i,s}^\top\mathbf{B}_{t,i,s}(\mathbf{B}_{t,i,s-1} - \mathbf{B}_{t,i,s})^\top\mathbf{B}_*\mathbf{w}_{*,i}\mathbf{w}_{*,i}^\top\mathbf{B}_*^\top\mathbf{B}_{t,i,s} \\
&\qquad + \alpha^2\mathbf{B}_{t,i,s}^\top\mathbf{B}_{t,i,s}\mathbf{\Delta}_{t,i,s-1}\mathbf{w}_{t,i,s-1}\mathbf{w}_{*,i}^\top\mathbf{B}_*^\top\mathbf{B}_{t,i,s}\| \\
&\quad\leq \alpha\|\mathbf{\Delta}_{t,i,s}\mathbf{B}_{t,i,s}^\top\mathbf{B}_*\mathbf{w}_{*,i}\mathbf{w}_{*,i}^\top\mathbf{B}_*^\top\mathbf{B}_{t,i,s}\| \\
&\qquad + \alpha^2\|\mathbf{B}_{t,i,s}^\top\mathbf{B}_{t,i,s}\mathbf{w}_{t,i,s-1}\mathbf{e}_{t,i,s-1}^\top\mathbf{B}_*\mathbf{w}_{*,i}\mathbf{w}_{*,i}^\top\mathbf{B}_*^\top\mathbf{B}_{t,i,s}\| \\
&\qquad + \alpha^2\|\mathbf{B}_{t,i,s}^\top\mathbf{B}_{t,i,s}\mathbf{\Delta}_{t,i,s-1}\mathbf{w}_{t,i,s-1}\mathbf{w}_{*,i}^\top\mathbf{B}_*^\top\mathbf{B}_{t,i,s}\| \\
&\quad= 7c_3\alpha^2\tau L_{\max}^4\kappa_{\max}^2E_0^{-1} + 9\alpha^2L_{\max}^4.
\end{aligned} \tag{16}$$

Thus,

$$\begin{aligned}
\|\mathbf{\Delta}_{t,i,s+1}\|_2 &\leq \|\mathbf{\Delta}_{t,i,s}\|_2 + 2\alpha^2\|\mathbf{B}_{t,i,s}^\top\mathbf{G}_{t,i,s}\| + \alpha^3\|\mathbf{G}_{t,i,s}^\top\mathbf{G}_{t,i,s}\| \\
&\leq \|\mathbf{\Delta}_{t,i,s}\|_2 + 46c_3\alpha^4\tau L_{\max}^4\kappa_{\max}^2E_0^{-1} + 81\alpha^4L_{\max}^4 \\
&\vdots \\
&\leq \|\mathbf{\Delta}_t\|_2 + 46c_3\alpha^4\tau^2L_{\max}^4\kappa_{\max}^2E_0^{-1} + 81\alpha^4\tau L_{\max}^4 \\
&\leq c_3\alpha^2\tau L_{\max}^2\kappa_{\max}^2E_0^{-1} + 46c_3\alpha^4\tau^2L_{\max}^4\kappa_{\max}^2E_0^{-1} + 81\alpha^4\tau L_{\max}^4 \\
&\leq 2c_3\alpha^2\tau L_{\max}^2\kappa_{\max}^2E_0^{-1}
\end{aligned} \tag{17}$$

by choice of c_3 and α sufficiently small. □

Lemma 5. $A_{2,t,i}(s) \cap A_{3,t,i}(s+1) \cap A_3(t) \implies A_{4,t,i}(s+1)$.

Proof. Note that

$$\begin{aligned}
\|\mathbf{B}_{*,\perp}^\top\mathbf{B}_{t,i,s+1}\|_2 &= \|\mathbf{B}_{*,\perp}^\top\mathbf{B}_{t,i,s}(\mathbf{I}_k - \alpha\mathbf{w}_{t,i,s}\mathbf{w}_{t,i,s}^\top)\|_2 \\
&\leq \|\mathbf{B}_{*,\perp}^\top\mathbf{B}_{t,i,s}\|_2 \\
&\vdots \\
&\leq \|\mathbf{B}_{*,\perp}^\top\mathbf{B}_t\|_2
\end{aligned} \tag{18}$$

where the first inequality follows since $\|\mathbf{w}_{t,i,s}\| \leq 2\sqrt{\alpha}L_{\max}$ (by $A_{2,t,i}(s)$) and α is sufficiently small, and the last inequality follows by recursively applying the first inequality for all local iterations leading up to s. Thus

$$\mathrm{dist}_{t,i,s} \leq \frac{\|\mathbf{B}_t\|_2}{\sigma_{\min}(\mathbf{B}_{t,i,s})}\,\mathrm{dist}_t \leq \sqrt{\frac{1+c_3\alpha^2\tau L_{\max}^2\kappa_{\max}^2 E_0^{-1}}{1-2c_3\alpha^2\tau L_{\max}^2\kappa_{\max}^2 E_0^{-1}}}\,\mathrm{dist}_t \leq 2\,\mathrm{dist}_t\,.$$

□

Lemma 6. $\cap_{i\in\mathcal{I}_t}\big(A_{2,t,i}(\tau-1)\cap A_{3,t,i}(\tau-1)\big)\cap A_2(t)\cap A_3(t) \implies A_1(t+1)$.

Proof. Expanding $\mathbf{w}_{t+1}$ yields

$$\begin{aligned}
\mathbf{w}_{t+1} &= \tfrac{1}{m}\sum_{i\in\mathcal{I}_t}\mathbf{w}_{t,i,\tau} \\
&= \tfrac{1}{m}\sum_{i\in\mathcal{I}_t}\boldsymbol{\Delta}_{t,i,\tau-1}\mathbf{w}_{t,i,\tau-1} + \alpha\mathbf{B}_{t,i,\tau-1}^\top\mathbf{B}_*\mathbf{w}_{*,i} \\
&= \alpha\mathbf{B}_t^\top\mathbf{B}_*\bar{\mathbf{w}}_{*,t} + \tfrac{1}{m}\sum_{i\in\mathcal{I}_t}\boldsymbol{\Delta}_{t,i,\tau-1}\mathbf{w}_{t,i,\tau-1} + \alpha(\mathbf{B}_{t,i,\tau-1}-\mathbf{B}_t)^\top\mathbf{B}_*\mathbf{w}_{*,i} \\
&= \frac{1}{n}\sum_{i\in\mathcal{I}_t}\alpha(\mathbf{B}_{t,i,\tau-1}-\mathbf{B}_t)^\top\mathbf{B}_*\mathbf{w}_{*,i} + \alpha\boldsymbol{\Delta}_{t,i,\tau-1}\mathbf{B}_{t,i,\tau-2}^\top\mathbf{B}_*\mathbf{w}_{*,i} \\
&\qquad + \alpha\boldsymbol{\Delta}_{t,i,\tau-1}\boldsymbol{\Delta}_{t,i,\tau-2}\mathbf{w}_{t,i,\tau-2} + \alpha\mathbf{B}_t^\top\mathbf{B}_*\bar{\mathbf{w}}_{*,t} \\
&= \alpha\mathbf{B}_t^\top\mathbf{B}_*\bar{\mathbf{w}}_{*,t} + \alpha\boldsymbol{\Delta}_t\mathbf{B}_t^\top\mathbf{B}_*\bar{\mathbf{w}}_{*,t} \\
&\quad + \tfrac{1}{m}\sum_{i\in\mathcal{I}_t}\alpha(\mathbf{B}_{t,i,\tau-1}-\mathbf{B}_t)^\top\mathbf{B}_*\mathbf{w}_{*,i} + \alpha(\boldsymbol{\Delta}_{t,i,\tau-1}\mathbf{B}_{t,i,\tau-2}^\top - \boldsymbol{\Delta}_t\mathbf{B}_t^\top)\mathbf{B}_*\mathbf{w}_{*,i} \\
&\qquad + \boldsymbol{\Delta}_{t,i,\tau-1}\boldsymbol{\Delta}_{t,i,\tau-2}\mathbf{w}_{t,i,\tau-2} \\
&= \alpha\mathbf{B}_{t+1}^\top\mathbf{B}_*\bar{\mathbf{w}}_{*,t+1} + \alpha\boldsymbol{\Delta}_{t+1}\mathbf{B}_{t+1}^\top\mathbf{B}_*\bar{\mathbf{w}}_{*,t+1} \\
&\quad + \alpha\mathbf{B}_{t+1}^\top\mathbf{B}_*(\bar{\mathbf{w}}_{*,t}-\bar{\mathbf{w}}_{*,t+1}) + \alpha\boldsymbol{\Delta}_{t+1}\mathbf{B}_{t+1}^\top\mathbf{B}_*(\bar{\mathbf{w}}_{*,t}-\bar{\mathbf{w}}_{*,t+1}) \\
&\quad + \alpha(\mathbf{B}_t-\mathbf{B}_{t+1})^\top\mathbf{B}_*\bar{\mathbf{w}}_{*,t} + \alpha(\boldsymbol{\Delta}_t\mathbf{B}_t-\boldsymbol{\Delta}_{t+1}\mathbf{B}_{t+1})^\top\mathbf{B}_*\bar{\mathbf{w}}_{*,t} \\
&\quad + \tfrac{1}{m}\sum_{i\in\mathcal{I}_t}\alpha(\mathbf{B}_{t,i,\tau-1}-\mathbf{B}_t)^\top\mathbf{B}_*\mathbf{w}_{*,i} + \alpha(\boldsymbol{\Delta}_{t,i,\tau-1}\mathbf{B}_{t,i,\tau-2}^\top - \boldsymbol{\Delta}_t\mathbf{B}_t^\top)\mathbf{B}_*\mathbf{w}_{*,i} \\
&\qquad + \boldsymbol{\Delta}_{t,i,\tau-1}\boldsymbol{\Delta}_{t,i,\tau-2}\mathbf{w}_{t,i,\tau-2}
\end{aligned} \tag{19}$$

The remainder of the proof lies in bounding the error terms, which are all terms in the RHS of (19) besides the terms in the first line. First, by A_0 and the triangle inequality, we have

$$\|\bar{\mathbf{w}}_{*,t}-\bar{\mathbf{w}}_{*,t+1}\| \leq \|\bar{\mathbf{w}}_{*,t}-\bar{\mathbf{w}}_*\| + \|\bar{\mathbf{w}}_{*,t+1}-\bar{\mathbf{w}}_*\| \leq 8\alpha^2 L_{\max}^3$$

Thus, by $A_3(t+1)$, we have

$$\begin{aligned}
\|\alpha\mathbf{B}_{t+1}^\top\mathbf{B}_*(\bar{\mathbf{w}}_{*,t}-\bar{\mathbf{w}}_{*,t+1})\| &\leq 1.1\sqrt{\alpha}\|\bar{\mathbf{w}}_{*,t}-\bar{\mathbf{w}}_{*,t+1}\| \leq 9\alpha^{2.5}L_{\max}^3 \\
\|\alpha\boldsymbol{\Delta}_{t+1}\mathbf{B}_{t+1}^\top\mathbf{B}_*(\bar{\mathbf{w}}_{*,t}-\bar{\mathbf{w}}_{*,t+1})\| &\leq 1.1\sqrt{\alpha}\|\boldsymbol{\Delta}_{t+1}\|\|\bar{\mathbf{w}}_{*,t}-\bar{\mathbf{w}}_{*,t+1}\| \leq 18c_3\alpha^{4.5}\tau L_{\max}^5\kappa_{\max}^2 E_0^{-1}
\end{aligned}$$

Next, we can bound the difference between the locally-updated representation and the global representation as follows, for any $s \in \{1,\ldots,\tau\}$

$$\|\mathbf{B}_{t,i,s}-\mathbf{B}_t\|_2 \leq \sum_{r=1}^{s}\|\mathbf{B}_{t,i,r}-\mathbf{B}_{t,i,r-1}\|_2 \leq \alpha\sum_{r=1}^{s}\|\mathbf{e}_{t,i,r-1}\mathbf{w}_{t,i,r-1}^\top\|_2 \leq 7\alpha^{1.5}sL_{\max}^2 \tag{20}$$

using $A_2(t), A_3(t), A_{2,t,i}(\tau-1)$ and $A_{3,t,i}(\tau-1)$ to control the norms of $\mathbf{w}_{t,i,s-1}$ and $\mathbf{B}_{t,i,s-1}$. From (20) it follows that

$$\begin{aligned}
\|\mathbf{B}_{t+1}-\mathbf{B}_t\|_2 &\le \tfrac{1}{m}\sum_{i\in\mathcal{I}_t}\|\mathbf{B}_{t,i,\tau}-\mathbf{B}_t\|_2 \le 7\alpha^{1.5}\tau L_{\max}^2 \\
\|\mathbf{B}_{t,i,\tau-2}\mathbf{\Delta}_{t,i,\tau-1}-\mathbf{B}_t\mathbf{\Delta}_t\|_2 &\le \|\mathbf{B}_{t,i,\tau-2}-\mathbf{B}_t\|_2+\alpha\|\mathbf{B}_{t,i,\tau-2}\mathbf{B}_{t,i,\tau-1}^\top\mathbf{B}_{t,i,\tau-1}-\mathbf{B}_t\mathbf{B}_t^\top\mathbf{B}_t\|_2 \\
&\le \|\mathbf{B}_{t,i,\tau-2}-\mathbf{B}_t\|_2+\alpha\|(\mathbf{B}_{t,i,\tau-2}-\mathbf{B}_t)\mathbf{B}_{t,i,\tau-1}^\top\mathbf{B}_{t,i,\tau-1}\|_2 \\
&\quad+\alpha\|\mathbf{B}_t(\mathbf{B}_{t,i,\tau-1}-\mathbf{B}_t)^\top\mathbf{B}_{t,i,\tau-1}\|_2 \\
&\quad+\alpha\|\mathbf{B}_t\mathbf{B}_t^\top(\mathbf{B}_{t,i,\tau-1}-\mathbf{B}_t)\|_2 \\
&\le \|\mathbf{B}_{t,i,\tau-2}-\mathbf{B}_t\|_2+\alpha\|\mathbf{B}_{t,i,\tau-2}-\mathbf{B}_t\|\|\mathbf{B}_{t,i,\tau-1}^\top\mathbf{B}_{t,i,\tau-1}\|_2 \\
&\quad+\alpha\|\mathbf{B}_t\|\|\mathbf{B}_{t,i,\tau-1}-\mathbf{B}_t\|\|\mathbf{B}_{t,i,\tau-1}\|_2 \\
&\quad+\alpha\|\mathbf{B}_t\mathbf{B}_t^\top\|\|\mathbf{B}_{t,i,\tau-1}-\mathbf{B}_t\| \\
&\le 31\alpha^{1.5}\tau L_{\max}^2 \\
\|\mathbf{B}_t\mathbf{\Delta}_t-\mathbf{B}_{t+1}\mathbf{\Delta}_{t+1}\|_2 &\le 31\alpha^{1.5}\tau L_{\max}^2 \qquad (21)
\end{aligned}$$

Also, we have by $A_{2,t,i}(\tau-1)$ and $A_{3,t,i}(\tau-1)$,

$$\|\mathbf{\Delta}_{t,i,\tau-1}\mathbf{\Delta}_{t,i,\tau-2}\mathbf{w}_{t,i,\tau-2}\|_2 \le 8c_3^2\alpha^{4.5}\tau^2L_{\max}^5\kappa_{\max}^4E_0^{-2}. \qquad (22)$$

Thus, using these bounds with (19), we obtain

$$\begin{aligned}
\|\mathbf{w}_{t+1}-\alpha(\mathbf{I}_k+\mathbf{\Delta}_{t+1})\mathbf{B}_{t+1}^\top\mathbf{B}_*\bar{\mathbf{w}}_{*,t+1}\|_2 &\le 82\alpha^{2.5}\tau L_{\max}^3+(8c_3^2+12c_3)\alpha^{4.5}\tau^2L_{\max}^5\kappa_{\max}^4E_0^{-2} \\
&\le 91\alpha^{2.5}\tau L_{\max}^3
\end{aligned}$$

to complete the proof, where we have used that α is sufficiently small in the last inequality. □

Lemma 7. $\cap_{i\in\mathcal{I}_t}A_{2,t,i}(\tau) \implies A_2(t+1)$

Proof. By the triangle inequality and $\cap_{i\in\mathcal{I}_t}A_{2,t,i}(\tau)$, we have

$$\|\mathbf{w}_{t+1}\| = \left\|\tfrac{1}{m}\sum_{i\in\mathcal{I}_t}\mathbf{w}_{t,i,\tau}\right\| \le \tfrac{1}{m}\sum_{i\in\mathcal{I}_t}\|\mathbf{w}_{t,i,\tau}\| \le 2\sqrt{\alpha}L_{\max}$$

as desired. □

Lemma 8. $A_3(t)\cap A_4(t) \implies \sigma_{\min}^2(\mathbf{B}_t^\top\mathbf{B}_*) \ge \frac{0.1}{\alpha}E_0$.

Proof. First note that

$$\begin{aligned}
\sigma_{\min}^2(\mathbf{B}_t^\top\mathbf{B}_*) &\ge \sigma_{\min}^2(\mathbf{R}_t)\sigma_{\min}^2(\hat{\mathbf{B}}_t^\top\mathbf{B}_*) \\
&\ge \tfrac{0.9}{\alpha}\sigma_{\min}^2(\hat{\mathbf{B}}_t^\top\mathbf{B}_*) \qquad (23) \\
&= \tfrac{0.9}{\alpha}(1-\|\hat{\mathbf{B}}_t^\top\mathbf{B}_{*,\perp}\|_2^2) \\
&= \tfrac{0.9}{\alpha}(1-\mathrm{dist}_t^2) \qquad (24)
\end{aligned}$$

where $\hat{\mathbf{B}}_t\mathbf{R}_t=\mathbf{B}_t$ is the QR factorization of $\mathbf{B}_t$. Next, we would like to show the RHS is at most $(2+\delta_0)/3$. Using $A_3(t)$ and $A_4(t)$, we obtain

$$\begin{aligned}
\mathrm{dist}_t &= \|\mathbf{B}_{*,\perp}^\top\hat{\mathbf{B}}_t\|_2 \\
&\le \tfrac{1}{\sigma_{\min}(\mathbf{B}_t)}\|\mathbf{B}_{*,\perp}^\top\mathbf{B}_t\|_2 \\
&\ \ \vdots \\
&\le \tfrac{1}{\sigma_{\min}(\mathbf{B}_{t+1})}(1-0.04\alpha^2\tau E_0\mu^2)^t\|\mathbf{B}_{*,\perp}^\top\mathbf{B}_0\|_2 \\
&\le \tfrac{\sigma_{\max}(\mathbf{B}_0)}{\sigma_{\min}(\mathbf{B}_t)}(1-0.04\alpha^2\tau E_0\mu^2)^t\delta_0 \\
&\le \tfrac{\sqrt{1+\|\mathbf{\Delta}_0\|_2}/\sqrt{\alpha}}{\sqrt{1-\|\mathbf{\Delta}_t\|_2}/\sqrt{\alpha}}\delta_0
\end{aligned}$$

Next we use that $\|\mathbf{\Delta}_0\| \leq \alpha^2 \tau L_{\max}^2 \kappa_{\max}^2 \leq 0.1(1-\delta_0)^2$ by choice of initialization and choice of α, and similarly $\|\mathbf{\Delta}_t\| \leq \alpha^2 \tau L_{\max}^2 \kappa_{\max}^2 E_0^{-1} \leq 0.1(1-\delta_0)^2/(1-\delta_0^2)$. Let $c \coloneqq 0.1$. Then we have

$$\begin{aligned}
\frac{\sqrt{1+\|\mathbf{\Delta}_0\|_2}/\sqrt{\alpha}}{\sqrt{1-\|\mathbf{\Delta}_t\|_2}/\sqrt{\alpha}}\delta_0 &\leq \frac{\sqrt{1+c(1-\delta_0)^2}}{\sqrt{1-c(1-\delta_0)^2/(1-\delta_0^2)}}\delta_0 \\
&= \frac{\sqrt{1+c(1-\delta_0)^2}}{\sqrt{1-c(1-\delta_0)/(1+\delta_0)}}\delta_0 \\
&= \frac{\sqrt{1+\delta_0+c(1-\delta_0)^2(1+\delta_0)}}{\sqrt{1-c+(1+c)\delta_0}}\delta_0
\end{aligned}$$

Now, observe that

$$\begin{aligned}
&\frac{\sqrt{1+\delta_0+c(1-\delta_0)^2(1+\delta_0)}}{\sqrt{1-c+(1+c)\delta_0}}\delta_0 \leq \tfrac{2+\delta_0}{3} \\
\iff\ & \tfrac{1+\delta_0+c(1-\delta_0)^2(1+\delta_0)}{1-c+(1+c)\delta_0}\delta_0^2 \leq \tfrac{4+4\delta_0+\delta_0^2}{9} \\
\iff\ & (1+c)\delta_0^2 + \delta_0^3 - c\delta_0^4 + c\delta_0^5 \leq (4-4c+8\delta_0+8\delta_0^2+(1+c)\delta_0^3)/9 \\
\iff\ & c\delta_0^5 - c\delta_0^4 + \tfrac{8-c}{9}\delta_0^3 + \tfrac{1+9c}{9}\delta_0^2 - \tfrac{8}{9}\delta_0 - \tfrac{4-4c}{9} \leq 0 \qquad (25)
\end{aligned}$$

where (25) holds for all $\delta_0 \in [0,1)$ and $c = 0.1$, therefore we have

$$\mathrm{dist}_t \leq \frac{\sqrt{1+\|\mathbf{\Delta}_0\|_2}/\sqrt{\alpha}}{\sqrt{1-\|\mathbf{\Delta}_t\|_2}/\sqrt{\alpha}}\delta_0 \leq \tfrac{2+\delta_0}{3}. \qquad (26)$$

Thus, using (24), we obtain

$$\begin{aligned}
\sigma_{\min}^2(\mathbf{B}_t^\top \mathbf{B}_*) &\geq \tfrac{0.9}{\alpha}\left(1 - \tfrac{4+4\delta_0+\delta_0^2}{9}\right) \\
&\geq \tfrac{0.9}{\alpha}\left(1 - \tfrac{8+\delta_0^2}{9}\right) \\
&= \tfrac{0.9}{9\alpha}E_0 \\
&= \tfrac{0.1}{\alpha}E_0
\end{aligned}$$

as desired. □

Lemma 9. $\cap_{i\in\mathcal{I}_t}\big(\cap_{h=1}^4 A_{h,t,i}(\tau)\big) \cap A_1(t) \cap A_2(t) \cap A_3(t) \cap A_5(t) \implies A_3(t+1)$.

Proof. We aim to write $\mathbf{\Delta}_{t+1} = \frac{1}{2}(\mathbf{I}_k - \mathbf{P}_t)\mathbf{\Delta}_t + \frac{1}{2}\mathbf{\Delta}_t(\mathbf{I}_k - \mathbf{P}_t) + \mathbf{Z}_t$ for a positive definite matrix $\mathbf{P}_t$ and a perturbation matrix $\mathbf{Z}_t$. This will yield the inequality $\|\mathbf{\Delta}_{t+1}\|_2 \leq (1-\lambda_{\min}(\mathbf{P}_t))\|\mathbf{\Delta}_t\|_2 + \|\mathbf{Z}_t\|_2$. Assuming $\lambda_{\min}(\mathbf{P}_t)$ and $\|\mathbf{Z}_t\|_2$ scale appropriately (defined later), this inequality combined with inductive hypothesis $A_5(t)$ will give the desired upper bound on $\|\mathbf{\Delta}_{t+1}\|_2$ (this is because the upper bound on $\|\mathbf{Z}_t\|_2$ scales with dist_t, so $A_5(t)$ contributes to controlling $\|\mathbf{Z}_t\|_2$). The proof therefore relies on showing the existence of appropriate $\mathbf{P}_t$ and $\mathbf{Z}_t$.

First recall $\mathbf{\Delta}_t \coloneqq \mathbf{I} - \alpha\mathbf{B}_t^\top\mathbf{B}_t$ and $\bar{\mathbf{\Delta}}_t \coloneqq \mathbf{I}_d - \alpha\mathbf{B}_t\mathbf{B}_t^\top$. Let $\mathbf{G}_t \coloneqq \frac{1}{\alpha}(\mathbf{B}_t - \mathbf{B}_{t+1})$, i.e. $\mathbf{G}_t$ satisfies $\mathbf{B}_{t+1} = \mathbf{B}_t - \alpha\mathbf{G}_t$. Then

$$\mathbf{\Delta}_{t+1} = \mathbf{I}_k - \alpha\mathbf{B}_{t+1}^\top\mathbf{B}_{t+1} = \mathbf{\Delta}_t + \alpha^2\mathbf{B}_t^\top\mathbf{G}_t + \alpha^2\mathbf{G}_t^\top\mathbf{B}_t - \alpha^3\mathbf{G}_t^\top\mathbf{G}_t \qquad (27)$$

The key is showing that $\alpha^2\mathbf{B}_t^\top\mathbf{G}_t = -\frac{1}{2}\mathbf{\Delta}_t\mathbf{P}_t + \mathbf{Z}_t'$ for appropriate $\mathbf{P}_t$ and $\mathbf{Z}_t'$. Then, by (27), we will have $\mathbf{\Delta}_{t+1} = \frac{1}{2}(\mathbf{I}_k - \mathbf{P}_t)\mathbf{\Delta}_t + \frac{1}{2}\mathbf{\Delta}_t(\mathbf{I}_k - \mathbf{P}_t) + \mathbf{Z}_t$ as desired, where $\mathbf{Z}_t = \mathbf{Z}_t' + (\mathbf{Z}_t')^\top - \alpha^3\mathbf{G}_t^\top\mathbf{G}_t$.

Notice that $\mathbf{G}_t$ is the average across clients of the sum of their local gradients on every local update. In particular, we have

$$\mathbf{G}_t = (\mathbf{B}_t\mathbf{w}_t - \mathbf{B}_*\bar{\mathbf{w}}_{*,t})\mathbf{w}_t^\top + \tfrac{1}{m}\sum_{i\in\mathcal{I}_t}\sum_{s=1}^{\tau-1}(\mathbf{B}_{t,i,s}\mathbf{w}_{t,i,s} - \mathbf{B}_*\mathbf{w}_{*,i})\mathbf{w}_{t,i,s}^\top \qquad (28)$$

We will unroll the gradients for the first two local updates only, in order to obtain a negative term that will contribute to the contraction of $\|\mathbf{\Delta}_t\|$ (i.e. $\mathbf{P}_t$ will be extracted from the gradients for the first two local updates). The remaining terms will belong to $\mathbf{Z}_t$ and must be upper bounded (i.e. $\|\mathbf{\Delta}_{t+1}\|$

can grow due to local updates beyond the second local update, but we will show that it can't grow too much). In particular, we have

$$
\begin{aligned}
\mathbf{G}_t &= (\mathbf{B}_t\mathbf{w}_t - \mathbf{B}_*\bar{\mathbf{w}}_{*,t})\mathbf{w}_t^\top + \tfrac{1}{m}\sum_{i\in\mathcal{I}_t}(\mathbf{B}_{t,i,1}\mathbf{w}_{t,i,1} - \mathbf{B}_*\mathbf{w}_{*,i})\mathbf{w}_{t,i,1}^\top \\
&\quad + \tfrac{1}{m}\sum_{i\in\mathcal{I}_t}\sum_{s=2}^{\tau-1}(\mathbf{B}_{t,i,s}\mathbf{w}_{t,i,s} - \mathbf{B}_*\mathbf{w}_{*,i})\mathbf{w}_{t,i,s}^\top \\
&= (\mathbf{B}_t\mathbf{w}_t - \mathbf{B}_*\bar{\mathbf{w}}_{*,t})\mathbf{w}_t^\top - \alpha\bar{\boldsymbol{\Delta}}_t\mathbf{B}_*\tfrac{1}{m}\sum_{i\in\mathcal{I}_t}\mathbf{w}_{*,i}\mathbf{w}_{*,i}^\top\mathbf{B}_*^\top\mathbf{B}_t - \bar{\boldsymbol{\Delta}}_t\mathbf{B}_*\bar{\mathbf{w}}_{*,t}\mathbf{w}_t^\top\boldsymbol{\Delta}_t \\
&\quad + \tfrac{1}{m}\sum_{i\in\mathcal{I}_t}\alpha^2(\mathbf{B}_t\mathbf{w}_t - \mathbf{B}_*\mathbf{w}_{*,i})\mathbf{w}_t^\top\mathbf{B}_t^\top\mathbf{B}_*\mathbf{w}_{*,i}\mathbf{w}_{t,i,1}^\top \\
&\quad + \tfrac{1}{m}\sum_{i\in\mathcal{I}_t}(\mathbf{B}_t - \alpha(\mathbf{B}_t\mathbf{w}_t - \mathbf{B}_*\mathbf{w}_{*,i})\mathbf{w}_t^\top)\boldsymbol{\Delta}_t\mathbf{w}_t\mathbf{w}_{t,i,1}^\top \\
&\quad + \tfrac{1}{m}\sum_{i\in\mathcal{I}_t}\sum_{s=2}^{\tau-1}(\mathbf{B}_{t,i,s}\mathbf{w}_{t,i,s} - \mathbf{B}_*\mathbf{w}_{*,i})\mathbf{w}_{t,i,s}^\top
\end{aligned}
$$

Multiplying both sides by $\mathbf{B}_t^\top$, and using the fact that $\mathbf{B}_t^\top\bar{\boldsymbol{\Delta}}_t = \boldsymbol{\Delta}_t\mathbf{B}_t^\top$, we obtain

$$
\begin{aligned}
\mathbf{B}_t^\top\mathbf{G}_t &= \mathbf{B}_t^\top(\mathbf{B}_t\mathbf{w}_t - \mathbf{B}_*\bar{\mathbf{w}}_{*,t})\mathbf{w}_t^\top - \alpha\boldsymbol{\Delta}_t\mathbf{B}_t^\top\mathbf{B}_*\tfrac{1}{m}\sum_{i\in\mathcal{I}_t}\mathbf{w}_{*,i}\mathbf{w}_{*,i}^\top\mathbf{B}_*^\top\mathbf{B}_t - \boldsymbol{\Delta}_t\mathbf{B}_t^\top\mathbf{B}_*\bar{\mathbf{w}}_{*,t}\mathbf{w}_t^\top\boldsymbol{\Delta}_t \\
&\quad - \mathbf{B}_t^\top\tfrac{1}{m}\sum_{i\in\mathcal{I}_t}\alpha^2(\mathbf{B}_t\mathbf{w}_t - \mathbf{B}_*\mathbf{w}_{*,i})\mathbf{w}_t^\top\mathbf{B}_t^\top\mathbf{B}_*\mathbf{w}_{*,i}\mathbf{w}_{t,i,1}^\top \\
&\quad + \mathbf{B}_t^\top\tfrac{1}{m}\sum_{i\in\mathcal{I}_t}(\mathbf{B}_t - \alpha(\mathbf{B}_t\mathbf{w}_t - \mathbf{B}_*\mathbf{w}_{*,i})\mathbf{w}_t^\top)\boldsymbol{\Delta}_t\mathbf{w}_t\mathbf{w}_{t,i,1}^\top \\
&\quad + \mathbf{B}_t^\top\tfrac{1}{m}\sum_{i\in\mathcal{I}_t}\sum_{s=2}^{\tau-1}(\mathbf{B}_{t,i,s}\mathbf{w}_{t,i,s} - \mathbf{B}_*\mathbf{w}_{*,i})\mathbf{w}_{t,i,s}^\top \\
&= -\alpha\boldsymbol{\Delta}_t\mathbf{B}_t^\top\mathbf{B}_*\tfrac{1}{m}\sum_{i\in\mathcal{I}_t}\mathbf{w}_{*,i}\mathbf{w}_{*,i}^\top\mathbf{B}_*^\top\mathbf{B}_t + \mathbf{N}_t
\end{aligned} \tag{29}
$$

where the first term is a negative term that helps $\|\boldsymbol{\Delta}_{t+1}\|$ stay small, and the remaining terms are given by

$$
\begin{aligned}
\mathbf{N}_t \coloneqq\ & \mathbf{B}_t^\top(\mathbf{B}_t\mathbf{w}_t - \mathbf{B}_*\bar{\mathbf{w}}_{*,t})\mathbf{w}_t^\top - \boldsymbol{\Delta}_t\mathbf{B}_t^\top\mathbf{B}_*\bar{\mathbf{w}}_{*,t}\mathbf{w}_t^\top\boldsymbol{\Delta}_t \\
& - \mathbf{B}_t^\top \tfrac{1}{m}\sum_{i\in\mathcal{I}_t}\alpha^2(\mathbf{B}_t\mathbf{w}_t - \mathbf{B}_*\mathbf{w}_{*,i})\mathbf{w}_t^\top\mathbf{B}_t^\top\mathbf{B}_*\mathbf{w}_{*,i}\mathbf{w}_{t,i,1}^\top \\
& + \mathbf{B}_t^\top \tfrac{1}{m}\sum_{i\in\mathcal{I}_t}(\mathbf{B}_t - \alpha(\mathbf{B}_t\mathbf{w}_t - \mathbf{B}_*\mathbf{w}_{*,i})\mathbf{w}_t^\top)\boldsymbol{\Delta}_t\mathbf{w}_t\mathbf{w}_{t,i,1}^\top \\
& + \mathbf{B}_t^\top \tfrac{1}{m}\sum_{i\in\mathcal{I}_t}\sum_{s=2}^{\tau-1}(\mathbf{B}_{t,i,s}\mathbf{w}_{t,i,s} - \mathbf{B}_*\mathbf{w}_{*,i})\mathbf{w}_{t,i,s}^\top \\
=\ & \mathbf{B}_t^\top(\mathbf{B}_t\mathbf{w}_t - \mathbf{B}_*\bar{\mathbf{w}}_{*,t})\mathbf{w}_t^\top + \mathbf{B}_t^\top\mathbf{B}_t\boldsymbol{\Delta}_t\mathbf{w}_t\tfrac{1}{m}\sum_{i\in\mathcal{I}_t}\mathbf{w}_{t,i,1}^\top \\
& - \mathbf{B}_t^\top \tfrac{1}{m}\sum_{i\in\mathcal{I}_t}\alpha^2(\mathbf{B}_t\mathbf{w}_t - \mathbf{B}_*\mathbf{w}_{*,i})\mathbf{w}_t^\top\mathbf{B}_t^\top\mathbf{B}_*\mathbf{w}_{*,i}\mathbf{w}_{t,i,1}^\top \\
& - \mathbf{B}_t^\top \tfrac{1}{m}\sum_{i\in\mathcal{I}_t}\alpha(\mathbf{B}_t\mathbf{w}_t - \mathbf{B}_*\mathbf{w}_{*,i})\mathbf{w}_t^\top\boldsymbol{\Delta}_t\mathbf{w}_t\mathbf{w}_{t,i,1}^\top \\
& - \boldsymbol{\Delta}_t\mathbf{B}_t^\top\mathbf{B}_*\bar{\mathbf{w}}_{*,t}\mathbf{w}_t^\top\boldsymbol{\Delta}_t + \mathbf{B}_t^\top \tfrac{1}{m}\sum_{i\in\mathcal{I}_t}\sum_{s=2}^{\tau-1}(\mathbf{B}_{t,i,s}\mathbf{w}_{t,i,s} - \mathbf{B}_*\mathbf{w}_{*,i})\mathbf{w}_{t,i,s}^\top \\
=\ & \underbrace{\mathbf{B}_t^\top(\mathbf{B}_t\mathbf{w}_t - \mathbf{B}_*\bar{\mathbf{w}}_{*,t})\mathbf{w}_t^\top + \alpha\mathbf{B}_t^\top\mathbf{B}_t\boldsymbol{\Delta}_t\mathbf{w}_t\bar{\mathbf{w}}_{*,t}^\top\mathbf{B}_*^\top\mathbf{B}_t}_{=:\mathbf{E}_1} \\
& \underbrace{- \tfrac{1}{m}\sum_{i\in\mathcal{I}_t}\alpha\mathbf{B}_t^\top(\mathbf{B}_t\mathbf{w}_t - \mathbf{B}_*\mathbf{w}_{*,i})\mathbf{w}_t^\top\mathbf{w}_{t,i,1}\mathbf{w}_{t,i,1}^\top}_{=:\mathbf{E}_2} \\
& + \underbrace{\boldsymbol{\Delta}_t\mathbf{B}_t^\top(\mathbf{B}_t\mathbf{w}_t - \mathbf{B}_*\bar{\mathbf{w}}_{*,t})\mathbf{w}_t^\top\boldsymbol{\Delta}_t}_{=:\mathbf{E}_3} + \underbrace{\mathbf{B}_t^\top \tfrac{1}{m}\sum_{i\in\mathcal{I}_t}\sum_{s=2}^{\tau-1}(\mathbf{B}_{t,i,s}\mathbf{w}_{t,i,s} - \mathbf{B}_*\mathbf{w}_{*,i})\mathbf{w}_{t,i,s}^\top}_{=:\mathbf{E}_4} \qquad (30)
\end{aligned}
$$

To get from the first to the second equation we expanded the fourth term in the first equation. Now we need to upper bound the spectral norm of each of the terms $\mathbf{E}_i$. The matrices $\mathbf{E}_2$ and $\mathbf{E}_3$ are straightforward to control; we will take care of them shortly. For now we are concerned with $\mathbf{E}_1$. In order to control this matrix, we must use the fact that $\mathbf{w}_t$ is close to a matrix times $\bar{\mathbf{w}}_{*,t}$. This will allow us to subsume the dominant term from $\mathbf{E}_1$ into the negative term in (29). In particular, note that by $A_1(t)$, we have $\mathbf{w}_t = \alpha\mathbf{B}_t^\top\mathbf{B}_*\bar{\mathbf{w}}_{*,t} + \alpha\boldsymbol{\Delta}_t\mathbf{B}_t^\top\mathbf{B}_*\bar{\mathbf{w}}_{*,t} + \mathbf{h}_t$, where $\|\mathbf{h}_t\|_2 \le 91\alpha^{2.5}\tau L_{\max}^3$. This implies that

$$
\begin{aligned}
\mathbf{B}_t^\top(\mathbf{B}_t\mathbf{w}_t - \mathbf{B}_*\bar{\mathbf{w}}_{*,t}) &= \mathbf{B}_t^\top(\alpha\mathbf{B}_t\mathbf{B}_t^\top\mathbf{B}_*\bar{\mathbf{w}}_{*,t} - \mathbf{B}_*\bar{\mathbf{w}}_{*,t}) + \alpha\boldsymbol{\Delta}_t\mathbf{B}_t^\top\mathbf{B}_t\mathbf{B}_t^\top\mathbf{B}_*\bar{\mathbf{w}}_{*,t} + \mathbf{B}_t^\top\mathbf{B}_t\mathbf{h}_t \\
&= -\boldsymbol{\Delta}_t\mathbf{B}_t^\top\mathbf{B}_*\bar{\mathbf{w}}_{*,t} + \alpha\boldsymbol{\Delta}_t\mathbf{B}_t^\top\mathbf{B}_t\mathbf{B}_t^\top\mathbf{B}_*\bar{\mathbf{w}}_{*,t} + \mathbf{B}_t^\top\mathbf{B}_t\mathbf{h}_t \\
&= -\boldsymbol{\Delta}_t^2\mathbf{B}_t^\top\mathbf{B}_*\bar{\mathbf{w}}_{*,t} + \mathbf{B}_t^\top\mathbf{B}_t\mathbf{h}_t \qquad (31)
\end{aligned}
$$

Making this substitution in $\mathbf{E}_1$, we obtain,

$$
\begin{aligned}
\mathbf{E}_1 &= -\boldsymbol{\Delta}_t^2\mathbf{B}_t^\top\mathbf{B}_*\bar{\mathbf{w}}_{*,t}\mathbf{w}_t^\top + \mathbf{B}_t^\top\mathbf{B}_t\mathbf{h}_t\mathbf{w}_t^\top + \alpha\mathbf{B}_t^\top\mathbf{B}_t\boldsymbol{\Delta}_t\mathbf{w}_t\bar{\mathbf{w}}_{*,t}^\top\mathbf{B}_*^\top\mathbf{B}_t \\
&= -\boldsymbol{\Delta}_t^2\mathbf{B}_t^\top\mathbf{B}_*\bar{\mathbf{w}}_{*,t}\mathbf{w}_t^\top + \mathbf{B}_t^\top\mathbf{B}_t\mathbf{h}_t\mathbf{w}_t^\top - \boldsymbol{\Delta}_t^2\mathbf{w}_t\bar{\mathbf{w}}_{*,t}^\top\mathbf{B}_*^\top\mathbf{B}_t + \boldsymbol{\Delta}_t\mathbf{w}_t\bar{\mathbf{w}}_{*,t}^\top\mathbf{B}_*^\top\mathbf{B}_t \\
&= -\boldsymbol{\Delta}_t^2\mathbf{B}_t^\top\mathbf{B}_*\bar{\mathbf{w}}_{*,t}\mathbf{w}_t^\top + \mathbf{B}_t^\top\mathbf{B}_t\mathbf{h}_t\mathbf{w}_t^\top - \boldsymbol{\Delta}_t^2\mathbf{w}_t\bar{\mathbf{w}}_{*,t}^\top\mathbf{B}_*^\top\mathbf{B}_t \\
&\quad + \boldsymbol{\Delta}_t(\alpha\boldsymbol{\Delta}_t\mathbf{B}_t^\top\mathbf{B}_*\bar{\mathbf{w}}_{*,t} + \mathbf{h}_t)\bar{\mathbf{w}}_{*,t}^\top\mathbf{B}_*^\top\mathbf{B}_t + \alpha\boldsymbol{\Delta}_t\mathbf{B}_t^\top\mathbf{B}_*\bar{\mathbf{w}}_{*,t}\bar{\mathbf{w}}_{*,t}^\top\mathbf{B}_*^\top\mathbf{B}_t. \qquad (32)
\end{aligned}
$$

The dominant term in (32) is the last term. Specifically, we have,

$$
\begin{aligned}
&\|\mathbf{E}_1 - \alpha \mathbf{\Delta}_t \mathbf{B}_t^\top \mathbf{B}_* \bar{\mathbf{w}}_{*,t} \bar{\mathbf{w}}_{*,t}^\top \mathbf{B}_*^\top \mathbf{B}_t\| \\
&\quad \leq \|\mathbf{\Delta}_t^2 \mathbf{B}_t^\top \mathbf{B}_* \bar{\mathbf{w}}_{*,t} \mathbf{w}_t^\top\| + \|\mathbf{B}_t^\top \mathbf{B}_t \mathbf{h}_t \mathbf{w}_t^\top\| + \|\mathbf{\Delta}_t^2 \mathbf{w}_t \bar{\mathbf{w}}_{*,t}^\top \mathbf{B}_*^\top \mathbf{B}_t\| \\
&\qquad + \|\mathbf{\Delta}_t(\alpha \mathbf{\Delta}_t \mathbf{B}_t^\top \mathbf{B}_* \bar{\mathbf{w}}_{*,t} + \mathbf{h}_t) \bar{\mathbf{w}}_{*,t}^\top \mathbf{B}_*^\top \mathbf{B}_t\| \\
&\quad \leq \|\mathbf{\Delta}_t^2 \mathbf{B}_t^\top \mathbf{B}_* \bar{\mathbf{w}}_{*,t} \mathbf{w}_t^\top\| + \|\mathbf{\Delta}_t^2 \mathbf{w}_t \bar{\mathbf{w}}_{*,t}^\top \mathbf{B}_*^\top \mathbf{B}_t\| + \alpha \|\mathbf{\Delta}_t^2 \mathbf{B}_t^\top \mathbf{B}_* \bar{\mathbf{w}}_{*,t} \bar{\mathbf{w}}_{*,t}^\top \mathbf{B}_*^\top \mathbf{B}_t\| \\
&\qquad + \|\mathbf{B}_t^\top \mathbf{B}_t \mathbf{h}_t \mathbf{w}_t^\top\| + \|\mathbf{\Delta}_t \mathbf{h}_t \bar{\mathbf{w}}_{*,t}^\top \mathbf{B}_*^\top \mathbf{B}_t\| \\
&\quad \leq 5.5 c_3^2 \alpha^4 \tau^2 L_{\max}^6 \kappa_{\max}^4 E_0^{-2} + 2.2 \times 91 \alpha^2 \tau L_{\max}^4 + 1.1 \times 91 c_3 \alpha^4 \tau^2 L_{\max}^6 \kappa_{\max}^2 E_0^{-1} \quad (33) \\
&\quad \leq (206 + 101/c_3) \alpha^2 \tau L_{\max}^4 \quad (34)
\end{aligned}
$$

where (33) follows by applying the Cauchy-Schwarz inequality to each of the terms in the previous inequality, and using $A_2(t), A_3(t)$, and our bound on $\mathbf{h}_t$ (from $A_1(t)$), and (34) follows as α is sufficiently small. The last first term term can be subsumed by completing a square as follows. Combining (29), (30) and (32) yields

$$
\begin{aligned}
\mathbf{B}_t^\top \mathbf{G}_t &= -\alpha \mathbf{\Delta}_t \mathbf{B}_t^\top \mathbf{B}_* \tfrac{1}{m} \sum_{i \in \mathcal{I}_t} \mathbf{w}_{*,i} \mathbf{w}_{*,i}^\top \mathbf{B}_*^\top \mathbf{B}_t + \mathbf{E}_1 - \mathbf{E}_2 + \mathbf{E}_3 + \mathbf{E}_4 \\
&= -\alpha \mathbf{\Delta}_t \mathbf{B}_t^\top \mathbf{B}_* \tfrac{1}{m} \sum_{i \in \mathcal{I}_t} \mathbf{w}_{*,i} \mathbf{w}_{*,i}^\top \mathbf{B}_*^\top \mathbf{B}_t + \alpha \mathbf{\Delta}_t \mathbf{B}_t^\top \mathbf{B}_* \bar{\mathbf{w}}_{*,t} \bar{\mathbf{w}}_{*,t}^\top \mathbf{B}_*^\top \mathbf{B}_t \\
&\quad + (\mathbf{E}_1 - \alpha \mathbf{\Delta}_t \mathbf{B}_t^\top \mathbf{B}_* \bar{\mathbf{w}}_{*,t} \bar{\mathbf{w}}_{*,t}^\top \mathbf{B}_*^\top \mathbf{B}_t) - \mathbf{E}_2 + \mathbf{E}_3 + \mathbf{E}_4 \\
&= -\alpha \mathbf{\Delta}_t \mathbf{B}_t^\top \mathbf{B}_* \tfrac{1}{m} \sum_{i \in \mathcal{I}_t} (\mathbf{w}_{*,i} - \bar{\mathbf{w}}_{*,t})(\mathbf{w}_{*,i} - \bar{\mathbf{w}}_{*,t})^\top \mathbf{B}_*^\top \mathbf{B}_t \\
&\quad + (\mathbf{E}_1 - \alpha \mathbf{\Delta}_t \mathbf{B}_t^\top \mathbf{B}_* \bar{\mathbf{w}}_{*,t} \bar{\mathbf{w}}_{*,t}^\top \mathbf{B}_*^\top \mathbf{B}_t) - \mathbf{E}_2 + \mathbf{E}_3 + \mathbf{E}_4 \\
&= -\tfrac{1}{2\alpha^2} \mathbf{\Delta}_t \mathbf{P}_t + \tfrac{1}{\alpha^2} \mathbf{Z}_t' \quad (35)
\end{aligned}
$$

where $\mathbf{P}_t = 2\alpha^3 \mathbf{B}_t^\top \mathbf{B}_* \frac{1}{m} \sum_{i \in \mathcal{I}_t} (\mathbf{w}_{*,i} - \bar{\mathbf{w}}_{*,t})(\mathbf{w}_{*,i} - \bar{\mathbf{w}}_{*,t})^\top \mathbf{B}_*^\top \mathbf{B}_t$ and

$$
\mathbf{Z}_t' := \alpha^2 (\mathbf{E}_1 - \alpha \mathbf{\Delta}_t \mathbf{B}_t^\top \mathbf{B}_* \bar{\mathbf{w}}_{*,t} \bar{\mathbf{w}}_{*,t}^\top \mathbf{B}_*^\top \mathbf{B}_t) - \alpha^2 \mathbf{E}_2 + \alpha^2 \mathbf{E}_3 + \alpha^2 \mathbf{E}_4
$$

we have performed the desired decomposition; it remains to show that $\lambda_{\min}(\mathbf{P}_t)$ and $\|\mathbf{Z}_t'\|_2$ scale appropriately. First we lower bound $\lambda_{\min}(\mathbf{P}_t)$.

$$
\begin{aligned}
\lambda_{\min}(\mathbf{P}_t) &= \lambda_{\min}\left(2\alpha^3 \mathbf{B}_t^\top \mathbf{B}_* \tfrac{1}{m} \sum_{i \in \mathcal{I}_t} (\mathbf{w}_{*,i} - \bar{\mathbf{w}}_{*,t})(\mathbf{w}_{*,i} - \bar{\mathbf{w}}_{*,t})^\top \mathbf{B}_*^\top \mathbf{B}_t\right) \\
&\geq 2\alpha^3 \sigma_{\min}(\mathbf{B}_t^\top \mathbf{B}_*)^2 \lambda_{\min}\left(\tfrac{1}{m} \sum_{i \in \mathcal{I}_t} (\mathbf{w}_{*,i} - \bar{\mathbf{w}}_{*,t})(\mathbf{w}_{*,i} - \bar{\mathbf{w}}_{*,t})^\top\right) \\
&\geq 0.2\alpha^2 E_0 \lambda_{\min}\left(\tfrac{1}{m} \sum_{i \in \mathcal{I}_t} (\mathbf{w}_{*,i} - \bar{\mathbf{w}}_{*,t})(\mathbf{w}_{*,i} - \bar{\mathbf{w}}_{*,t})^\top\right) \quad (36) \\
&\geq 0.2\alpha^2 E_0 \lambda_{\min}\left(\tfrac{1}{M} \sum_{i=1}^{M} (\mathbf{w}_{*,i} - \bar{\mathbf{w}}_*)(\mathbf{w}_{*,i} - \bar{\mathbf{w}}_*)^\top\right) \\
&\quad - 0.2\alpha^2 E_0 \left\| \tfrac{1}{m} \sum_{i \in \mathcal{I}_t} \mathbf{w}_{*,i} \mathbf{w}_{*,i}^\top - \tfrac{1}{M} \sum_{i'=1}^{M} \mathbf{w}_{*,i'} \mathbf{w}_{*,i'}^\top \right\| \\
&\quad - 0.2\alpha^2 E_0 \left\| \mathbf{w}_{*,t} \mathbf{w}_{*,t}^\top - \bar{\mathbf{w}}_* \bar{\mathbf{w}}_*^\top \right\| \\
&\geq 0.15\alpha^2 E_0 \mu^2 - 6\alpha^4 E_0 L_{\max}^4 \quad (37) \\
&\geq 0.15\alpha^2 E_0 \mu^2 \quad (38)
\end{aligned}
$$

where (36) follows by Lemma 8, (37) follows by Assumption 2 and A_0, and (38) follows as $\alpha^2 \leq \frac{1}{120\kappa_*^2 L_{\max}^2}$. Now we upper bound $\|\mathbf{Z}_t'\|_2$. We have already upper bounded $\|\mathbf{E}_1 -$

$\alpha \mathbf{\Delta}_t \mathbf{B}_t^\top \mathbf{B}_* \bar{\mathbf{w}}_{*,t} \bar{\mathbf{w}}_{*,t}^\top \mathbf{B}_*^\top \mathbf{B}_t \|$ in (34). We next upper bound $\|\mathbf{E}_2\|_2$ and $\|\mathbf{E}_3\|_2$ by $A_2(t), A_3(t)$, and $A_{2,i,t}(1)$. We have

$$\|\alpha^2 \mathbf{E}_2\|_2 \leq 32\alpha^4 L_{\max}^4$$
$$\|\alpha^2 \mathbf{E}_3\|_2 \leq 28 c_3^2 \alpha^6 \tau^2 L_{\max}^6 \kappa_{\max}^2 E_0^{-2}$$

using the triangle and Cauchy-Schwarz inequalities. Now we turn to $\|\alpha^2 \mathbf{E}_4\|_2$. Recall that $\mathbf{E}_4$ is the sum of local gradients across all clients and all local updates beyond the first local update. We show that these gradients are sufficiently small such that $\|\mathbf{\Delta}_{t+1}\|_2$ cannot grow beyond the desired threshold.

Recall that $\mathbf{E}_4 = \sum_{s=2}^{\tau-1} \mathbf{B}_t^\top \mathbf{e}_{t,i,s} \mathbf{w}_{t,i,s}^\top$. To bound this sum it is critical to control the evolution of $\mathbf{e}_{t,i,s}$. The idea is to split $\mathbf{e}_{t,i,s}$ into its projection onto $\mathrm{col}(\mathbf{B}_{t,i,s-1}) \approx \mathrm{col}(\mathbf{B}_t)$ and its projection onto $\mathrm{col}(\mathbf{B}_{t,i,s-1})^\perp \approx \mathrm{col}(\mathbf{B}_t)^\perp$. Then, we can show that the magnitude of the projection onto $\mathrm{col}(\mathbf{B}_{t,i,s-1})$ is going to zero very fast (the head is quickly learned, meaning it fits the product as much as it can with what it has to work with, i.e. $\mathrm{col}(\mathbf{B}_{t,i,s-1})$). On the other hand, the magnitude of the projection onto $\mathrm{col}(\mathbf{B}_{t,i,s-1})^\perp$ is slowly going to zero, since this reducing this error requires changing the representation and the representation changes slower than the head. The saving grace is that this error is proportional to $\mathrm{dist}(\mathbf{B}_{t,i,s-1}, \mathbf{B}_*)$, which for all s is linearly converging to zero with t.

To show this, pick any $i \in \mathcal{I}_t$ and let $\hat{\mathbf{B}}_{t,i,s}, \mathbf{R}_{t,i,s}$ denote the QR-factorization of $\mathbf{B}_{t,i,s}$. Define $\tilde{\mathbf{\Delta}}_{t,i,s-1} \coloneqq \hat{\mathbf{B}}_{t,i,s-1} \hat{\mathbf{B}}_{t,i,s-1}^\top - \alpha \mathbf{B}_{t,i,s-1} \mathbf{B}_{t,i,s-1}^\top$ and $\omega_{t,i,s-1} \coloneqq \alpha \mathbf{w}_{t,i,s-1}^\top \mathbf{\Delta}_{t,i,s-1} \mathbf{w}_{t,i,s} + \alpha^2 \mathbf{w}_{t,i,s-1}^\top \mathbf{B}_{t,i,s-1}^\top \mathbf{B}_* \mathbf{w}_{*,i}$. By expanding $\mathbf{e}_{t,i,s}$, we find

$$\begin{aligned}
&\mathbf{e}_{t,i,s} \\
&= (\mathbf{I}_d - \alpha \mathbf{B}_{t,i,s-1} \mathbf{B}_{t,i,s-1}^\top - \alpha \mathbf{w}_{t,i,s-1}^\top \mathbf{\Delta}_{t,i,s-1} \mathbf{w}_{t,i,s} \mathbf{I}_d - \alpha^2 \mathbf{w}_{t,i,s-1}^\top \mathbf{B}_{t,i,s-1}^\top \mathbf{B}_* \mathbf{w}_{*,i} \mathbf{I}_d) \mathbf{e}_{t,i,s-1} \\
&= (\mathbf{I}_d - \hat{\mathbf{B}}_{t,i,s-1} \hat{\mathbf{B}}_{t,i,s-1}^\top) \mathbf{e}_{t,i,s-1} + \big(\tilde{\mathbf{\Delta}}_{t,i,s-1} - \omega_{t,i,s-1} \mathbf{I}_d\big) \mathbf{e}_{t,i,s-1} \\
&= (\mathbf{I}_d - \hat{\mathbf{B}}_{t,i,s-1} \hat{\mathbf{B}}_{t,i,s-1}^\top) \mathbf{e}_{t,i,s-1} + \big(\tilde{\mathbf{\Delta}}_{t,i,s-1} - \omega_{t,i,s-1} \mathbf{I}_d\big)(\mathbf{I}_d - \hat{\mathbf{B}}_{t,i,s-2} \hat{\mathbf{B}}_{t,i,s-2}^\top) \mathbf{e}_{t,i,s-2} \\
&\quad + \big(\tilde{\mathbf{\Delta}}_{t,i,s-1} - \omega_{t,i,s-1} \mathbf{I}_d\big)\big(\tilde{\mathbf{\Delta}}_{t,i,s-2} - \omega_{t,i,s-2} \mathbf{I}_d\big) \mathbf{e}_{t,i,s-2} \qquad (39)
\end{aligned}$$

Therefore,

$$\begin{aligned}
\mathbf{B}_t^\top \mathbf{e}_{t,i,s} &= \mathbf{B}_t^\top (\mathbf{I}_d - \hat{\mathbf{B}}_{t,i,s-1} \hat{\mathbf{B}}_{t,i,s-1}^\top) \mathbf{e}_{t,i,s-1} \\
&\quad + \mathbf{B}_t^\top \big(\tilde{\mathbf{\Delta}}_{t,i,s-1} - \omega_{t,i,s-1} \mathbf{I}_d\big)(\mathbf{I}_d - \hat{\mathbf{B}}_{t,i,s-2} \hat{\mathbf{B}}_{t,i,s-2}^\top) \mathbf{e}_{t,i,s-2} \\
&\quad + \mathbf{B}_t^\top \big(\tilde{\mathbf{\Delta}}_{t,i,s-1} - \omega_{t,i,s-1} \mathbf{I}_d\big)\big(\tilde{\mathbf{\Delta}}_{t,i,s-2} - \omega_{t,i,s-2} \mathbf{I}_d\big) \mathbf{e}_{t,i,s-2} \qquad (40)
\end{aligned}$$

For the first term, we have

$$\begin{aligned}
&\|\mathbf{B}_t^\top (\mathbf{I}_d - \hat{\mathbf{B}}_{t,i,s-1} \hat{\mathbf{B}}_{t,i,s-1}^\top) \mathbf{e}_{t,i,s-1}\|_2 \\
&\quad \leq \|\mathbf{B}_{t,i,s-1}^\top (\mathbf{I}_d - \hat{\mathbf{B}}_{t,i,s-1} \hat{\mathbf{B}}_{t,i,s-1}^\top) \mathbf{e}_{t,i,s-1}\|_2 \\
&\qquad + \|(\mathbf{B}_t - \mathbf{B}_{t,i,s-1})^\top (\mathbf{I}_d - \hat{\mathbf{B}}_{t,i,s-1} \hat{\mathbf{B}}_{t,i,s-1}^\top) \mathbf{e}_{t,i,s-1}\|_2 \\
&\quad = \|(\mathbf{B}_t - \mathbf{B}_{t,i,s-1})^\top (\mathbf{I}_d - \hat{\mathbf{B}}_{t,i,s-1} \hat{\mathbf{B}}_{t,i,s-1}^\top) \mathbf{e}_{t,i,s-1}\|_2 \qquad (41) \\
&\quad \leq \|(\mathbf{I}_d - \hat{\mathbf{B}}_{t,i,s-1} \hat{\mathbf{B}}_{t,i,s-1}^\top) \mathbf{e}_{t,i,s-1}\|_2 \sum_{r=1}^{s-1} \|\mathbf{B}_{t,i,r} - \mathbf{B}_{t,i,r-1}\|_2 \qquad (42) \\
&\quad \leq 7 \|(\mathbf{I}_d - \hat{\mathbf{B}}_{t,i,s-1} \hat{\mathbf{B}}_{t,i,s-1}^\top) \mathbf{B}_* \mathbf{w}_{*,i}\|_2 \alpha^{1.5} \tau L_{\max}^2 \qquad (43) \\
&\quad \leq 8\alpha^{1.5} \tau L_{\max}^3 \,\mathrm{dist}_t \qquad (44)
\end{aligned}$$

where (41) follows since $\mathbf{B}_{t,i,s-1}^\top (\mathbf{I}_d - \hat{\mathbf{B}}_{t,i,s-1} \hat{\mathbf{B}}_{t,i,s-1}^\top) = \mathbf{0}$, (42) follows using the Cauchy-Schwarz and triangle inequalities, (43) follows using that $(\mathbf{I}_d - \hat{\mathbf{B}}_{t,i,s-1} \hat{\mathbf{B}}_{t,i,s-1}^\top) \mathbf{B}_{t,i,s-1} = \mathbf{0}$ and applying $A_{2,t,i}(\tau)$ and $A_{3,t,i}(\tau)$, (44) follows by the fact that $\|(\mathbf{I}_d - \hat{\mathbf{B}}_{t,i,s-1} \hat{\mathbf{B}}_{t,i,s-1}^\top) \mathbf{B}_*\| = \mathrm{dist}(\mathbf{B}_{t,i,s}, \mathbf{B}_*) \leq 1.1\,\mathrm{dist}_t$ by $A_{4,t,i}(\tau)$. For the second term in (40), note that

$$\begin{aligned}
|\omega_{t,i,s-1}| &\leq \alpha |\mathbf{w}_{t,i,s-1}^\top \mathbf{\Delta}_{t,i,s-1} \mathbf{w}_{t,i,s-1}| + \alpha^2 |\mathbf{w}_{t,i,s-1}^\top \mathbf{B}_{t,i,s-1}^\top \mathbf{B}_* \mathbf{w}_{*,i}| \\
&\leq 8 c_3 \alpha^4 \tau L_{\max}^4 \kappa_{\max}^2 E_0^{-1} + 2.2 \alpha^{1.5} L_{\max}^2 \\
&\leq 3\alpha^2 L_{\max}^2 \qquad (45)
\end{aligned}$$

As a result, we have

$$
\begin{aligned}
&\|\mathbf{B}_t^\top \big(\tilde{\mathbf{\Delta}}_{t,i,s-1} - \omega_{t,i,s-1}\mathbf{I}_d\big)(\mathbf{I}_d - \hat{\mathbf{B}}_{t,i,s-2}\hat{\mathbf{B}}_{t,i,s-2}^\top)\mathbf{e}_{t,i,s-2}\|_2 \\
&\qquad \le \|\mathbf{B}_t^\top \tilde{\mathbf{\Delta}}_{t,i,s-1}(\mathbf{I}_d - \hat{\mathbf{B}}_{t,i,s-2}\hat{\mathbf{B}}_{t,i,s-2}^\top)\mathbf{e}_{t,i,s-2}\|_2 \\
&\qquad\quad + |\omega_{t,i,s-1}|\|\mathbf{B}_t^\top(\mathbf{I}_d - \hat{\mathbf{B}}_{t,i,s-2}\hat{\mathbf{B}}_{t,i,s-2}^\top)\mathbf{e}_{t,i,s-2}\|_2 \\
&\qquad \le \|\mathbf{B}_t^\top \tilde{\mathbf{\Delta}}_{t,i,s-1}(\mathbf{I}_d - \hat{\mathbf{B}}_{t,i,s-2}\hat{\mathbf{B}}_{t,i,s-2}^\top)\mathbf{e}_{t,i,s-2}\|_2 \\
&\qquad\quad + 3.3\alpha^{1.5}L_{\max}^2\|(\mathbf{I}_d - \hat{\mathbf{B}}_{t,i,s-2}\hat{\mathbf{B}}_{t,i,s-2}^\top)\mathbf{B}_*\mathbf{w}_{*,i}\|_2 \\
&\qquad \le \|\mathbf{B}_t^\top \tilde{\mathbf{\Delta}}_{t,i,s-1}(\mathbf{I}_d - \hat{\mathbf{B}}_{t,i,s-2}\hat{\mathbf{B}}_{t,i,s-2}^\top)\mathbf{e}_{t,i,s-2}\|_2 \\
&\qquad\quad + 3.7\alpha^{1.5}L_{\max}^3\,\mathrm{dist}_t \qquad (46)
\end{aligned}
$$

where (46) follows by $A_{4,t,i}(\tau)$, and

$$
\begin{aligned}
&\|\mathbf{B}_t^\top \tilde{\mathbf{\Delta}}_{t,i,s-1}(\mathbf{I}_d - \hat{\mathbf{B}}_{t,i,s-2}\hat{\mathbf{B}}_{t,i,s-2}^\top)\mathbf{e}_{t,i,s-2}\|_2 \\
&\quad \le \|\mathbf{B}_t^\top \hat{\mathbf{B}}_{t,i,s-1}\hat{\mathbf{B}}_{t,i,s-1}^\top(\mathbf{I}_d - \hat{\mathbf{B}}_{t,i,s-2}\hat{\mathbf{B}}_{t,i,s-2}^\top)\mathbf{e}_{t,i,s-2}\|_2 \\
&\qquad + \alpha\|\mathbf{B}_t^\top \mathbf{B}_{t,i,s-1}\mathbf{B}_{t,i,s-1}^\top(\mathbf{I}_d - \hat{\mathbf{B}}_{t,i,s-2}\hat{\mathbf{B}}_{t,i,s-2}^\top)\mathbf{e}_{t,i,s-2}\|_2 \\
&\quad = \|\mathbf{B}_t^\top \hat{\mathbf{B}}_{t,i,s-1}(\mathbf{R}_{t,i,s-1}^{-1})^\top\mathbf{B}_{t,i,s-1}^\top(\mathbf{I}_d - \hat{\mathbf{B}}_{t,i,s-2}\hat{\mathbf{B}}_{t,i,s-2}^\top)\mathbf{e}_{t,i,s-2}\|_2 \\
&\qquad + \alpha\|\mathbf{B}_t^\top \mathbf{B}_{t,i,s-1}\mathbf{B}_{t,i,s-1}^\top(\mathbf{I}_d - \hat{\mathbf{B}}_{t,i,s-2}\hat{\mathbf{B}}_{t,i,s-2}^\top)\mathbf{e}_{t,i,s-2}\|_2 \\
&\quad = \alpha\|\mathbf{B}_t^\top \hat{\mathbf{B}}_{t,i,s-1}(\mathbf{R}_{t,i,s-1}^{-1})^\top\mathbf{w}_{t,i,s-2}\mathbf{e}_{t,i,s-2}^\top(\mathbf{I}_d - \hat{\mathbf{B}}_{t,i,s-2}\hat{\mathbf{B}}_{t,i,s-2}^\top)\mathbf{e}_{t,i,s-2}\|_2 \\
&\qquad + \alpha^2\|\mathbf{B}_t^\top \mathbf{B}_{t,i,s-1}\mathbf{w}_{t,i,s-2}\mathbf{e}_{t,i,s-2}^\top(\mathbf{I}_d - \hat{\mathbf{B}}_{t,i,s-2}\hat{\mathbf{B}}_{t,i,s-2}^\top)\mathbf{e}_{t,i,s-2}\|_2 \qquad (47) \\
&\quad \le 44\alpha^{1.5}L_{\max}^3\,\mathrm{dist}_t \qquad (48)
\end{aligned}
$$

where (47) follows since $\mathbf{B}_{t,i,s-2}(\mathbf{I}_d - \hat{\mathbf{B}}_{t,i,s-2}\hat{\mathbf{B}}_{t,i,s-2}^\top) = \mathbf{0}$ and (48) follows using the Cauchy-Schwarz inequality, $A_3(t)$, $A_{2,t,i}(\tau)$, $A_{3,t,i}(\tau)$, and $A_{4,t,i}(\tau)$. Next, recalling that $\hat{\mathbf{B}}_{t,i,s}\mathbf{R}_{t,i,s}$ is the QR-factorization of $\mathbf{B}_{t,i,s}$, we have, for any s,

$$
\begin{aligned}
\|\tilde{\mathbf{\Delta}}_{t,i,s-1}\| &= \|\hat{\mathbf{B}}_{t,i,s-1}\hat{\mathbf{B}}_{t,i,s-1}^\top - \alpha\mathbf{B}_{t,i,s-1}\mathbf{B}_{t,i,s-1}^\top\| \\
&\le \|\hat{\mathbf{B}}_{t,i,s-1}(\mathbf{I}_k - \alpha\mathbf{R}_{t,i,s-1}\mathbf{R}_{t,i,s-1}^\top)\hat{\mathbf{B}}_{t,i,s-1}^\top\| \\
&\le \|\mathbf{I}_k - \alpha\mathbf{R}_{t,i,s-1}\mathbf{R}_{t,i,s-1}^\top\| \\
&\le \max(|1-\alpha\sigma_{\min}^2(\mathbf{B}_{t,i,s-1})|, |1-\alpha\sigma_{\max}^2(\mathbf{B}_{t,i,s-1})|) \qquad (49) \\
&\le \max(|1-\alpha\tfrac{1-\|\mathbf{\Delta}_{t,i,s-1}\|}{\alpha}|, |1-\alpha\tfrac{1+\|\mathbf{\Delta}_{t,i,s-1}\|}{\alpha})|) \\
&= \|\mathbf{\Delta}_{t,i,s-1}\| \\
&\le 2c_3\alpha^2\tau L_{\max}^2\kappa_{\max}^2 E_0^{-1} \qquad (50)
\end{aligned}
$$

where (49) follows by Weyl's inequality and (50) follows by $A_{3,t,i}(s-1)$. Furthermore, $\|\tilde{\mathbf{\Delta}}_{t,i,s-1} + \omega_{t,i,s-1}\mathbf{I}_d\| \le 2c_3\alpha^2\tau L_{\max}^2\kappa_{\max}^2 E_0^{-1} + 3\alpha^2 L_{\max}^2 \le 3c_3\alpha^2\tau L_{\max}^2\kappa_{\max}^2 E_0^{-1}$ for any s. Thus, for the

third term in (40), for any $s > 2$,

$$
\begin{aligned}
&\|\mathbf{B}_t^\top \big(\tilde{\mathbf{\Delta}}_{t,i,s-1} - \omega_{t,i,s-1}\mathbf{I}_d\big)\big(\tilde{\mathbf{\Delta}}_{t,i,s-2} - \omega_{t,i,s-2}\mathbf{I}_d\big)\mathbf{e}_{t,i,s-2}\|_2 \\
&= \|\mathbf{B}_t^\top \big(\tilde{\mathbf{\Delta}}_{t,i,s-1} - \omega_{t,i,s-1}\mathbf{I}_d\big)\big(\tilde{\mathbf{\Delta}}_{t,i,s-2} - \omega_{t,i,s-2}\mathbf{I}_d\big)(\tilde{\mathbf{\Delta}}_{t,i,s-3} - \omega_{t,i,s-3}\mathbf{I}_d)\mathbf{e}_{t,i,s-3}\|_2 \\
&\quad + \|\mathbf{B}_t^\top \big(\tilde{\mathbf{\Delta}}_{t,i,s-1} - \omega_{t,i,s-1}\mathbf{I}_d\big)\big(\tilde{\mathbf{\Delta}}_{t,i,s-2} - \omega_{t,i,s-2}\mathbf{I}_d\big)(\mathbf{I}_d - \hat{\mathbf{B}}_{t,i,s-3}\hat{\mathbf{B}}_{t,i,s-3}^\top)\mathbf{e}_{t,i,s-3}\|_2 \\
&\le \|\mathbf{B}_t^\top \big(\tilde{\mathbf{\Delta}}_{t,i,s-1} - \omega_{t,i,s-1}\mathbf{I}_d\big)\big(\tilde{\mathbf{\Delta}}_{t,i,s-2} - \omega_{t,i,s-2}\mathbf{I}_d\big)(\tilde{\mathbf{\Delta}}_{t,i,s-3} - \omega_{t,i,s-3}\mathbf{I}_d)\mathbf{e}_{t,i,s-3}\|_2 \\
&\quad + 10c_3^2\alpha^{3.5}\tau^2 L_{\max}^5\kappa_{\max}^4 E_0^{-2}\,\mathrm{dist}_t \\
&\vdots \\
&\le \left\|\mathbf{B}_t^\top \prod_{r=1}^{s}\big(\tilde{\mathbf{\Delta}}_{t,i,s-r} - \omega_{t,i,s-r}\mathbf{I}_d\big)\mathbf{e}_{t,i,s-r}\right\|_2 \\
&\quad + 10c_3^2\alpha^{3.5}\tau^2 L_{\max}^5\kappa_{\max}^4 E_0^{-2}\,\mathrm{dist}_t \sum_{r=0}^{s}(3c_3)^r\alpha^{2r}\tau^r L_{\max}^{2r}\kappa_{\max}^{2r}E_0^{-r} \\
&\le \left\|\mathbf{B}_t^\top \prod_{r=1}^{s}\big(\tilde{\mathbf{\Delta}}_{t,i,s-r} - \omega_{t,i,s-r}\mathbf{I}_d\big)\mathbf{e}_{t,i,s-r}\right\|_2 + \frac{10c_3^2\alpha^{3.5}\tau^2 L_{\max}^5\kappa_{\max}^4 E_0^{-2}\,\mathrm{dist}_t}{1 - 3c_3\alpha^2\tau L_{\max}^2\kappa_{\max}^2 E_0^{-1}} \\
&\le 3.5\times(3c_3)^s\alpha^{2s-0.5}\tau^s L_{\max}^{2s+1}\kappa_{\max}^{2s}E_0^{-s} + 15c_3^2\alpha^{3.5}\tau^2 L_{\max}^5\kappa_{\max}^4 E_0^{-2}\,\mathrm{dist}_t \qquad (51)
\end{aligned}
$$

and for $s = 2$ we have

$$
\begin{aligned}
&\|\mathbf{B}_t^\top \big(\tilde{\mathbf{\Delta}}_{t,i,s-1} - \omega_{t,i,s-1}\mathbf{I}_d\big)\big(\tilde{\mathbf{\Delta}}_{t,i,s-2} - \omega_{t,i,s-2}\mathbf{I}_d\big)\mathbf{e}_{t,i,s-2}\|_2 \\
&\qquad \le 3.5\times(3c_3)^2\alpha^{3.5}\tau^2 L_{\max}^5\kappa_{\max}^4 E_0^{-2}. \qquad (52)
\end{aligned}
$$

Thus, using $\|\mathbf{w}_{t,i,s}\|_2 \le 2\sqrt{\alpha}L_{\max}$ with (40), (44), (46), (48), (51), and (52), we have

$$
\begin{aligned}
\|\alpha^2\mathbf{E}_4\|_2 &\le 2\alpha^{2.5}L_{\max}\sum_{s=2}^{\tau-1}\Bigg(3.5\times(3c_3)^2\alpha^{2s-0.5}\tau^s L_{\max}^{2s+1}\kappa_{\max}^{2s}E_0^{-2s} \\
&\qquad + 15c_3^2\alpha^{3.5}\tau^2 L_{\max}^5\kappa_{\max}^4\,\mathrm{dist}_t + (8\tau+48)\alpha^{1.5}L_{\max}^3\,\mathrm{dist}_t\Bigg) \\
&\le \frac{63c_3^2\alpha^6\tau^2 L_{\max}^6\kappa_{\max}^4 E_0^{-2}}{1 - 3c_s\alpha^2\tau L_{\max}^2\kappa_{\max}^2 E_0^{-1}} + (30c_3^2\alpha^6\tau^3 L_{\max}^6\kappa_{\max}^4 E_0^{-2} + 66\alpha^4\tau^2 L_{\max}^4)\,\mathrm{dist}_t \\
&\le 90c_3^2\alpha^6\tau^2 L_{\max}^6\kappa_{\max}^4 E_0^{-2} + 94\alpha^4\tau^2 L_{\max}^4\,\mathrm{dist}_t
\end{aligned}
$$

where the last inequality follows by choice of α. Combining all terms, we obtain

$$
\begin{aligned}
\|\mathbf{\Delta}_{t+1}\|_2 &\le (1 - 0.15\alpha^2 E_0\mu^2)\|\mathbf{\Delta}_t\|_2 + (206 + 101/c_3)\alpha^4\tau L_{\max}^4 + 32\alpha^4 L_{\max}^4 \\
&\quad + 118c_3^2\alpha^6\tau^2 L_{\max}^6\kappa_{\max}^4 E_0^{-2} + 94\alpha^4\tau^2 L_{\max}^4\,\mathrm{dist}_t \\
&\le (1 - 0.15\alpha^2 E_0\mu^2)\|\mathbf{\Delta}_t\|_2 + (340 + 101/c_3)\alpha^4\tau L_{\max}^4 + 94\alpha^4\tau^2 L_{\max}^4\,\mathrm{dist}_t \qquad (53) \\
&\vdots \\
&\le (1 - 0.15\alpha^2 E_0\mu^2)^t\|\mathbf{\Delta}_0\|_2 \\
&\quad + \sum_{t'=1}^{t}(1 - 0.15\alpha^2 E_0\mu^2)^{t-t'}\big((340 + 101/c_3)\alpha^4\tau L_{\max}^4 + 94\alpha^4\tau^2 L_{\max}^4\,\mathrm{dist}_{t'}\big) \\
&\le \|\mathbf{\Delta}_0\|_2 + (340 + 101/c_3)\alpha^4\tau L_{\max}^4\sum_{t'=1}^{t}(1 - 0.15\alpha^2 E_0\mu^2)^{t-t'} \\
&\quad + 94\alpha^4\tau^2 L_{\max}^4\sum_{t'=1}^{t}(1 - 0.04\alpha^2\tau E_0\mu^2)^{t'} \qquad (54) \\
&\le \|\mathbf{\Delta}_0\|_2 + (7(340 + 101/c_3) + 25\times 94)\alpha^2\tau L_{\max}^2\kappa_{\max}^2 E_0^{-1} \\
&\le \alpha^2\tau L_{\max}^2\kappa_{\max}^2 + (4730 + 101/c_3)\alpha^2\tau L_{\max}^2\kappa_{\max}^2 E_0^{-1} \\
&\le c_3\alpha^2\tau L_{\max}^2\kappa_{\max}^2 \qquad (55)
\end{aligned}
$$

where (53) follows by choice of $\alpha \leq \frac{1-\delta_0}{c_3\sqrt{\tau}L_{\max}^2\kappa_{\max}^2} \leq \frac{E_0}{c_3\sqrt{\tau}L_{\max}^2\kappa_{\max}^2}$, (54) follows from $A_5(t)$, and the last inequality is due to $c_3 = 4800$.

□

Lemma 10. $\cap_{i\in\mathcal{I}_t}\big(A_{1,t,i}(\tau)\cap A_{2,t,i}(\tau)\cap A_{3,t,i}(\tau)\big)\cap A_2(t) \implies A_4(t+1)$.

Proof. We have

$$\mathbf{B}_{t+1} = \mathbf{B}_t\left(\frac{1}{m}\sum_{i\in\mathcal{I}_t}\prod_{s=0}^{\tau-1}(\mathbf{I}_k - \alpha\mathbf{w}_{t,i,s}\mathbf{w}_{t,i,s}^\top)\right) + \hat{\mathbf{B}}_*\left(\frac{\alpha}{m}\sum_{i\in\mathcal{I}_t}\mathbf{w}_{*,i}\sum_{s=0}^{\tau-1}\mathbf{w}_{t,i,s}^\top\prod_{r=s+1}^{\tau-1}(\mathbf{I}_k - \alpha\mathbf{w}_{t,i,r}\mathbf{w}_{t,i,r}^\top)\right)$$

which implies

$$\mathbf{B}_{*,\perp}^\top\mathbf{B}_{t+1} = \mathbf{B}_{*,\perp}^\top\mathbf{B}_t(\mathbf{I} - \alpha\mathbf{w}_t\mathbf{w}_t^\top)\left(\frac{1}{m}\sum_{i\in\mathcal{I}_t}\prod_{s=1}^{\tau-1}(\mathbf{I}_k - \alpha\mathbf{w}_{t,i,s}\mathbf{w}_{t,i,s}^\top)\right) \tag{56}$$

We can expand the right product of $\mathbf{B}_t(\mathbf{I} - \alpha\mathbf{w}_t\mathbf{w}_t^\top)$ using the binomial expansion as follows:

$$\begin{aligned}\frac{1}{m}\sum_{i\in\mathcal{I}_t}\prod_{s=1}^{\tau-1}(\mathbf{I}_k - \alpha\mathbf{w}_{t,i,s}\mathbf{w}_{t,i,s}^\top) = \mathbf{I}_k &- \frac{\alpha}{m}\sum_{i\in\mathcal{I}_t}\sum_{s=1}^{\tau-1}\mathbf{w}_{t,i,s}\mathbf{w}_{t,i,s}^\top \\ &+ \frac{\alpha^2}{m}\sum_{i\in\mathcal{I}_t}\sum_{s=1}^{\tau-1}\sum_{s^{(1)}=s+1}^{\tau-1}\mathbf{w}_{t,i,s}\mathbf{w}_{t,i,s}^\top\mathbf{w}_{t,i,s^{(1)}}\mathbf{w}_{t,i,s^{(1)}}^\top \\ &- \cdots + \mathrm{sign}(\tau)\frac{\alpha^\tau}{m}\sum_{i\in\mathcal{I}_t}\prod_{s=1}^{\tau-1}\mathbf{w}_{t,i,s}\mathbf{w}_{t,i,s}^\top\end{aligned}$$

Recall that each $\|\mathbf{w}_{t,i,s}\|_2 \leq 2\sqrt{\alpha}L_{\max}$. Thus, after the identity, the spectral norm of the first set of summations has spectral norm at most $4\alpha^2\tau L_{\max}^2$, the second set has specral norm at most $16\alpha^4\tau^2L_{\max}^4$, and so on. We in fact use the first set of summations as a negative term, and bound all subsequent sets of summations as errors, exploiting the fact that their norms are geometrically decaying. In particular, we have:

$$\begin{aligned}\left\|\frac{1}{m}\sum_{i\in\mathcal{I}_t}\prod_{s=1}^{\tau-1}(\mathbf{I}_k - \alpha\mathbf{w}_{t,i,s}\mathbf{w}_{t,i,s}^\top)\right\|_2 &\leq \left\|\mathbf{I}_k - \frac{\alpha}{m}\sum_{i\in\mathcal{I}_t}\sum_{s=1}^{\tau-1}\mathbf{w}_{t,i,s}\mathbf{w}_{t,i,s}^\top\right\|_2 + \sum_{z=2}^{\tau-1}(4\alpha^2\tau L_{\max}^2)^z \\ &\leq \left\|\mathbf{I}_k - \frac{\alpha}{m}\sum_{i\in\mathcal{I}_t}\sum_{s=1}^{\tau-1}\mathbf{w}_{t,i,s}\mathbf{w}_{t,i,s}^\top\right\|_2 + \frac{4\alpha^4\tau^2L_{\max}^4}{1-4\alpha^2\tau L_{\max}^2} \\ &\leq \left\|\mathbf{I}_k - \frac{\alpha}{m}\sum_{i\in\mathcal{I}_t}\sum_{s=1}^{\tau-1}\mathbf{w}_{t,i,s}\mathbf{w}_{t,i,s}^\top\right\|_2 + 5\alpha^4\tau^2L_{\max}^4\end{aligned} \tag{57}$$

Next, we use $\|\mathbf{w}_{t,i,s} - \alpha\mathbf{B}_{t,i,s-1}^\top\mathbf{B}_*\mathbf{w}_{*,i}\| \leq 4c_3\alpha^{2.5}\tau L_{\max}^3\kappa_{\max}^2E_0^{-1}$ for all $s \geq 1$ to obtain

$$\begin{aligned}\left\|\mathbf{I}_k - \frac{\alpha}{m}\sum_{i\in\mathcal{I}_t}\sum_{s=1}^{\tau-1}\mathbf{w}_{t,i,s}\mathbf{w}_{t,i,s}^\top\right\|_2 \leq &\left\|\mathbf{I}_k - \frac{\alpha^3}{m}\sum_{i\in\mathcal{I}_t}\sum_{s=1}^{\tau-1}\mathbf{B}_{t,i,s-1}^\top\mathbf{B}_*\mathbf{w}_{*,i}\mathbf{w}_{*,i}^\top\mathbf{B}_*^\top\mathbf{B}_{t,i,s-1}\right\|_2 \\ &+ 13c_3\alpha^4\tau^2L_{\max}^4\kappa_{\max}^2E_0^{-1}\end{aligned} \tag{58}$$

Next, we have for any $s-1 \in \{1, \ldots, \tau-1\}$,

$$\begin{aligned}
\|\mathbf{B}_{t,i,s-1} - \mathbf{B}_t\|_2 = \|\mathbf{B}_{t,i,s-1} - \mathbf{B}_{t,i,0}\|_2 &\leq \sum_{r=1}^{s-1} \|\mathbf{B}_{t,i,r} - \mathbf{B}_{t,i,r-1}\|_2 \\
&\leq \alpha \sum_{r=1}^{s-1} \|\mathbf{e}_{t,i,r-1}\|_2 \|\mathbf{w}_{t,i,r-1}\|_2 \\
&\leq 7\alpha^{1.5}(s-1)L_{\max}^2
\end{aligned}$$

Thus,

$$\begin{aligned}
&\left\| \mathbf{I}_k - \frac{\alpha^3}{m} \sum_{i \in \mathcal{I}_t} \sum_{s=1}^{\tau-1} \mathbf{B}_{t,i,s-1}^\top \mathbf{B}_* \mathbf{w}_{*,i} \mathbf{w}_{*,i}^\top \mathbf{B}_*^\top \mathbf{B}_{t,i,s-1} \right\|_2 \\
&\qquad \leq \left\| \mathbf{I}_k - \frac{\alpha^3}{m} \sum_{i \in \mathcal{I}_t} \sum_{s=1}^{\tau-1} \mathbf{B}_t^\top \mathbf{B}_* \mathbf{w}_{*,i} \mathbf{w}_{*,i}^\top \mathbf{B}_*^\top \mathbf{B}_t \right\|_2 \\
&\qquad\quad + \left\| \frac{\alpha^3}{m} \sum_{i \in \mathcal{I}_t} \sum_{s=1}^{\tau-1} (\mathbf{B}_t - \mathbf{B}_{t,i,s-1})^\top \mathbf{B}_* \mathbf{w}_{*,i} \mathbf{w}_{*,i}^\top \mathbf{B}_*^\top \mathbf{B}_{t,i,s-1} \right\|_2 \\
&\qquad\quad + \left\| \frac{\alpha^3}{m} \sum_{i \in \mathcal{I}_t} \sum_{s=1}^{\tau-1} \mathbf{B}_t^\top \mathbf{B}_* \mathbf{w}_{*,i} \mathbf{w}_{*,i}^\top \mathbf{B}_*^\top (\mathbf{B}_t - \mathbf{B}_{t,i,s-1}) \right\|_2 \\
&\qquad \leq \left\| \mathbf{I}_k - \frac{\alpha^3}{m} \sum_{i \in \mathcal{I}_t} \sum_{s=1}^{\tau-1} \mathbf{B}_t^\top \mathbf{B}_* \mathbf{w}_{*,i} \mathbf{w}_{*,i}^\top \mathbf{B}_*^\top \mathbf{B}_t \right\|_2 + 16\alpha^4(\tau-1)^2 L_{\max}^4. \qquad (59)
\end{aligned}$$

Furtheromre,

$$\begin{aligned}
&\left\| \mathbf{I}_k - \tfrac{\alpha^3}{m} \sum_{i \in \mathcal{I}_t} \sum_{s=1}^{\tau-1} \mathbf{B}_t^\top \mathbf{B}_* \mathbf{w}_{*,i} \mathbf{w}_{*,i}^\top \mathbf{B}_*^\top \mathbf{B}_t \right\|_2 \\
&= \left\| \mathbf{I}_k - \tfrac{\alpha^3(\tau-1)}{m} \sum_{i \in \mathcal{I}_t} \mathbf{B}_t^\top \mathbf{B}_* \mathbf{w}_{*,i} \mathbf{w}_{*,i}^\top \mathbf{B}_*^\top \mathbf{B}_t \right\|_2 \\
&\leq \left\| \mathbf{I}_k - \tfrac{\alpha^3(\tau-1)}{M} \sum_{i=1}^{M} \mathbf{B}_t^\top \mathbf{B}_* \mathbf{w}_{*,i} \mathbf{w}_{*,i}^\top \mathbf{B}_*^\top \mathbf{B}_t \right\|_2 \\
&\quad + \alpha^3(\tau-1)\|\mathbf{B}_t^\top \mathbf{B}_*\|_2^2 \left\| \tfrac{1}{m} \sum_{i \in \mathcal{I}_t} \left(\mathbf{w}_{*,i}\mathbf{w}_{*,i}^\top - \tfrac{1}{M} \sum_{i=1}^{M} \mathbf{w}_{*,i}\mathbf{w}_{*,i}^\top \right) \right\|_2 \\
&\leq \left\| \mathbf{I}_k - \tfrac{\alpha^3(\tau-1)}{M} \sum_{i=1}^{M} \mathbf{B}_t^\top \mathbf{B}_* \mathbf{w}_{*,i} \mathbf{w}_{*,i}^\top \mathbf{B}_*^\top \mathbf{B}_t \right\|_2 + 6\alpha^4(\tau-1)L_{\max}^4, \qquad (60)
\end{aligned}$$

noting that (60) follows since we are conditioning on the event A_0. Finally,

$$\begin{aligned}
&\left\| \mathbf{I}_k - \tfrac{\alpha^3(\tau-1)}{M} \sum_{i=1}^{M} \mathbf{B}_t^\top \mathbf{B}_* \mathbf{w}_{*,i} \mathbf{w}_{*,i}^\top \mathbf{B}_*^\top \mathbf{B}_t \right\|_2 \\
&\leq 1 - \alpha^3(\tau-1)\sigma_{\min}^2(\mathbf{B}_t^\top \mathbf{B}_*)\sigma_{\min}\left(\tfrac{1}{M} \sum_{i=1}^{M} \mathbf{w}_{*,i}\mathbf{w}_{*,i}^\top \right) \\
&\leq 1 - \alpha^3(\tau-1)\sigma_{\min}^2(\mathbf{B}_t^\top \mathbf{B}_*)\sigma_{\min}\left(\tfrac{1}{M} \sum_{i=1}^{M} \mathbf{w}_{*,i}\mathbf{w}_{*,i}^\top - \bar{\mathbf{w}}_*\bar{\mathbf{w}}_*^\top \right) \\
&= 1 - \alpha^3(\tau-1)\sigma_{\min}(\mathbf{B}_t^\top \mathbf{B}_*)^2\sigma_{\min}\left(\tfrac{1}{M} \sum_{i=1}^{M} (\mathbf{w}_{*,i} - \bar{\mathbf{w}}_*)(\mathbf{w}_{*,i} - \bar{\mathbf{w}}_*)^\top \right) \\
&\leq 1 - 0.1\alpha^2(\tau-1)E_0\mu \qquad (61) \\
&\leq 1 - 0.05\alpha^2\tau E_0\mu \qquad (62)
\end{aligned}$$

where (61) follows by Lemma 8 and Assumption 2, and (62) follows since $\tau \geq 2$. Combining (62), (60), (59), (58), (57), and (56), we obtain

$$\begin{aligned}
\|\mathbf{B}_{*,\perp}^\top \mathbf{B}_{t+1}\|_2 &\leq \Big(1 - 0.05\alpha^2\tau E_0\mu^2 + 6\alpha^4(\tau-1)L_{\max}^4 + 16\alpha^4(\tau-1)^2 L_{\max}^4 \\
&\qquad + 13c_3\alpha^4\tau^2 L_{\max}^4 \kappa_{\max}^2 E_0^{-1} + 5\alpha^4\tau^2 L_{\max}^4 \Big) \|\mathbf{B}_{*,\perp}^\top \mathbf{B}_t\|_2 \\
&\leq \big(1 - 0.05\alpha^2\tau E_0\mu^2 + (24/c_3^2)\alpha^2\tau E_0\mu^2 + (13/c_3)\alpha^2\tau E_0\mu^2\big)\|\mathbf{B}_{*,\perp}^\top \mathbf{B}_t\|_2 \\
&\leq (1 - 0.04\alpha^2\tau E_0\mu^2)\|\mathbf{B}_{*,\perp}^\top \mathbf{B}_t\|_2 \qquad (63)
\end{aligned}$$

using $\alpha^2\tau \leq \frac{(1-\delta_0)^2}{c_3^2\tau\kappa_{\max}^4 L_{\max}^2} \leq \frac{E_0^2}{c_3^3\tau\kappa_{\max}^4 L_{\max}^2}$ and $c_3 > 1305$. □

Lemma 11. $A_3(t+1) \cap A_4(t+1) \cap A_5(t) \implies A_5(t+1)$

Proof. We use the contraction of $\|\mathbf{B}_{*,\perp}^\top \mathbf{B}_s\|_2$ ($A_4(t)$) and the fact that $\|\mathbf{\Delta}_s\|_2$ is small for all $s \in [t]$ ($A_5(t)$), as in Lemma 8, to obtain

$$\begin{aligned}
\mathrm{dist}_{t+1} &= \|\mathbf{B}_{*,\perp}^\top \hat{\mathbf{B}}_{t+1}\|_2 \\
&\leq \tfrac{1}{\sigma_{\min}(\mathbf{B}_{t+1})}\|\mathbf{B}_{*,\perp}^\top \mathbf{B}_{t+1}\|_2 \\
&\leq \tfrac{1}{\sigma_{\min}(\mathbf{B}_{t+1})}(1 - 0.04\alpha^2\tau E_0\mu^2)\|\mathbf{B}_{*,\perp}^\top \mathbf{B}_t\|_2 \\
&\;\;\vdots \\
&\leq \tfrac{1}{\sigma_{\min}(\mathbf{B}_{t+1})}(1 - 0.04\alpha^2\tau E_0\mu^2)^t\|\mathbf{B}_{*,\perp}^\top \mathbf{B}_0\|_2 \\
&\leq \tfrac{\sigma_{\max}(\mathbf{B}_0)}{\sigma_{\min}(\mathbf{B}_{t+1})}(1 - 0.04\alpha^2\tau E_0\mu^2)^t\delta_0 \\
&\leq \tfrac{\sqrt{1+\|\mathbf{\Delta}_0\|_2}/\sqrt{\alpha}}{\sqrt{1-\|\mathbf{\Delta}_{t+1}\|_2}/\sqrt{\alpha}}(1 - 0.04\alpha^2\tau E_0\mu^2)^t\delta_0
\end{aligned}$$

Now, we argue as in (26) (with $\|\mathbf{\Delta}_t\|$ replaced by $\|\mathbf{\Delta}_{t+1}$ without anything changing in the analysis) to find $\frac{\sqrt{1+\|\mathbf{\Delta}_0\|_2}/\sqrt{\alpha}}{\sqrt{1-\|\mathbf{\Delta}_{t+1}\|_2}/\sqrt{\alpha}}\delta_0 \leq \frac{2+\delta_0}{3} \leq 1$. Thus $\mathrm{dist}_{t+1} \leq (1 - 0.04\alpha^2\tau E_0\mu^2)^t$ as desired. □

B.2 Proof of Proposition 1

Proposition 2 (Distributed GD lower bound)**.** *Suppose we are in the setting described in Section 3 and $d > k > 1$. Then for any set of ground-truth heads $\{\mathbf{w}_{*,i}\}_{i=1}^M$, full-rank initialization $\mathbf{B}_0 \in \mathbb{R}^{d\times k}$, initial distance $\delta_0 \in (0, 1/2]$, step size $\alpha > 0$, and number of rounds T, there exists $\mathbf{B}_* \in \mathcal{O}^{d\times k}$ satisfying $\mathrm{dist}(\mathbf{B}_0, \mathbf{B}_*) = \delta_0$ and $\mathrm{dist}(\mathbf{B}_T^{D\text{-}GD}, \mathbf{B}_*) \geq 0.7\delta_0$, where*

$\mathbf{B}_T^{\text{D-GD}} \equiv \mathbf{B}_T^{\text{D-GD}}(\mathbf{B}_0, \mathbf{B}_*, \{\mathbf{w}_{*,i}\}_{i=1}^M, \alpha)$ *is the result of D-GD with step size* α *and initialization* $\mathbf{B}_0$ *in the setting with ground-truth representation* $\mathbf{B}_*$ *and ground-truth heads* $\{\mathbf{w}_{*,i}\}_{i=1}^M$.

Proof. Recall that $\mathbf{B}_T^{\text{D-GD}}(\mathbf{B}_0, \mathbf{B}_*, \{\mathbf{w}_{*,i}\}_{i=1}^M, \alpha)$ is the result of D-GD with step size α and initialization $\mathbf{B}_0$ on the system with ground-truth representation $\mathbf{B}_*$ and ground-truth heads $\{\mathbf{w}_{*,i}\}_{i=1}^M$.

There are two disjoint cases: (1) for all $\mathbf{B}_* \in \mathcal{B} \coloneqq \{\mathbf{B} \in \mathcal{O}^{d\times k} : \operatorname{dist}(\mathbf{B}_0, \mathbf{B}) = \delta_0, \mathbf{B}\bar{\mathbf{w}}_* \in \operatorname{col}(\mathbf{B}_0)\}$, $\operatorname{dist}(\mathbf{B}_T^{\text{D-GD}}(\mathbf{B}_0, \mathbf{B}_*, \{\mathbf{w}_{*,i}\}_{i=1}^M, \alpha), \mathbf{B}_*) \geq 0.7\delta_0$, or (2) there exists some $\mathbf{B}_* \in \mathcal{B}$ such that $\operatorname{dist}(\mathbf{B}_T^{\text{D-GD}}(\mathbf{B}_0, \mathbf{B}_*, \{\mathbf{w}_{*,i}\}_{i=1}^M, \alpha), \mathbf{B}_*) < 0.7\delta_0$. If case (1) holds then the proof is complete. Otherwise, let $\mathbf{B}_* \in \mathcal{B}$ such that $\operatorname{dist}(\mathbf{B}_T^{\text{D-GD}}(\mathbf{B}_0, \mathbf{B}_*, \{\mathbf{w}_{*,i}\}_{i=1}^M, \alpha), \mathbf{B}_*) < 0.7\delta_0$. We will show that there exists another $\mathbf{B}_{*'} \in \mathcal{B}$ such that $\operatorname{dist}(\mathbf{B}_T^{\text{D-GD}}(\mathbf{B}_0, \mathbf{B}_{*'}, \{\mathbf{w}_{*,i}\}_{i=1}^M, \alpha), \mathbf{B}_{*'}) \geq \delta_0$, so D-GD cannot guarantee to recover the ground-truth representation, completing the proof.

Consider case (2). Without loss of generality we can write $\mathbf{B}_0 = \frac{1}{\|\bar{\mathbf{w}}_*\|}\mathbf{B}_*\bar{\mathbf{w}}_*\mathbf{v}_0^\top + \tilde{\mathbf{B}}_0\tilde{\mathbf{V}}_0^\top$ for some $\mathbf{v}_0 \in \mathbb{R}^k : \|\mathbf{v}_0\| = 1$, $\tilde{\mathbf{B}}_0 \in \mathcal{O}^{d\times k-1} : \tilde{\mathbf{B}}_0^\top\mathbf{B}_*\bar{\mathbf{w}}_* = \mathbf{0}$, $\tilde{\mathbf{V}}_0 \in \mathcal{O}^{k\times k-1} : \tilde{\mathbf{V}}_0^\top\mathbf{v}_0 = \mathbf{0}$ using the SVD, since $\mathbf{B}_*\bar{\mathbf{w}}_* \in \operatorname{col}(\mathbf{B}_0)$. Likewise, we can write $\mathbf{B}_* = \frac{1}{\|\bar{\mathbf{w}}_*\|^2}\mathbf{B}_*\bar{\mathbf{w}}_*\bar{\mathbf{w}}_*^\top + \tilde{\mathbf{B}}_*\tilde{\mathbf{V}}_*^\top$ for some $\tilde{\mathbf{B}}_* \in \mathcal{O}^{d\times k-1} : \tilde{\mathbf{B}}_*^\top\mathbf{B}_*\bar{\mathbf{w}}_* = \mathbf{0}$, $\tilde{\mathbf{V}}_* \in \mathcal{O}^{k\times k-1} : \tilde{\mathbf{V}}_*^\top\bar{\mathbf{w}}_* = \mathbf{0}$. Using these decompositions, we can see that

$$
\begin{aligned}
\mathbf{B}_*\mathbf{B}_*^\top &= \big(\tfrac{1}{\|\bar{\mathbf{w}}_*\|^2}\mathbf{B}_*\bar{\mathbf{w}}_*\bar{\mathbf{w}}_*^\top + \tilde{\mathbf{B}}_*\tilde{\mathbf{V}}_*^\top\big)\big(\tfrac{1}{\|\bar{\mathbf{w}}_*\|^2}\mathbf{B}_*\bar{\mathbf{w}}_*\bar{\mathbf{w}}_*^\top + \tilde{\mathbf{B}}_*\tilde{\mathbf{V}}_*^\top\big)^\top \\
&= \tfrac{1}{\|\bar{\mathbf{w}}_*\|^4}\mathbf{B}_*\bar{\mathbf{w}}_*\bar{\mathbf{w}}_*^\top\bar{\mathbf{w}}_*\bar{\mathbf{w}}_*^\top\mathbf{B}_*^\top + \tfrac{1}{\|\bar{\mathbf{w}}_*\|^2}\mathbf{B}_*\bar{\mathbf{w}}_*\bar{\mathbf{w}}_*^\top\tilde{\mathbf{V}}_*\tilde{\mathbf{B}}_*^\top + \tfrac{1}{\|\bar{\mathbf{w}}_*\|^2}\tilde{\mathbf{B}}_*\tilde{\mathbf{V}}_*^\top\bar{\mathbf{w}}_*\bar{\mathbf{w}}_*^\top\mathbf{B}_*^\top \\
&\quad + \tilde{\mathbf{B}}_*\tilde{\mathbf{V}}_*^\top\tilde{\mathbf{V}}_*\tilde{\mathbf{B}}_*^\top \\
&= \tfrac{1}{\|\bar{\mathbf{w}}_*\|^2}\mathbf{B}_*\bar{\mathbf{w}}_*\bar{\mathbf{w}}_*^\top\mathbf{B}_*^\top + \tilde{\mathbf{B}}_*\tilde{\mathbf{B}}_*^\top
\end{aligned}
$$

and

$$
\begin{aligned}
\delta_0 &\coloneqq \operatorname{dist}(\mathbf{B}_0, \mathbf{B}_*) \\
&\coloneqq \|(\mathbf{I}_d - \mathbf{B}_*\mathbf{B}_*^\top)\mathbf{B}_0\| \\
&= \big\|\big(\mathbf{I}_d - \tfrac{1}{\|\bar{\mathbf{w}}_*\|^2}\mathbf{B}_*\bar{\mathbf{w}}_*\bar{\mathbf{w}}_*^\top\mathbf{B}_*^\top - \tilde{\mathbf{B}}_*\tilde{\mathbf{B}}_*^\top\big)\big(\tfrac{1}{\|\bar{\mathbf{w}}_*\|}\mathbf{B}_*\bar{\mathbf{w}}_*\mathbf{v}_0^\top + \tilde{\mathbf{B}}_0\tilde{\mathbf{V}}_0^\top\big)\big\| \\
&= \big\|\big(\mathbf{I}_d - \tfrac{1}{\|\bar{\mathbf{w}}_*\|^2}\mathbf{B}_*\bar{\mathbf{w}}_*\bar{\mathbf{w}}_*^\top\mathbf{B}_*^\top - \tilde{\mathbf{B}}_*\tilde{\mathbf{B}}_*^\top\big)\tfrac{1}{\|\bar{\mathbf{w}}_*\|}\mathbf{B}_*\bar{\mathbf{w}}_*\mathbf{v}_0^\top \\
&\quad + \big(\mathbf{I}_d - \tfrac{1}{\|\bar{\mathbf{w}}_*\|^2}\mathbf{B}_*\bar{\mathbf{w}}_*\bar{\mathbf{w}}_*^\top\mathbf{B}_*^\top - \tilde{\mathbf{B}}_*\tilde{\mathbf{B}}_*^\top\big)\tilde{\mathbf{B}}_0\tilde{\mathbf{V}}_0^\top\big\| \\
&= \big\|\big(\mathbf{I}_d - \tfrac{1}{\|\bar{\mathbf{w}}_*\|^2}\mathbf{B}_*\bar{\mathbf{w}}_*\bar{\mathbf{w}}_*^\top\mathbf{B}_*^\top - \tilde{\mathbf{B}}_*\tilde{\mathbf{B}}_*^\top\big)\tilde{\mathbf{B}}_0\tilde{\mathbf{V}}_0^\top\big\| \\
&= \big\|\big(\mathbf{I}_d - \tilde{\mathbf{B}}_*\tilde{\mathbf{B}}_*^\top\big)\tilde{\mathbf{B}}_0\tilde{\mathbf{V}}_0^\top\big\| \\
&= \big\|\big(\mathbf{I}_d - \tilde{\mathbf{B}}_*\tilde{\mathbf{B}}_*^\top\big)\tilde{\mathbf{B}}_0\big\| \\
&= \operatorname{dist}(\tilde{\mathbf{B}}_0, \tilde{\mathbf{B}}_*).
\end{aligned} \tag{64}
$$

Next, let $\mathbf{B}_{*'} = \frac{1}{\|\bar{\mathbf{w}}_*\|^2}\mathbf{B}_*\bar{\mathbf{w}}_*\bar{\mathbf{w}}_*^\top + (2\tilde{\mathbf{B}}_0\tilde{\mathbf{B}}_0^\top\tilde{\mathbf{B}}_* - \tilde{\mathbf{B}}_*)\tilde{\mathbf{V}}_*^\top$. We first check that $\mathbf{B}_{*'} \in \mathcal{O}^{d\times k}$:

$$
\begin{aligned}
\mathbf{B}_{*'}^\top\mathbf{B}_{*'} &= \big(\tfrac{1}{\|\bar{\mathbf{w}}_*\|^2}\mathbf{B}_*\bar{\mathbf{w}}_*\bar{\mathbf{w}}_*^\top + (2\tilde{\mathbf{B}}_0\tilde{\mathbf{B}}_0^\top\tilde{\mathbf{B}}_* - \tilde{\mathbf{B}}_*)\tilde{\mathbf{V}}_*^\top\big)^\top\big(\tfrac{1}{\|\bar{\mathbf{w}}_*\|^2}\mathbf{B}_*\bar{\mathbf{w}}_*\bar{\mathbf{w}}_*^\top + (2\tilde{\mathbf{B}}_0\tilde{\mathbf{B}}_0^\top\tilde{\mathbf{B}}_* - \tilde{\mathbf{B}}_*)\tilde{\mathbf{V}}_*^\top\big) \\
&= \tfrac{1}{\|\bar{\mathbf{w}}_*\|^2}\bar{\mathbf{w}}_*\bar{\mathbf{w}}_*^\top + \tilde{\mathbf{V}}_*(2\tilde{\mathbf{B}}_0\tilde{\mathbf{B}}_0^\top\tilde{\mathbf{B}}_* - \tilde{\mathbf{B}}_*)^\top(2\tilde{\mathbf{B}}_0\tilde{\mathbf{B}}_0^\top\tilde{\mathbf{B}}_* - \tilde{\mathbf{B}}_*)\tilde{\mathbf{V}}_*^\top \qquad (65) \\
&= \tfrac{1}{\|\bar{\mathbf{w}}_*\|^2}\bar{\mathbf{w}}_*\bar{\mathbf{w}}_*^\top + \tilde{\mathbf{V}}_*(4\tilde{\mathbf{B}}_*^\top\tilde{\mathbf{B}}_0\tilde{\mathbf{B}}_0^\top\tilde{\mathbf{B}}_0\tilde{\mathbf{B}}_0^\top\tilde{\mathbf{B}}_* - 4\tilde{\mathbf{B}}_*^\top\tilde{\mathbf{B}}_0\tilde{\mathbf{B}}_0^\top\tilde{\mathbf{B}}_* + \tilde{\mathbf{B}}_*^\top\tilde{\mathbf{B}}_*)\tilde{\mathbf{V}}_*^\top \\
&= \tfrac{1}{\|\bar{\mathbf{w}}_*\|^2}\bar{\mathbf{w}}_*\bar{\mathbf{w}}_*^\top + \tilde{\mathbf{V}}_*\tilde{\mathbf{V}}_*^\top \\
&= [\tilde{\mathbf{V}}_*, \tfrac{1}{\|\bar{\mathbf{w}}_*\|}\bar{\mathbf{w}}_*][\tilde{\mathbf{V}}_*, \tfrac{1}{\|\bar{\mathbf{w}}_*\|}\bar{\mathbf{w}}_*]^\top \\
&= \mathbf{I}_k \qquad (66)
\end{aligned}
$$

as desired, where (65) follows since $\tilde{\mathbf{B}}_*^\top \mathbf{B}_* \bar{\mathbf{w}}_* = \tilde{\mathbf{B}}_0^\top \mathbf{B}_* \bar{\mathbf{w}}_* = \mathbf{0}$, and (66) follows since $[\tilde{\mathbf{V}}_*, \frac{1}{\|\bar{\mathbf{w}}_*\|}\bar{\mathbf{w}}_*] \in \mathcal{O}^{k\times k}$ by the definition of the SVD. Furthermore,

$$
\begin{aligned}
\operatorname{dist}(\mathbf{B}_0, \mathbf{B}_{*'}) &= \|(\mathbf{I}_d - \mathbf{B}_0\mathbf{B}_0^\top)\mathbf{B}_{*'}\| \\
&= \|(\mathbf{I}_d - \tfrac{1}{\|\bar{\mathbf{w}}_*\|^2}\mathbf{B}_*\bar{\mathbf{w}}_*\bar{\mathbf{w}}_*^\top\mathbf{B}_*^\top - \tilde{\mathbf{B}}_0\tilde{\mathbf{B}}_0^\top)\big(\tfrac{1}{\|\bar{\mathbf{w}}_*\|^2}\mathbf{B}_*\bar{\mathbf{w}}_*\bar{\mathbf{w}}_*^\top + (2\tilde{\mathbf{B}}_0\tilde{\mathbf{B}}_0^\top\tilde{\mathbf{B}}_* - \tilde{\mathbf{B}}_*)\tilde{\mathbf{V}}_*^\top\big)\| \\
&= \|(\mathbf{I}_d - \tfrac{1}{\|\bar{\mathbf{w}}_*\|^2}\mathbf{B}_*\bar{\mathbf{w}}_*\bar{\mathbf{w}}_*^\top\mathbf{B}_*^\top - \tilde{\mathbf{B}}_0\tilde{\mathbf{B}}_0^\top)\tfrac{1}{\|\bar{\mathbf{w}}_*\|^2}\mathbf{B}_*\bar{\mathbf{w}}_*\bar{\mathbf{w}}_*^\top \\
&\quad + (\mathbf{I}_d - \tfrac{1}{\|\bar{\mathbf{w}}_*\|^2}\mathbf{B}_*\bar{\mathbf{w}}_*\bar{\mathbf{w}}_*^\top\mathbf{B}_*^\top - \tilde{\mathbf{B}}_0\tilde{\mathbf{B}}_0^\top)(2\tilde{\mathbf{B}}_0\tilde{\mathbf{B}}_0^\top\tilde{\mathbf{B}}_* - \tilde{\mathbf{B}}_*)\tilde{\mathbf{V}}_*^\top\| \\
&= \|(\mathbf{I}_d - \tfrac{1}{\|\bar{\mathbf{w}}_*\|^2}\mathbf{B}_*\bar{\mathbf{w}}_*\bar{\mathbf{w}}_*^\top\mathbf{B}_*^\top - \tilde{\mathbf{B}}_0\tilde{\mathbf{B}}_0^\top)(2\tilde{\mathbf{B}}_0\tilde{\mathbf{B}}_0^\top\tilde{\mathbf{B}}_* - \tilde{\mathbf{B}}_*)\tilde{\mathbf{V}}_*^\top\| \\
&= \|(\mathbf{I}_d - \tilde{\mathbf{B}}_0\tilde{\mathbf{B}}_0^\top)(2\tilde{\mathbf{B}}_0\tilde{\mathbf{B}}_0^\top\tilde{\mathbf{B}}_* - \tilde{\mathbf{B}}_*)\tilde{\mathbf{V}}_*^\top\| \\
&= \|(\mathbf{I}_d - \tilde{\mathbf{B}}_0\tilde{\mathbf{B}}_0^\top)\tilde{\mathbf{B}}_*\tilde{\mathbf{V}}_*^\top\| \\
&= \|(\mathbf{I}_d - \tilde{\mathbf{B}}_0\tilde{\mathbf{B}}_0^\top)\tilde{\mathbf{B}}_*\| \\
&= \operatorname{dist}(\tilde{\mathbf{B}}_*, \tilde{\mathbf{B}}_0) \\
&= \delta_0 \qquad (67)
\end{aligned}
$$

where (67) follows from (64). Moreover, $\mathbf{B}_{*'}\bar{\mathbf{w}}_* = \mathbf{B}_*\bar{\mathbf{w}}_* \in \operatorname{col}(\mathbf{B}_0)$, thus $\mathbf{B}_{*'} \in \mathcal{B}$. Next,

$$
\begin{aligned}
\operatorname{dist}(\mathbf{B}_*, \mathbf{B}_{*'}) &= \|(\mathbf{I}_d - \mathbf{B}_*\mathbf{B}_*^\top)\mathbf{B}_{*'}\| \\
&= \|(\mathbf{I}_d - \tfrac{1}{\|\bar{\mathbf{w}}_*\|^2}\mathbf{B}_*\bar{\mathbf{w}}_*\bar{\mathbf{w}}_*^\top\mathbf{B}_*^\top - \tilde{\mathbf{B}}_*\tilde{\mathbf{B}}_*^\top)\big(\tfrac{1}{\|\bar{\mathbf{w}}_*\|^2}\mathbf{B}_*\bar{\mathbf{w}}_*\bar{\mathbf{w}}_*^\top + (2\tilde{\mathbf{B}}_0\tilde{\mathbf{B}}_0^\top\tilde{\mathbf{B}}_* - \tilde{\mathbf{B}}_*)\tilde{\mathbf{V}}_*^\top\big)\| \\
&= \|(\mathbf{I}_d - \tilde{\mathbf{B}}_*\tilde{\mathbf{B}}_*^\top)(2\tilde{\mathbf{B}}_0\tilde{\mathbf{B}}_0^\top\tilde{\mathbf{B}}_* - \tilde{\mathbf{B}}_*)\| \\
&= 2\|(\mathbf{I}_d - \tilde{\mathbf{B}}_*\tilde{\mathbf{B}}_*^\top)\tilde{\mathbf{B}}_0\tilde{\mathbf{B}}_0^\top\tilde{\mathbf{B}}_*\| \\
&\geq 2\|(\mathbf{I}_d - \tilde{\mathbf{B}}_*\tilde{\mathbf{B}}_*^\top)\tilde{\mathbf{B}}_0\|\sigma_{\min}(\tilde{\mathbf{B}}_0^\top\tilde{\mathbf{B}}_*) \\
&= 2\operatorname{dist}(\tilde{\mathbf{B}}_0, \tilde{\mathbf{B}}_*)\sqrt{1 - \operatorname{dist}^2(\tilde{\mathbf{B}}_0, \tilde{\mathbf{B}}_*)} \qquad (68) \\
&= 2\delta_0\sqrt{1 - \delta_0}
\end{aligned}
$$

where (68) follows since $\sigma_{\min}^2(\tilde{\mathbf{B}}_1^\top\tilde{\mathbf{B}}_2) + \sigma_{\max}^2((\mathbf{I}_d - \tilde{\mathbf{B}}_1\tilde{\mathbf{B}}_1^\top)\tilde{\mathbf{B}}_2) = 1$ for any $\tilde{\mathbf{B}}_1, \tilde{\mathbf{B}}_2 \in \mathcal{O}^{d,k-1}$.

Note that for D-GD the global update for the representation is

$$
\mathbf{B}_{t+1} = \mathbf{B}_t - \frac{\alpha}{M}\sum_{i=1}^{M}\nabla_{\mathbf{B}} f_i(\mathbf{B}_t, \mathbf{w}_t) = \mathbf{B}_t - \alpha(\mathbf{B}_t\mathbf{w}_t - \mathbf{B}_*\bar{\mathbf{w}}_*)\mathbf{w}_t^\top, \qquad (69)
$$

and similarly, the update for the head is $\mathbf{w}_{t+1} = \mathbf{w}_t - \alpha\mathbf{B}_t^\top(\mathbf{B}_t\mathbf{w}_t - \mathbf{B}_*\bar{\mathbf{w}}_*)$. Thus, the behavior of D-GD is indistinguishable in the settings with ground-truth representations $\mathbf{B}_{*'}, \mathbf{B}_*$ since $\mathbf{B}_{*'}\bar{\mathbf{w}}_* = \mathbf{B}_*\bar{\mathbf{w}}_*$. In particular, $\mathbf{B}_T^{\text{D-GD}}(\mathbf{B}_0, \mathbf{B}_*, \{\mathbf{w}_{*,i}\}_{i=1}^M, \alpha) = \mathbf{B}_T^{\text{D-GD}}(\mathbf{B}_0, \mathbf{B}_{*'}, \{\mathbf{w}_{*,i}\}_{i=1}^M, \alpha)$ Using this equality along with the triangle inequality yields

$$
\begin{aligned}
\operatorname{dist}(\mathbf{B}_T^{\text{D-GD}}(\mathbf{B}_0, \mathbf{B}_{*'}, \{\mathbf{w}_{*,i}\}_{i=1}^M, \alpha), \mathbf{B}_{*'}) &= \operatorname{dist}(\mathbf{B}_T^{\text{D-GD}}(\mathbf{B}_0, \mathbf{B}_*, \{\mathbf{w}_{*,i}\}_{i=1}^M, \alpha), \mathbf{B}_{*'}) \\
&\geq \operatorname{dist}(\mathbf{B}_*, \mathbf{B}_{*'}) - \operatorname{dist}(\operatorname{dist}(\mathbf{B}_T^{\text{D-GD}}(\mathbf{B}_0, \mathbf{B}_*, \{\mathbf{w}_{*,i}\}_{i=1}^M, \alpha), \mathbf{B}_*) \\
&\geq 2\delta_0\sqrt{1 - \delta_0^2} - 0.7\delta_0 \qquad (70) \\
&\geq (\sqrt{3} - 0.7)\delta_0 \qquad (71) \\
&\geq \delta_0
\end{aligned}
$$

as desired, where (70) follows by the definition of case (2) and (68), and (71) follows by $\delta_0 \in (0, 1/2]$. □

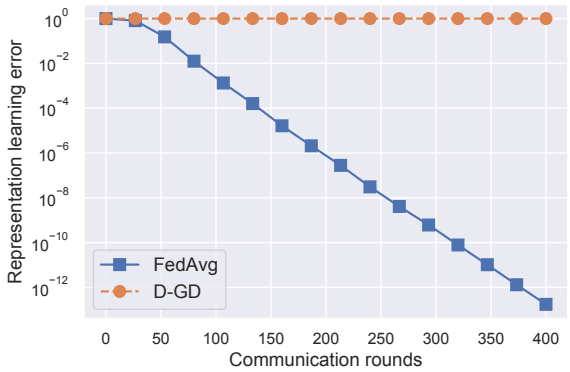

Figure 6: FedAvg with partial participation ($m = 10$, $M = 40$) learns the ground-truth representation at a linear rate.

C Experimental Details

C.1 Multi-task linear regression

The multi-task linear regression experiments consist of two stages: training and fine-tuning. During training, we track $\mathrm{dist}(\mathbf{B}_t, \mathbf{B}_*)$ in Figure 1 and the Frobenius norm of the gradient of (6), i.e. $(\|\mathbf{B}_t^\top(\mathbf{B}_t\mathbf{w}_t - \mathbf{B}_*\bar{\mathbf{w}}_*)\|_2^2 + \|(\mathbf{B}_t\mathbf{w}_t - \mathbf{B}_*\bar{\mathbf{w}}_*)\mathbf{w}_t^\top\|_F^2)^{1/2}$, in Figure 3(left). For fine-tuning, we track the squared Euclidean distance of the post-fine-tuned model from the ground-truth in Figure 3(right) for various numbers of fine-tuning samples n.

Each training trial consists of first sampling M ground truth heads $\mathbf{w}_{*,i} \sim \mathcal{N}(\mathbf{0}, \mathbf{I}_k)$ and a ground truth representation $\check{\mathbf{B}}_* \in \mathbb{R}^{d\times k}$ such that each element is i.i.d. sampled from a standard Gaussian distribution. Then, $\mathbf{B}_*$ is formed by computing the QR factorization of $\check{\mathbf{B}}_*$, i.e. $\mathbf{B}_*\mathbf{R}_* = \check{\mathbf{B}}$, where $\mathbf{R}_* \in \mathbb{R}^{k\times k}$ is upper triangular and $\mathbf{B}_* \in \mathcal{O}^{d\times k}$ has orthonormal columns. To initialize the model we set $\mathbf{w}_0 = \mathbf{0} \in \mathbb{R}^k$ and sample $\check{\mathbf{B}}_0 \in \mathbb{R}^{d\times k}$ such that each element is i.i.d. sampled from a standard Gaussian distribution, then compute $\mathbf{B}_0 = \frac{1}{\sqrt{\alpha}}\hat{\mathbf{B}}_0$ where $\hat{\mathbf{B}}_0 \in \mathcal{O}^{d\times k}$ is the matrix with orthonormal columns resulting from the QR factorization of $\check{\mathbf{B}}_0$. Then we run FedAvg with $\tau = 2$ and D-SGD on the population objective 6, with both sampling $m = M$ clients per round and using step size $\alpha = 0.4$. The training plots show quantities averaged over 10 independent trials.

For each fine-tuning trial, we similarly draw a new head $\mathbf{w}_{*,M+1} \sim \mathcal{N}(\mathbf{0}, \mathbf{I}_k)$, and data $\mathbf{x}_{M+1,j} \sim \mathcal{N}(\mathbf{0}, \mathbf{I}_k)$, $y_{M+1,j} = \langle \mathbf{B}_*\mathbf{w}_{*,i}, \mathbf{x}_{M+1,j}\rangle + \zeta_{M+1,j}$ where $\zeta_{M+1,j} \sim \mathcal{N}(0, 0.01)$. Then we run GD on the empirical loss $\frac{1}{2n}\sum_{j=1}^n(\langle \mathbf{B}\mathbf{w}, \mathbf{x}_{M+1,j}\rangle - \mathbf{y}_{M+1,j})^2$ for $\tau' = 200$ iterations with step size $\alpha = 0.01$. The fine-tuning plot shows average results over 10 independent, end-to-end trials (starting with training), and the error bars give standard deviations.

Remark 1 (Full participation)**.** *Although the aforementioned experiments used full participation ($m = M$), this condition is not required for FedAvg to learn the ground-truth representation. Figure 6 plots the representation learning error in the same setting as Figure 1 but with $m = 10$ (and $M = 40$) and one can see that FedAvg again learns the representation.*

Remark 2 (Convergence to stationary point of the global objective)**.** *The literature has thus far focused on analyzing the rates at which FedAvg converges to a stationary point of the global objective* (1)*, which prior works have shown requires step size diminishing with T to achieve at-best sublinear convergence in nonconvex data heterogeneous settings. In contrast, Theorem 1 and Figure 4 show that FedAvg with* fixed *step size converges* linearly *to the ground-truth representation despite* not converging *to a stationary point of the global objective.*

C.2 Image classification

The CNN used in the image classification experiments has six convolutional layers with ReLU activations and max pooling after every other layer. On top of the six convolutional layers is a 3-layer MLP with ReLU activations.

All models are trained with a step size of $\alpha = 0.1$ after tuning in $\{0.5, 0.1, 0.05, 0.01, 0.005\}$ and selecting the best α that yields the smallest training loss. In all cases, $m = 0.1M$. We use the SGD optimizer with weight decay 10^{-4} and momentum 0.5. We train all models such that $T\tau = 125000$. Thus, D-SGD trains for $T = 125000$ rounds, since $\tau = 1$ in this case. Likewise, for FedAvg with $\tau = 50$, $T = 2500$ training rounds are executed. The batch size is 10 in all cases. We also experimented with larger batch sizes for D-SGD but they did not improve performance.

Each client has 500 training samples in all cases. Thus, FedAvg with $\tau = 50$ is equivalent to FedAvg with one local epoch. For the experiments with C classes per client for all clients, each client has the same number of images from each class. For the experiment testing fine-tuning performance on new classes from the same dataset, the first 80 classes for CIFAR100 are used for training, while classes 80-99 are reserved for new clients. For fine-tuning, 10 epochs of SGD are executed on the training data for the new client. For fine-tuning on CIFAR10, each new client has images from all 10 classes, and equal numbers of samples per class for training. For fine-tuning on CIFAR100, each new client has images from all 20 classes, with equal numbers of samples from each class for training when possible, and either 2 or 3 samples from each class otherwise (when the number of fine-tuning samples equals 50). Accuracies are top 1 accuracies evaluated on 2000 test samples per client for CIFAR10 and 400 test samples per client for the last 20 classes of CIFAR100.

To compute the layer-wise similarities in Figure 2, we use the Centered Kernel Alignment (CKA) similarity metric, which is the most common metric used to measure the similarity between neural networks [13]. CKA similarity between model layers is evaluated by feeding the same input through both networks and computing the similarity between the outputs of the layers. The similarity metric is invariant to rotations and isotropic scaling of the layer outputs [13]. We use the code from [76] to compute CKA similarity.

For Figure 4, the cosine similarity is evaluated by first feeding n images from class c through the trained network and storing the output of the network layer before the final linear layer to obtain the features $\{\mathbf{f}_1^c, \ldots, \mathbf{f}_n^c\}$, where each $\mathbf{f}_i^c \in \mathbb{R}^{512}$. Then, to obtain the average cosine similarity between features from classes c and c', we compute $\frac{1}{n}\sum_{i=1}^{n} \frac{|\langle \mathbf{f}_i^c, \mathbf{f}_i^{c'} \rangle|}{\|\mathbf{f}_i^c\| \|\mathbf{f}_i^{c'}\|}$. We use $n = 25$.

All experiments were performed on two 8GB NVIDIA GeForce RTX 2070 GPUs.